Universitat Autònoma de Barcelona

Novel molecular tools to study mycoplama cells

Ana M Martínez Mariscal

ADVERTIMENT. L'accés als continguts d'aquesta tesi queda condicionat a l'acceptació de les condicions d'ús establertes per la següent llicència Creative Commons: http://cat.creativecommons.org/?page_id=184

ADVERTENCIA. El acceso a los contenidos de esta tesis queda condicionado a la aceptación de las condiciones de uso establecidas por la siguiente licencia Creative Commons: http://es.creativecommons.org/blog/licencias/

WARNING. The access to the contents of this doctoral thesis it is limited to the acceptance of the use conditions set by the following Creative Commons license: https://creativecommons.org/licenses/?lang=en

Novel molecular tools to study mycoplama cells

Ana M Martínez Mariscal

2017

Doctoral dissertation submitted to fulfill the requirements to obtain the Doctor of Philosophy Degree in Biochemistry, Molecular Biology and Biomedicine

This work has been performed at the Institut de Biotecnologia i de Biomedicina and the Biochemistry and Molecular Biology Department of Universitat Autònoma de Barcelona under the supervision of Dr. Jaume Piñol Ribas and Dr. Enrique Querol Murillo

Dr. Jaume Piñol Ribas Dr. Enrique Querol Murillo

08193-Cerdanyola del Vallès Phone +34935868952 ana.martinez.mariscal@uab.cat

A mis padres, Rufino y Antonia

1. Table of contents

1. TABLE OF CONTENTS V

2. ABBREVIATIONS IX

3. INTRODUCTION 1

3.1 THE CLASS MOLLICUTES 1

3.1.1 Mycoplasma genitalium 5

3.1.2 Mycoplasma pneumoniae 6

3.2 CYTOSKELETON AND MORPHOLOGY 6

3.2.1 A complex ultrastructure: the terminal organelle 8

3.2.2 Motility of mycoplasmas 15

3.2.3 Cell division 17

3.2.4 Infection process mediated through adhesion 20

3.3 GENETIC TOOLS FOR THE STUDY OF MINIMAL CELLS 21

4. OBJECTIVES 23

CHAPTER I: MYCOPLASMA GENITALIUM TERMINAL ORGANELLE PROTEINS LOCALIZED BY EYFP TAGGING IN A P32-MCHERRY BACKGROUND 25

4.1 INTRODUCTION 25

4.2 RESULTS 26

4.2.1 eYFP-tagged mutants in a P32-mCherry background 26

4.2.2 Localization of the different terminal organelle proteins by epifluorescence microscopy analysis 31

4.2.3 Localization of terminal organelle proteins quantitatively 34

4.3 DISCUSSION 36

5. CHAPTER II: ALL-IN-ONE CONSTRUCT FOR GENOME ENGINEERING USING CRE-LOX TECHNOLOGY IN MYCOPLASMA GENITALIUM 43

5.1 INTRODUCTION 43

5.2 RESULTS 44

5.2.1 Stability of suicide vectors in M. genitalium 44

5.2.2 Evaluation of the Cre-Lox system 45

5.2.3 Cre expression under the control of an inducible promoter 48

5.2.4 Stability of lox66 cassettes in long term uninduced cultures 52

Table of contents

5.3 DISCUSSION 53

6. CHAPTER III: IMPLEMENTATION OF ICRISPR FOR GENE KNOCK-DOWN IN MYCOPLASMA PNEUMONIAE 57

6.1 INTRODUCTION 57

6.2 RESULTS 58

6.2.1 Introducing dCas9 in M. pneumoniae cells bearing the Venus fluorescent protein 58

6.2.2 Down regulation of Venus expression in M. pneumoniae dCas9 cells 60

6.2.3 Analysis of Venus by epifluorescence microscopy 62

6.3 DISCUSSION 66

7. GENERAL DISCUSSION 69

8. CONCLUSIONS 73

9. MATERIALS AND METHODS 77

9.1 BACTERIAL GROWTH AND STRAINS 77

9.1.1 E. coli strains culture 77

9.1.2 M. genitalium strains culture 78

9.1.2.1 Medium and component preparation 78

9.1.2.2 M. genitalium cultures 80

9.1.2.3 M. genitalium transformation 81

9.2 DNA MANIPULATIONS AND MOLECULAR CLONING 82

9.2.1 Plasmid DNA extraction 82

9.2.2 Genomic DNA extraction from M. genitalium cultures 82

9.2.3 DNA quantification 83

9.2.4 DNA sequencing 83

9.2.5 DNA restriction 83

9.2.6 DNA ligation 83

9.2.7 DNA agarose electrophoresis 83

9.2.8 DNA PCR amplification 84

9.3 RNA EXTRACTION AND QPCR ANALYSES 84

9.4 SDS-PAGE AND WESTERN BLOTTING 84

9.4.1 Protein extraction and quantification 84

9.4.2 SDS-PAGE (Sodium Dodecyl Sulfate Polyacrylamide Gel Electrophoresis) 85

9.4.3 Gel Staining 85

9.4.4 Western Blot 86

9.5 EPIFLUORESCENCE MICROSCOPY 87

Table of contents

10. APPENDICES 89

10.1 APPENDIX I: PLASMID CONSTRUCTIONS 89

10.1.1 Plasmids used in Chapter I 89

10.1.1.1 Minitransposons with eYFP 89

10.1.1.2 pP140:eYFP 90

10.1.1.3 pP110:eYFP 91

10.1.2 Plasmids used in Chapter II 92

10.1.2.1 pGmRS 92

10.1.2.2 pMTnTc66Cat66 92

10.1.2.3 pGmRSCre 93

10.1.2.4 pΔMG_217Cre 94

10.1.3 Plasmids used in Chapter III 96

10.1.3.1 TnPac_dCas9ind 96

10.1.3.2 TnPac_dCas9cons 97

10.2 APPENDIX II: OLIGONUCLEOTIDES 98

10.2.1 Oligonucleotides used in Chapter I 98

10.2.2 Oligonucleotides used in Chapter II 101

10.2.3 Oligonucleotides used in Chapter III 102

10.3 APPENDIX III: TRANSPOSON LOCALIZATION OF THE SELECTED CLONES BEARING THE DIFFERENT EYFP FUSIONS 103

10.4 APPENDIX IV: STATISTICAL ANALYSIS OF FLUORESCENCE DISTANCES 105

10.4.1 Distance between P32 protein and DNA 105

10.4.2 Distance between target protein fused with eYFP and DNA 106

10.5 APPENDIX V: PXYL/TETO$_2$MOD PROMOTER 107

11. BIBLIOGRAPHY 109

2. Abbreviations

aac-aph	acetyltransferase(6′)-Ie-phosphotransfer¬ase(2″)-Ia [AAC(6′)-Ie-APH(2″)-Ia
ATCC	American Type Culture Collection
ATP	adenosine triphosphate
BSA	bovine serum albumin
β-Gal	β-galactosidase
bla	ampicillin resistance gene.
cat	chloramphenicol acetyl transferase gene
CmR	chloramphenicol resistance gene
CFP	cyan fluorescent protein
cfu	colony-forming unit
C-ter	carboxy-terminus
dNTP	deoxy-nucleotide triphosphate
EAGR	enriched aromatic and glycine residues
EDTA	ethylenediamintetraacetic
EYFP	enhanced yellow fluorescent protein
EGFP	enhanced green fluorescent protein
FBS	fetal bovine serum
GmR	gentamicin resistance gene
HMDS	Hexamethyldisiloxane
HA	haemadsoption
HEPES	4-(2-hydroxyethyl)-1-piperazineethanesulfonic acid
HMW	high molecular weight
kb	kilobase
kDa	kilodalton
LB	lysogenic broth
LHR	left homology region
mA	miliampere

Abbreviations

Mr	molecular relative mass (anciently known as molecular weight)
N-ter	amino terminal
o/n	overnight
ORF	open reading frame
PBS	phosphate buffer saline
PCR	polymerase chain reaction
pDNA	plasmidic DNA
RBS	ribosome binding site
RHR	right homology region
RPM	revolutions per minute
SDS	sodium dodecyl sulphate
SDS-PAGE	SDS-polyacrilanúde gel electrophoresis
SEM	scanning electron microscopy
SP4	spiroplasma medium 4
TEMED	N,N,N,N'-tetramethhylethane-1,2-diamine
tetM438	tetracycline resistance gene with MG_438 promoter
Tris	2-Amino-2-hydroxymethyl-propane-1,3-diol
Trp	tryptophan
TO	terminal organelle
V	volt
WT	wild type
YFP	yellow fluorescent protein
X-Gal	5-bromo-4-chloro-3-indolyl-β-D-galactopyranoside

3. Introduction

3.1 The class Mollicutes

The class Mollicutes ("molli", soft, "cutes", skin, in Latin) is used in taxonomy to include and distinguish those microorganisms lacking the cell wall. This class, as it is detailed in Table 3.1, includes the genus *Mycoplasma, Ureaplasma, Entomoplasma, Mesoplasma, Spiroplasma, Acholeplasma, Anaeroplasma, Asteroleplasma* and the undefined taxonomic status *Phytoplasma.* These microorganisms have arisen from gram-positive bacteria (Woese et al., 1980) and are closely related to *Lactobacillus* genus (Weisburg et al., 1989).

All of them present common characteristics that distinguish them from other eubacteria (Table 3.2) such as a small size, a low G+C content, the presence of cholesterol in the membrane of most spices and only one or two tRNA operons which leads to a fewer tRNA genes than other bacteria (Razin et al., 1998). Another feature of some mycoplasmas is the formation of a characteristic fried-egg colonies when growing in agar medium (Figure 3.1). The lack of the peptidoglycan layer explains their sensitivity to osmotic shock, their pleomorphic shape and confers them resistance to penicillins. In some species, the codon UGA encodes the Trp (Table 3.2) instead of the usual STOP codon. This trait complicates the heterologous protein expression and site directed mutagenesis or suppressor strains must be used to efficiently express recombinant proteins in most host models (Hames et al., 2005, Smiley and Minion, 1993).

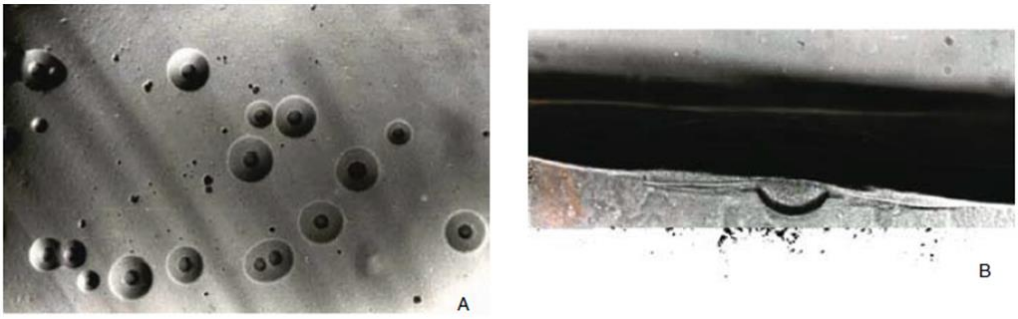

Figure 3.1. ***Acholeplasma Iaidlawii*** **colonies on mycoplasma agar at 50X magnification. A.** View from above shows the characteristic "fried-egg" shape due to a central zone embedded in the agar and a peripheral zone on the surface. **B.** Vertical section of a colony shows the central zone embedded in the agar and a theperipheral zone on the surface. Pictures from (Razin, 2006)

Table 3.1. Major characteristics and taxonomy of the Mollicutes (Razin, 2006)

Classification	No. of recognized species	Genome size (kb)	Genome G+C (mol%)	Cholesterol requirement	Distinctive properties	Habitat
Mycoplasmataceae						
Genus I: *Mycoplasma*	107 (11)[a]	580–1350	23–40	Yes	Optimum growth 37°C	Humans and animals
Genus II: *Ureaplasma*	7	760–1170	27–30	Yes	Urease positive	Humans and animals
Entomoplasmataceae						
Genus I: *Entomoplasma*	6	790–1140	27–29	Yes	Optimum growth 30°C	Insects and plants
Genus II: Mesoplasma	12	870–1100	27–30	No	Optimum growth 30°C	Insects and plants
Spiroplasmataceae						
Genus I: *Spiroplasma*	34	780–2220	24–31	Yes	Helical filaments	Insects and plants
Acholeplasmataceae						
Genus I: *Acholeplasma*	14	1500–1650	26–36	No	Optimum growth 30–37°C	Animals and plant surfaces
Anaeroplasmataceae						
Genus I: Anaeroplasma	4	1500–1600	29–34	Yes	Obligate anaerobes, oxygen sensitive	Bovine-ovine rumen
Genus II: Asteroleplasma	1	1500	40	No		
Undefined taxonomic status						
Phytoplasma	ND[b]	530–1185	23–29	ND	Uncultured in vitro	Insects and plants

Abbreviation: ND, not determined.

[a]The number of Candidatus species is given in parentheses and includes the hemoplasmas (*Eperythrozoon* and *Haemobartonella*) recently transferred to the genus *Mycoplasma* (Neimark et al., 2001).

[b]The taxonomic status of the uncultured phytoplasmas has not been finally defined; seven Candidatus *Phytoplasma* spp. have so far been published.

Table 3.2. Properties distinguishing Mollicutes from other eubacteria. Table from (Razin et al., 1998)

Property	Mollicutes	Other eubacteria
Cell wall	Absent	Present
Plasma membrane	Cholesterol present in most species	Cholesterol absent
Genome size	580–2,220 kb	1,050–>10,000 kb
G+C content of genome	23–40 mol%	25–75 mol%
No. of rRNA operons	1 or 2*	1–10
5S rRNA length	104–113 nt	>114 nt
No. of tRNA genes	30 (*M. capricolum*), 33 (*M. pneumoniae*)	84 (*B. subtilis*), 86 (*E. coli*)
UGA codon usage	Tryptophan codon in *Mycoplasma*, *Ureaplasma*, *Spiroplasma*, *Mesoplasma*	Stop codon
RNA polymerase	Rifampin resistant	Rifampin sensitive

* Three rRNA operons in *Mesoplasma lactucae*

Mollicutes present the smallest genomes ranging from 540 kb of *Mycoplasma parvum* (do Nascimento et al., 2013, do Nascimento et al., 2014) up to 1497 kb of *Acholeplasma laidlawii* (Lazarev et al., 2011). These reduced genome sizes are due to a reductive evolution process and leads to a limited number of biosynthetic routes. This low number of metabolic pathways explains their elevated nutrient requirements such as sterols, fatty acids, nucleotides and aminoacids (Pollack et al., 1997). Due to these elevated requirements, *mycoplasmas* have adopted an obligated parasitic life style and most of them are fastidious microorganisms when cultured in axenic conditions, requiring very complex media to grow (Razin et al., 1998). They are parasites of humans, mammals, reptiles, fish, insects and plants and usually present a high host and tissue specificity (Razin et al., 1998). The preferential infections sites for animal and human mycoplasmas are the urogenital and respiratory tract, mammary glands, joints and epithelial membranes. The obligatory anaerobic anaeroplasmas have been found only in the bovine and ovine rumen (Table 3.1) while spiroplasmas and phytoplasmas are spread in the gut, hemocoel and salivary glands of arthropods (Razin, 2006).

The genus *Mycoplasma* includes more than 100 of different species (Table 3.1), 16 of which are from human origin. Most of them are thought to be commensal conforming part of the natural flora of the respiratory and urogenital tracts but some species are considered pathogenic and can lead to acute or chronic infections (Table 3.3).

Table 3.3. *Mycoplasma* species from human origin. Table from (Taylor-Robinson and Jensen, 2011)

Species	Yr first isolated or named	Primary site colonized		Metabolism of:		Considered pathogenic
		Genital tract	Respiratory tract	Glucose	Arginine	
M. hominis	1937	+			+	+
M. fermentans	1952	+?		+	+	+
U. urealyticum[a]	1954	+				+
M. salivarium	1955		+		+	
M. primatum	1955		+		+	
M. pneumoniae	1962		+	+		+
M. orale	1964		+		+	
M. buccale	1965		+		+	
M. faucium	1965		+		+	
M. lipophilum	1974		+		+	
M. genitalium	1981	+		+		+
M. pirum	1985	+		+		?
M. spermatophilum	1991	+			+	?
M. penetrans	1991	+		+	+	?
M. amphoriforme	2005		+	+		?

[a] Metabolizes urea uniquely. In 2002, it was divided into *U. urealyticum* and *U. parvum*. ?, not certain.

3.1.1 *Mycoplasma genitalium*

M. genitalium is an emergent sexually transmitted human pathogen that infects the urogenital tract (Manhart et al., 2007). It has been isolated for the first time in the urogenital tract of two male with non-gonnococcal urethritis (NGU) (Tully et al., 1981). It causes between 20 and 35 % of the non-chlamydial NGU (McGowin and Anderson-Smits, 2011). In women, apart from causing urethritis, it has been related to other inflammatory syndromes of the reproductive tract such as cervicitis, pelvic inflammatory disease and infertility (McGowin and Anderson-Smits, 2011).

M. genitalium has been linked to AIDS by enhancing virus transmission and facilitating the development of this syndrome (Napierala Mavedzenge and Weiss, 2009, Taylor-Robinson and Jensen, 2011). Therefore, a possible HIV prevention would be the testing and treatment of *M. genitalium*-positive individuals in high-risk populations.

M. genitalium has been also detected in patients with cancer, including prostate and ovarian cancers and lymphomas (Namiki et al., 2009). However, its role in cancer development, like other *Mycoplasma* species, is still controversal and more epidemiological studies as well as a better understanding of malignant transformation are needed (Zarei et al., 2013, Idahl et al., 2011, Namiki et al., 2009).

3.1.2 *Mycoplasma pneumoniae*

M. pneumoniae, a human pathogen, infects the upper and lower respiratory tract of both children and adult causing primary atypical pneumonia with mild symptoms also known as "walking pneumonia" (Waites and Talkington, 2004) . It was isolated for the first time in 1944 in tissue culture from the sputum of a patient with primary atypical pneumonia (Eaton et al., 1944).

M. pneumoniae infections can occur both endemically and epidemically. This microorganism is responsible for about 4 to 8% of community-acquired bacterial pneumonias during periods of endemicity while its prevalence increases up to 70% (generally between 20 to 40%) in epidemic outbreaks (Waites et al., 2017). *M. pneumoniae* infection has also been related to chronic respiratory diseases such as bronchial asthma (Waites and Talkington, 2004, Kraft et al., 1998, Gil et al., 1993).

A significant milestone in mycoplasmology was the discovery of the CARDS (community-acquired respiratory distress syndrome) toxin, which displaced the paradigm that mycoplasmas were free of exotoxins (Kannan and Baseman, 2006, Waites et al., 2017). The production of this small protein has been directly related to the severity of disease (Techasaensiri et al., 2010).

3.2 Cytoskeleton and morphology

The majority of mycoplasma species are non-motile and present a pleomorphic and spherical morphology (Razin, 2006). However, despite its genomic simplicity, all motile species from *mollicutes* exhibit a complex cytoskeleton structure which confers them the ability to move. These structures differ in size and shape between species (Figure 3.2).

Spiroplasma species have a unique helical morphology, rotary motility and chemotaxis (Razin, 2006). Their internal structure is composed by a dumbbell-shaped structure at the tip connected by a flat ribbon-like structure that traces a line in the helical cell from the tip to the other pole (Figure 3.2A and B). The movement is thought to be achieved by coordinated changes in the length of these filamentous structures (Kurner et al., 2005).

The cytoskeleton found in mycoplasma cells from *M. pneumoniae* cluster shares many similarities between species (Hatchel and Balish, 2008). These cells present a flask shape with a characteristic protrusion called terminal organelle (TO) or attachment organelle (AO) (Figure 3.2C and D). This structure will be further detailed in the next section.

Mycoplasma mobile cells show a unique cytoskeletal structure reminding a jellyfish. This structure is composed by a bell solid structure at the cell head and dozens of tentacles connected to the bell (Miyata, 2010) (Figure 3.2E).

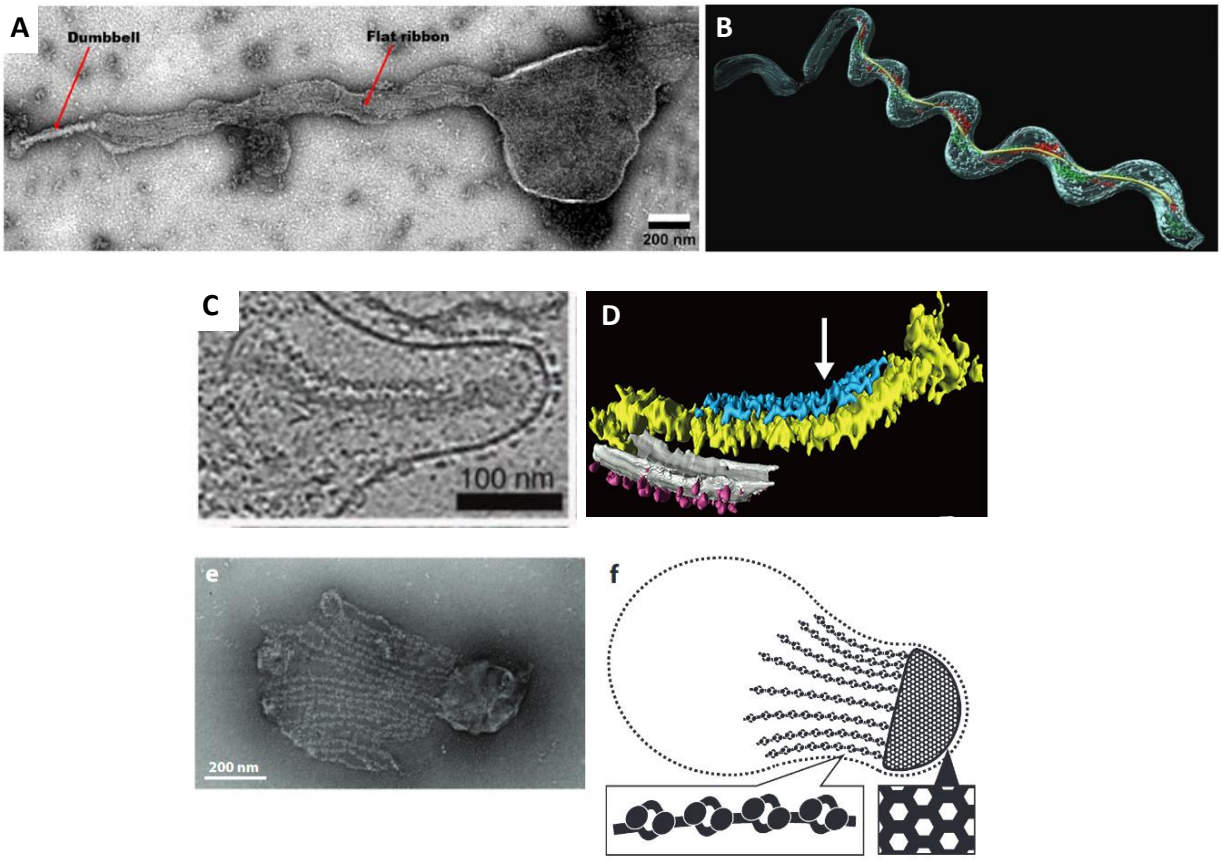

Figure 3.2. Images from different Mycoplasma cytoskeletons. A. Whole negative staining EM image of a *S. eriocheiris* cell extracted with 3% of Triton X-100 (Liu et al., 2017). **B.** 3D reconstruction by CET of *S. melliferum*. Image from (Kurner et al., 2005). **C.** Central slice of a top view of AO of *M. pneumoniae* from (Henderson and Jensen, 2006). **D.** 3D reconstruction by CET of the AO from *M. pneumoniae*. Image from (Miyata and Hamaguchi, 2016) **E.** Cytoskeletal structure of *M. mobile* visualized under negative-staining EM. The cell membrane and cytosol were removed by treatment with 0.1% Triton X-100. Image from (Miyata, 2010). **F.** Schematic of the cytoskeletal structure of a *M. mobile* cell from (Miyata, 2010).

3.2.1 A complex ultrastructure: the terminal organelle

Some *mycoplasma* species present a characteristic tip structure or a protrusion at one of the poles of the cell. It is called terminal organelle o attachment organelle in the members of *pneumoniae* cluster (Hatchel and Balish, 2008). The terminal organelle has been traditionally studied in *M. pneumoniae* and *M. genitalium* cells (Figure 3.3). This terminal organelle is involved in adhesion, gliding motility, cell division and virulence as it is further discused in next sections.

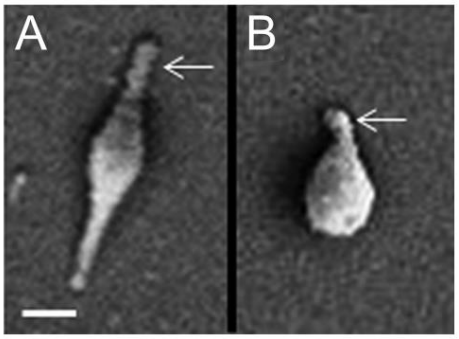

Figure 3.3. Scanning electron microgrphas of *M. pneumoniae* (A) and *M. genitalium* (B) cells. Terminal organelle is pointed with a white arrow. Images are shown at the same magnification. Scale bar 200 nm. Image from (Balish, 2014)

M. pneumoniae cytoskeleton was first observed in 1980 using different chemicals to remove the cell membrane, allowing the observation of the internal structure (Meng and Pfister, 1980). Further studies by cryo electron tomography improved the resolution of the different substructures forming the attachment organelle and generated 3D reconstructions of the electron-dense core (Seybert et al., 2006, Henderson and Jensen, 2006, Kawamoto et al., 2016). Based on these studies, 4 substructures conforming the cytoskeleton can be identified: (a) the adhesion complexes in the surface called nap, (b) the terminal button in the most apical region, (c) the segmented paired plates in the central region also called rod and (e) the wheel or bowl complex in the most proximal part. It must be stated that this electron-dense core is surrounded by an electron-lucent area, suggesting the presence of a low amount of proteins (Figure 3.4).

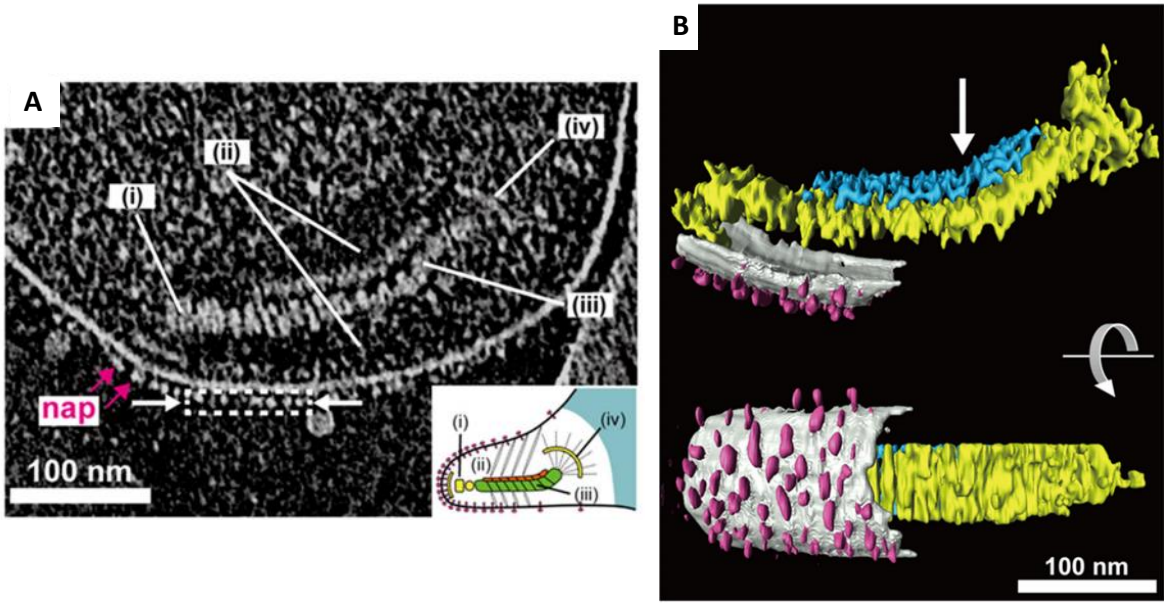

Figure 3.4. *M. pneumoniae* attachment organelle ultrastructure. A. Image of a 16 nm thick slice through the tomogram of an attachment organelle. The image shows a dense array of the knoblike particles on the membrane surface (nao), the terminal button (i), the translucent area (ii), the paired plates (iii) and the bowl or wheel complex (iv). The inset show a schematic diagram of the attachment organelle. **B.** Segmented 3D image of the reconstructed tomogram depicting the knoblike particles (pink), membranes (light grey) and thin (blue) and thick (yellow) plates. White arrow mark the bend. Images from (Kawamoto et al., 2016).

High-resolution studies of the *M. genitalium* terminal organelle have been recently performed. The treatment of *M. genitalium* cells with Triton X-100 to isolate the cytoskeleton structure shows a terminal organelle morphology very similar to its close relative *M. pneumoniae* with the difference of a less defined electron lucent area surrounding the terminal organelle (Gonzalez-Gonzalez, 2015) (Figure 3.5).

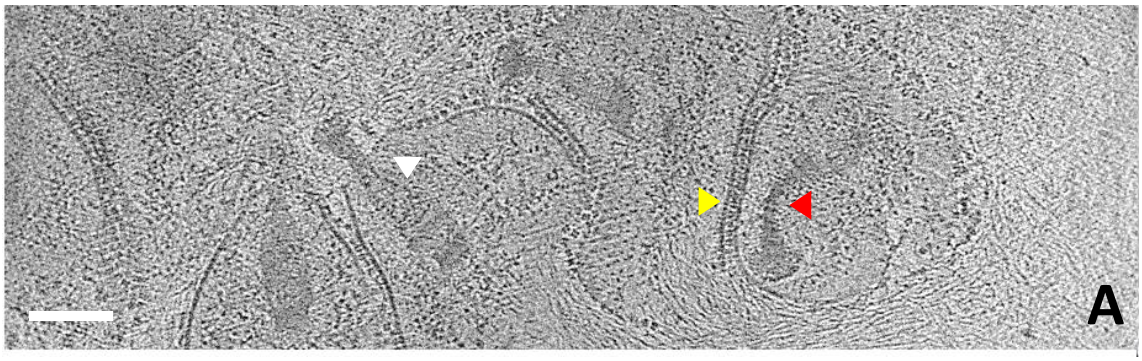

Figure 3.5. General view of ghost cells from *M. genitalium* by cryo-electron microscopy. The image shows the average projection of fifteen 0.85 nm thick slices through the reconstructed volume of G37 ghost cells treated with Triton X-100. White arrow indicates a top view of the cytoskeleton. Red arrow points a side view of the terminal organelle.

Yellow arrow indicates a junction of a nap with the adjacent mycoplasma membrane. Scale bar 100 nm. Image from (Gonzalez-Gonzalez, 2015)

The protein composition of the cytoskeleton has been studied by different mutant strains of *M. pneumoniae* and *M. genitalium* that present deficiencies in TO structure or function and by proteomic approaches after detergent treatment to isolate the cytoskeleton (Burgos et al., 2006, Pich et al., 2006a, Burgos et al., 2007, Pich et al., 2008, Burgos et al., 2008, Pich et al., 2009, Garcia-Morales et al., 2016, Parraga-Nino et al., 2012, Stevens and Krause, 1992, Hahn et al., 1998, Balish et al., 2001, Krause and Balish, 2001, Willby and Krause, 2002, Willby et al., 2004, Hasselbring et al., 2006a, Chaudhry et al., 2007, Relich and Balish, 2011, Cloward and Krause, 2011).

In *M. pneumoniae* these studies have been complemented with protein localization by immunofluorescence or using fluorescence proteins tagging the attachment organelle proteins (Seto and Miyata, 2003, Balish et al., 2003, Seto et al., 2001, Hasselbring et al., 2006b, Kenri et al., 2004, Hasselbring and Krause, 2007b, Cloward and Krause, 2009). Recently, a fluorescence microscopy and immuno electron microscopy study of different *M. pneumoniae* strains has assigned the proteins to the different substructures of the terminal organelle (Nakane et al., 2015).

In *M. genitalium* the exact localization of terminal organelle proteins has been only determined for MG217 and P32 (Burgos et al., 2008, Garcia-Morales et al., 2016). The assignment of the other TO proteins to the different substructures is based in their homology to *M. pneumoniae* proteins (see Table 3.4) and in the phenotypic analyses of the mutant strains.

Table 3.4. Orthologue terminal organelle proteins of *M. genitalium* and *M. pneumoniae.*

M. genitalium		*M. pneumoniae*			
Locus	**Protein**	**Locus**	**Protein**	**Identity (%)**	**Function**
MG_191	P140	MPN_141	P1	45	Adhesion
MG_192	P110	MPN_142	P40, P90	50	Adhesion
MG_200	MG200	MPN_119	TopJ	35	Gliding
MG_217	MG217	MPN_309	P65	42	Gliding
MG_218	HMW2	MPN_310	HMW2	57	Adhesion
MG_219	MG219	MPN_312	P24	16	Gliding
MG_269	MG269	MPN_387	MPN387		Gliding
MG_312	HMW1	MPN_447	HMW1	33	Adhesion
MG_317	HMW3	MPN_452	HMW3	33	Adhesion
MG_318	P32	MPN_453	P30	43	Adhesion
MG_386	MG386	MPN_567	P200	30	Gliding
MG_491	P41	MPN_311	P41	53	Gliding

Below are presented the proteins assigned to each substructure of the terminal organelle in basis of the previous studies cited. A drawing with the location of each proteins is shown in Figure 3.6.

Nap

The nap complex contains the adhesins located in the membrane that is surrounding the terminal organelle. It is formed by the P110 and P140 proteins in *M. genitalium* (Gonzalez-Gonzalez, 2015) and P1 and P40/P90 in *M. pneumoniae* (Nakane et al., 2015). In *M. pneumoniae* it has been determined that the nap complex contains two molecules of P1 adhesin and two molecules of P90 (Layh-Schmitt et al., 2000, Nakane et al., 2011) as well as for the P110 and P140 complex from *M. genitalium* (Scheffer et al., 2017). These proteins are essential for cell adhesion: real-time microscopy study with *M. pneumoniae* cells have shown that after the addition of anti-P1 antibody gliding cells were unbound from the glass surface (Seto et al., 2005). Moreover, P110 and P140 proteins are required for terminal organelle formation and cell division in *M. genitalium* (Pich et al., 2009, Burgos et al., 2006) and play a major role in gliding motility (Garcia-Morales et al., 2016).

Terminal Button

The terminal button is the most apical substructure. Proteins P30, P65 and HMW3 have been localized in the terminal button of *M. pneumoniae* (Nakane et al., 2015, Stevens and Krause, 1992, Jordan et al., 2001, Seto and Miyata, 2003, Seto et al., 2001).

P30 is a transmembrane protein located at the most apical region of the cell membrane, with its C-ter oriented toward the outside of the cell(Chang et al., 2011), and plays an important role in adhesion and gliding motility (Relich and Balish, 2011, Hasselbring et al., 2005, Romero-Arroyo et al., 1999). Interestingly, P32 from *M. genitalium*, can complement P30 function in *M. pneumoniae* strains lacking this protein (Relich and Balish, 2011) and it has been recently localized in *M. genitalium* TO (Garcia-Morales et al., 2016). It has been described that overexpression of P32 can stabilize P110 and P140 proteins, suggesting a close relationship between these three proteins (Garcia-Morales et al., 2016) and supporting its role in adhesion.

P65 needs the P30 for proper localization (Jordan et al., 2001). Although a mutant disrupting P65 coding gene have been isolated, it is not clear if its reduced gliding speed is directly due to P65 absence or to polar effects from transposon insertion affecting the stability of other terminal organelle proteins (Hasselbring et al., 2012). This last hypothesis is supported by the fact that MG217, which has been localized in the *M. genitalium* terminal button by TEM immunogold, determines the gliding direction by modifying the curvature of the terminal organelle (Burgos et al., 2008).

HMW3 protein is believed to anchor the terminal button to the electron-dense core (Nakane et al., 2015, Pich, 2008).

Segmented paired plates or rod

The segmented paired plates are the central part of the terminal organelle and are surrounded by an electron-lucent aera. The paired plates are composed by two striated plates separated by a gap of around 7nm (Henderson and Jensen, 2006, Seybert et al., 2006, Kawamoto et al., 2016) and a flexible bend of approximately 30 degrees in the middle. Thin and thick plate have been clearly defined in *M. pneunomiae* but have not been observed in *M. genitalium* rod structure.

HMW1 and HMW2 are the proteins localized in this substructure (Nakane et al., 2015, Balish et al., 2003). Both are proteins involved in cell morphology and adhesion and are critical for terminal organelle formation in both microorganisms(Pich et al., 2008, Burgos et al., 2007, Krause et al., 1997).(Popham et al., 1997, Hahn et al., 1998). HMW1 protein

from *M. genitalium* and *M. pneumoniae* are slightly different: while in *M. pneumoniae* it is a membrane-associated protein (Balish et al., 2001) it has not been found in cell membrane extracts from *M. genitalium* (Parraga-Nino et al., 2012). Moreover, *M. genitalium* HMW1 has a modular double function: C-ter domain is involved in cytadherence and terminal organelle assembly (as its *M. pneumoniae* homologue protein) while the N-ter domain is involved in gliding motility (Burgos et al., 2007). The N-ter domain contains a EAGR box (enriched in aromatic and glycine residues), supporting the implication of this EAGR motif in gliding motility (Calisto et al., 2012, Pich et al., 2006a, Balish et al., 2001, Cloward and Krause, 2009).

CpsG phosphomannomutase of *M. pneumoniae* has also been localized in this structure (Nakane et al., 2015) but its role in the terminal organelle is still unclear.

The recent finding that a *M. genitalium* mutant without HMW2 and overexpression of P32 can glide suggests that this structure is not directly involved in the movement generation (Garcia-Morales et al., 2016).

Wheel or bowl complex

The wheel or bowl complex is the structure located at the most proximal part of the terminal organelle. MPN387, P41, P200, TopJ, P24 and Lon proteins have been localized in the wheel complex (Kenri et al., 2004, Cloward and Krause, 2009, Nakane et al., 2015).

The proteins P200 and MG386, both containing EAGR domains, are involved in gliding motility but not in cell adhesion (Jordan et al., 2007, Pich et al., 2006a) as well as the proteins MPN387 and MG269 (Hasselbring and Krause, 2007a, Kawakita et al., 2016) (Lluch-Senar M., unpublished).

TopJ and MG200 proteins are involved in cell motility and also contain one EAGR box (Cloward and Krause, 2009, Pich et al., 2006a, Calisto et al., 2012). Moreover, their N-ter contain a DnaJ domain which has been shown to be involved in stabilizing the main adhesins in both strains (Cloward and Krause, 2011, Cloward and Krause, 2010, Broto, 2014). This adhesins stabilization explains the implication of these proteins in cell adhesion.

Protein P41 from *M. pneumoniae* and *M. genitalium* plays a key role in gliding motility (Hasselbring and Krause, 2007b, Hasselbring and Krause, 2007a, Martinelli et al., 2016). Moreover, it also has a role in connecting the attachment organelle to cell body since mutant strains lacking this protein present some terminal organelle detachments and the detached TO glides independently (Hasselbring and Krause, 2007b, Hasselbring and Krause, 2007a, Martinelli et al., 2016). Fluorescence studies of P41 in *M. pneumoniae* cells have shown that P41 is one of the earliest proteins incorporated in the nascent terminal organelles in the duplication process.

P24 and MG219 proteins are involved in gliding motility (Hasselbring and Krause, 2007b, Gonzalez-Gonzalez, 2015).

Interestingly, all the proteins localized in the wheel complex (except the Lon protease which has not been deeply studied) are involved in gliding motility but poorly related to adhesion in both organisms, supporting the idea that the wheel complex is the structure responsible for the movement generation(Miyata and Hamaguchi, 2016).

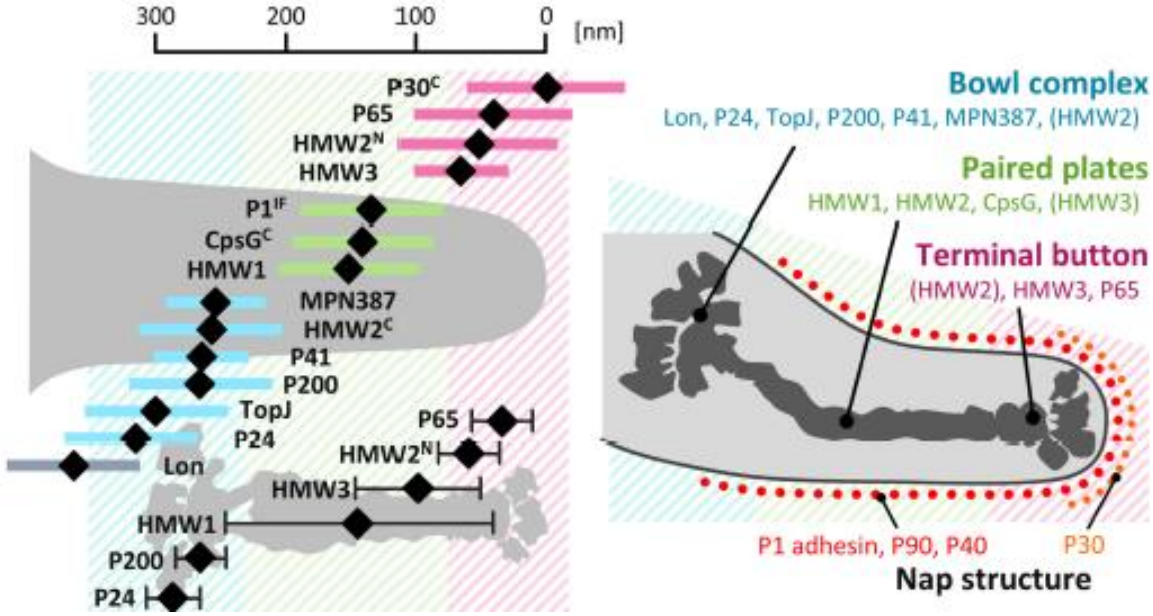

Figure 3.6. Scheme of component proteins localized in the attachment organelle. Left. Positions of proteins determined from EYFP fluorescence. The average position in individual cells relative to the cell edge is plotted with a black diamond and colored bars represent SD. **Right.** Scheme of the terminal organelle ultrastructure and the proteins assigned to each substructure. Colors in both panels indicate the localization groups: pink for the terminal button, green for the segmented paired plates, blue for the wheel complex and red for the nap. Image from (Nakane et al., 2015)

3.2.2 Motility of mycoplasmas

Only 13 species of *Mycoplasma* have been reported to be motile. All of them present a cytoskeleton structure, supporting the direct relationship between the cytoskeleton and the ability to glide (Hatchel and Balish, 2008)

Motile mycoplasmas glide over solid surfaces without using flagella, pili or other known machineries used by other bacteria (McBride, 2001, Jarrell and McBride, 2008). The mechanism behind this gliding motility of mycoplasmas is not completely understood but two different models have been proposed: the inchworm and centipede models (Miyata, 2008).

The best characterized mechanism is the described by *M. mobile* cells: the centipede model. This model is based in a motile machinery involving 4 main proteins (Gli349, Gli123, Gli521 and P42) that form a complex as a flexible leg. Multiple flexible legs are distributed in the cell membrane at the base of the tip structure and its coordinated cycle of attach – stroke - movement - realese will generate the cell movement (Figure 3.7). The movement generated by the ATP hydrolysis inside the cells is transmitted to these legs, which are connected to the internal cytoskeleton. This model has also been proposed to explain the movement of *M. pneumoniae* cells where the P1 adhesin complex would act as a leg (Miyata, 2010) (Miyata and Hamaguchi, 2016)

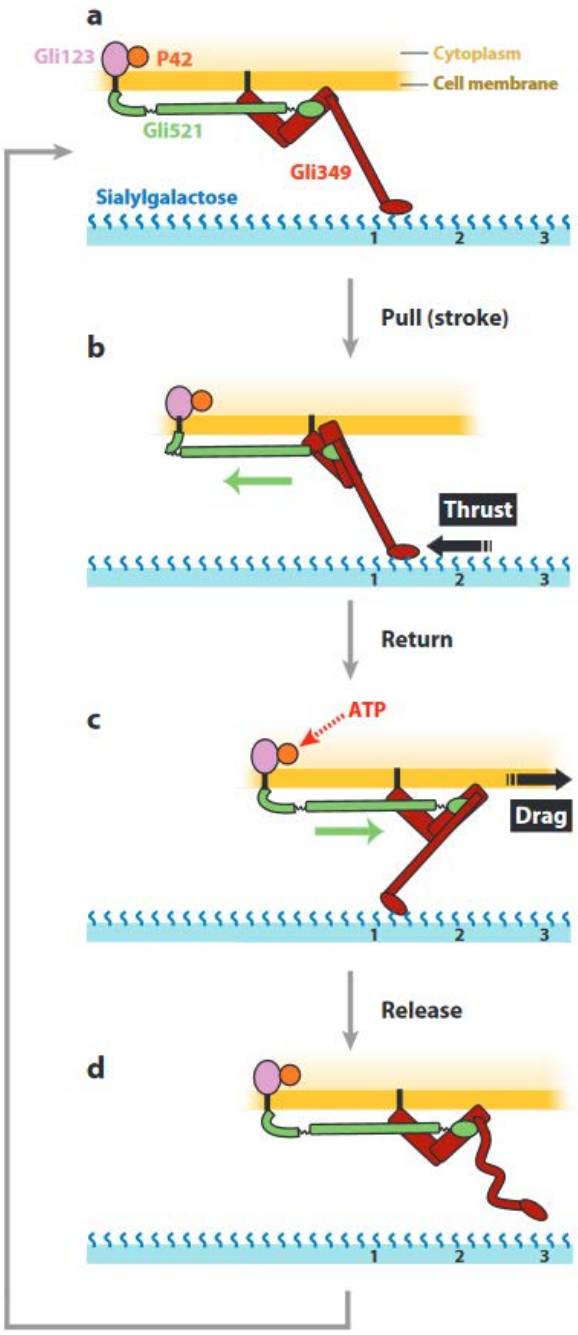

Figure 3.7. Model for centipede movement.
Image from (Miyata, 2010)

The inchworm model was based in the theory that longitudinal changes of the segmented paired plates drived the motion of cells by repetitive cycles of attach – contract – step – detach – extend (Wolgemuth et al., 2003) (Figure 3.8A). More recent studies by CET suggest that motion might be a consequence of changes in the bending of the segmented

paired plates (Seybert et al., 2006, Henderson and Jensen, 2006). It has been proposed that the wheel complex is the structure where the movement is generated and then is transmitted to the cell through the segmented paired plates while the terminal button will be in charge of the gliding direction determination. However, the mechanistic model for gliding motility is still controversial and recent studies have shown that the rod component is not essential for the gliding motility (Garcia-Morales et al., 2016)

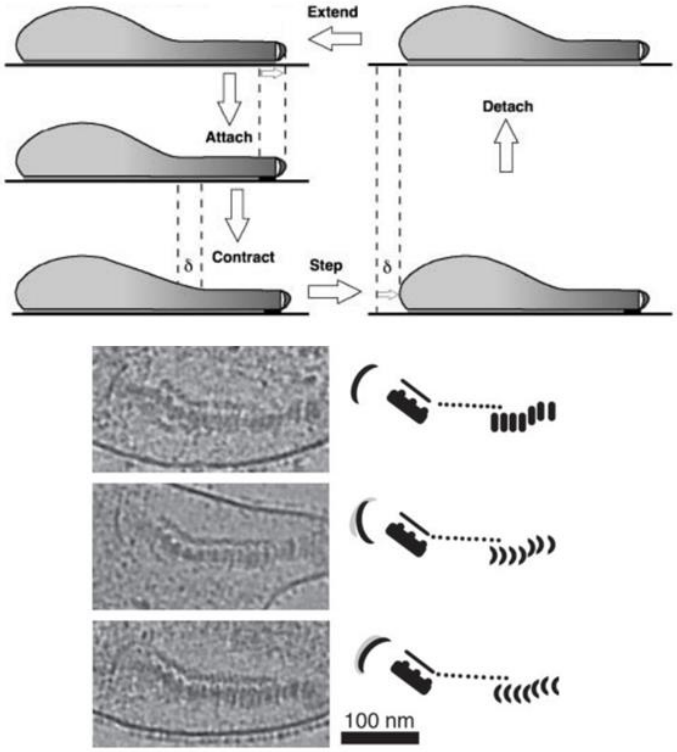

Figure 3.8. Inchworm model for explaining gliding motility. Images from (Wolgemuth et al., 2003) and (Henderson and Jensen, 2006).

3.2.3 Cell division

Mycoplasma cells divide by binary fission. Besides the role of their cytoskeleton in adhesion and gliding motility, this structure is also thought to participate in cell division (Razin, 2006). The process of cell division starts with the terminal organelle duplication. Once the new terminal organelle is completely formed and functional, it migrates to the opposite pole and the gliding motility of both terminal organelles help to the cytokinesis to

separate the daughter cells (Lluch-Senar et al., 2010, Hasselbring et al., 2006b, Balish, 2014). It has been reported that multiple organelle duplication can occur before the cytokinesis in *M. pneumoniae* cells (Figure 3.9a), suggesting a simultaneous initiation of cell division. However, in *M. genitalium* G37 cells, the frequency of cells with multiple organelles is much lower than in *M. pneumoniae*. This difference can be controlled by the proteins P110 and P140 since mutants with lower amounts of these proteins present a high increase in the cells with multiple organelles (Pich et al., 2009)

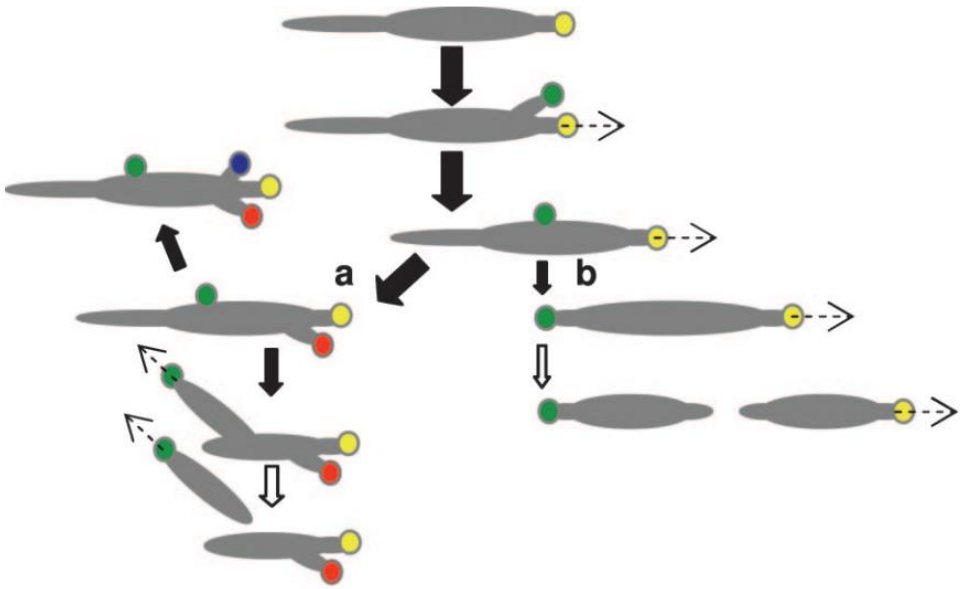

Figure 3.9. Model for *M. pneumoniae* terminal organelle duplication and growth cycle. Solid black arrows indicates the steps in the cell cycle, dashed arrows indicates the movement of the terminal organelle and white arrows indicates the cytokinesis. Scheme from (Hasselbring et al., 2006b)

A recent study with fluorescent proteins tagging some proteins conforming the attachment organelle of *M. pneumoniae* has enlighten the process of the terminal organelle formation during its replication (Hasselbring et al., 2006b). It seems that proteins are sequentially added when new terminal organelles are assembled. In this way, P41 protein is one of the firsts proteins identified in nascent terminal organelles, before that P30 and P65 could be detected. Since P41 is located in the wheel complex and P30 and P65 are located in the terminal button, the wheel complex could be the first structure that is assembled in nascent terminal organelles (Hasselbring et al., 2006b). This hypothesis is in disagreement with

electron microscopy images of *M. pneumoniae* cells where cells showing bipartite attachment organelles can be observed (Hegermann et al., 2002, Kawamoto et al., 2016) (Figure 3.10A). Cryo-electron microscopy images of *M. genitalium* cells also show cells with two terminal buttons, suggesting that the terminal organelle duplication may start from its most apical extreme (Figure 3.10B) (Gonzalez-Gonzalez, 2015). Therefore, more studies are required to fully understand the mechanism of terminal organelle duplication and division process.

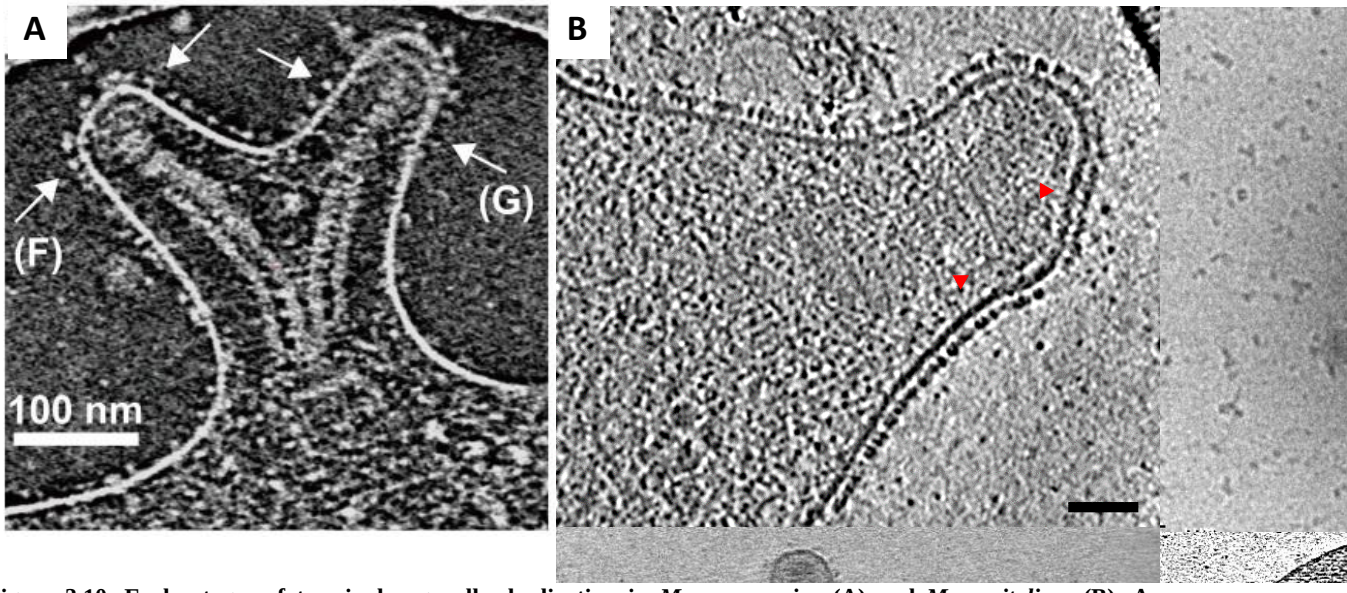

Figure 3.10. Early stages of terminal organelle duplication in *M. pneumoniae* (A) and *M. genitalium* (B). A. Bifurcated terminal organelle of *M. penumoniae.* White arrows point the two terminal organelles. Image from (Kawamoto et al., 2016)**B.** *M. genitalim* G37 cell in an early stage of terminal organelle division. Red arrows delimitate a nascent terminal button almost 90 º of the rod. Sacale bar 50 nm. Image from (Gonzalez-Gonzalez, 2015)

Interestingly, while FtsZ is essential in most bacteria, a *M. genitalium* viable mutant lacking the FtsZ gene has been engineered, suggesting that cells are able to perform binary fission without the FtsZ protein (Lluch-Senar et al., 2010, Jaffe et al., 2004). However, spontaneous adherence mutants, which appear quite frequently among wild-type cells, do not occur in appreciable numbers in the mutant lacking FtsZ, reinforcing the importance of the terminal organelle in the division process and suggesting that the gliding motility may be responsible for cytokinesis (Lluch-Senar et al., 2010). However, mutant strains with adhesion and gliding deficiencies (even pleomorphic mutants lacking the terminal organelle) have been isolated in *M. genitalium* and *M. pneumoniae.* This indicates that the gliding motility and FtsZ might be redundant systems for cytokinesis in these mycoplasmas.

3.2.4 Infection process mediated through adhesion

The adhesion of *mollicutes* to host cells is a prerequisite for the infection establishment. The loss of adhesion capacity is linked to the loss of infectivity as well as reversion to the cytadherence phenotype also reverts their virulence and infectivity (Razin, 2006). The adhesion of some mycoplasmas (i.e. *M. pneumoniae* and *M. mobile*) to the host cells has been demonstrated to be mediated by specific sialylated oligosaccharides that can be found in the membrane cell and would be recognized by adhsein proteins of the mycoplasma surface (Kasai et al., 2013, Nagai and Miyata, 2006, Loomes et al., 1984)

In vitro studies with vaginal epithelial cells have demonstrated that *M. genitalium* is able to be adhered to host cells, concretely through its terminal organelle as it can be observed in Figure 3.11A, and internalized (McGowin et al., 2009). The internalization mechanism is still unknown but it is characterized by a clathrin-coated membrane depressions where the attachment organelle is contacting the cell membrane (Mernaugh et al., 1993). After internalization *M. genitalium* cells are located in vacuoles adjacent to the nucleus but also distributed through the cytoplasm (Ueno et al., 2008, McGowin et al., 2009) . This internal localization aids this microorganism to escape from host immune system and explains its latent persistence in some cases after antibiotic treatments (McGowin et al., 2009, Cazanave et al., 2012). Regarding *in vivo* studies, *M. genitalium* cells have been found inside human vaginal cells of clinical samples using confocal immunoanalysis (Blaylock et al., 2004).

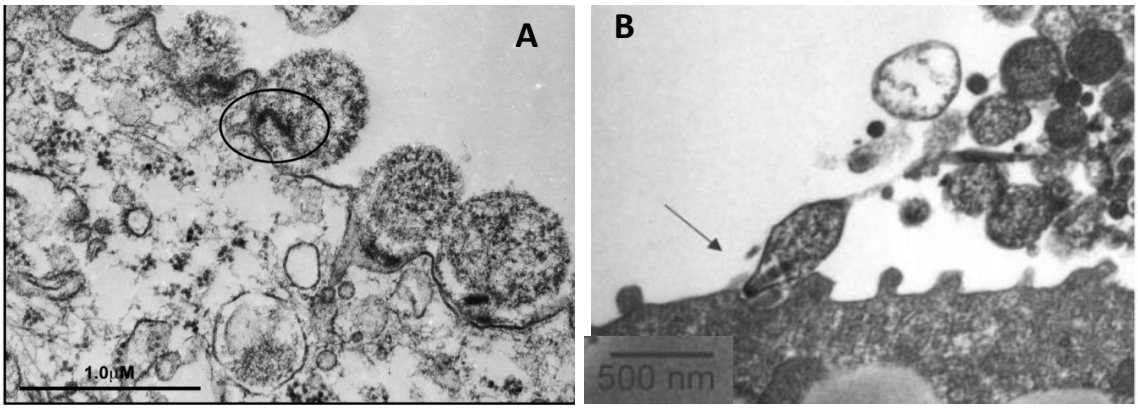

Figure 3.11. Electron microscopy images of Mycoplasma infection process. A. *M. genitalium* cells attached to the surface of epithelial cells after 3 h postinfection. The black circle encloses the terminal organelle cytoskeleton. Image from (McGowin et al., 2009). **B.** *M. pneumoniae* cell attached to tracheal epithelium cells of an infected hamster. Image from D.C. Krause in (Waites and Talkington, 2004).

As for other mycoplasmas, adhesion to host cells of *M. pneumoniae* is critical for its virulence and the attachment organelle plays a key role in this process (Figure 3.11B). Apart from adhesins located in the terminal organelle that binds to sialylated compounds (Kasai et al., 2013), it has been reported that proteins ef-Tu and E1 beta subunit of pyruvat deshydrogenase complex binds to fibronectin (Dallo et al., 2002, Balasubramanian et al., 2008), various subunits of pyruvate deshydrogenase and some glycolic enzymes also bind to plasminogen (Thomas et al., 2013, Grundel et al., 2015b, Grundel et al., 2015a) and glyceraldehydes-3phosphate deydrogenase has a moonlighting role in binding to fibrinogen (Dumke et al., 2011). All these proteins together may play a secondary role in adhesion to host cells once the attachment organelle has initiated the binding (Waites et al., 2017). Interestingly, a nearly nonmotile *M. pneumoniae* mutant (II-3R mutant) retaining most of its cyatadherence ability (about 60 % to wild-type cells) is avirulent (Szczepanek et al., 2012), suggesting that part of what makes terminal organelle essential for virulence is its implication in gliding motility apart from adhesion. Therefore proteins of the attachment organelle (Table 3.4) and the recently discovered CARDS toxin (Kannan and Baseman, 2006, Techasaensiri et al., 2010) are the main virulence factors of *mycoplasmas.*

3.3 Genetic tools for the study of minimal cells

Mycoplasmas have evolved from gram-positive ancestors by a process of massive genome reduction until being the self-replicating organisms with the smallest genomes known (Weisburg et al., 1989). Due to this evolutionary reduction process they are the most suitable cells for the study of the minimal genes essential for the life and determine the unsolved question of which is the minimal set of genes required for life (Glass et al., 2006b, Xavier et al., 2014).

However, despite their suitability for these studies, available genetic tools for engineering these microorganisms are limited. Replicative plasmids are only functional in some mycoplasma species such as *Mycoplasma hyopneumoniae* (Maglennon et al., 2013), *Mycoplasma capricolum subs. capricolum* , *M. pulmonis* (Cordova et al., 2002), *Mycoplasma gallisepticum* (Lee et al., 2008), *Mycoplasma imitans* (Lee et al., 2008), *Mycoplasma agalactiae* and *Mycoplasma bovis* (Sharma et al., 2015) while site directed mutagenesis by homologous recombination is also limited to *M. genitalium*

(Dhandayuthapani et al., 1999), *M. pulmonis* (Mahairas and Minion, 1989b) and some strains of *M. pneumoniae* (Krishnakumar et al., 2010). Therefore, the most extended technique is the use of transposons and minitransposons to deliver the desired sequences and to isolate randomly truncated mutants (Pich et al., 2006b, Hasselbring et al., 2006a, Pich et al., 2006a). Moreover, all of these techniques rely on the introduction of a antibiotic resistance gene and geneteic modifications in the same strain will be limited to the number or selective markers available and phenotypic analyses can be biased by the presence of selectable markers. For mycoplasmas 4 antibiotic resistance genes have been reported conferring resistance to gentamycin, tetracycline, chloramphenicol and puromycin (Mahairas and Minion, 1989a, Dybvig and Cassell, 1987, Hahn et al., 1999, Algire et al., 2009). In this work we present the implementation of state-of-the-art available techniques, such as Cre-lox system and iCRIPR, for genome engineering in mycoplasma cells (Chapters II and III).

4. Objectives

Chapter I: Mycoplasma genitalium terminal organelle proteins localized by eYFP tagging in a P32-mCherry background

- Obtaining a set of *M. genitalium* strains expressing eYFP fluorescent fusions with 15 different terminal organelle proteins.
- Analyze the relative position of each target protein using the P32 fluorescence as a reference marker.
- Quantitative analysis of the location of the different terminal organelle protein fusions.
- Assign the position of the different proteins to the main cytoskeleton structures of *M. genitalium*.

Chapter II: All-in-one construct for genome engineering using Cre-lox technology in *M. genitalium*

- Test the use of suicide plasmids for transient protein expression in *M. genitalium* cells.
- Test the excision of floxed DNA sequences by the Cre recombinase delivered by a suicide vector.
- Develop a non-leaky, inducible promoter for tightly control of the Cre expression.
- Design a plasmid vector to obtain unmarked *M. genitalium* mutants using the Cre-lox technology.

Chapter III: Implementation of iCRISPR for gene knock-down in *Mycoplasma pneumoniae*

- Implement the iCRISPR system to knock-down the expression of the *Venus* gene in a mutant strain of *M. penumoniae*.
- Test the expression of the dCas9 from *Streptoccocus pyogenes* under the control of the MG_438 constitutive promoter and an inducible promoter.
- Quantify the transcription repression of the *Venus* gene in the presence of dCas9 and a specific sgRNA.
- Perform an epifluorescence microscopy analysis of Venus protein abundance in the presence of dCas9 and a specific sgRNA.

Chapter I: *Mycoplasma genitalium* terminal organelle proteins localized by eYFP tagging in a P32-mCherry background

4.1 Introduction

Fluorescent proteins are a powerful tool that can be used for a multiple type of studies: from developmental neuroscience to determination of protein-protein interactions. Since the GFP was isolated from *Aequorea vicotria* (Shimomura et al., 1962), a wide spectrum of different fluorescent proteins covering all the visible range has been developed, either by isolating new fluorescent proteins from other organisms or reengineering the previous ones to improve their characteristics (brightness, stability, monomeric state…) or shift the emitted fluorescence (Karasawa et al., 2003, Zapata-Hommer and Griesbeck, 2003, Hadjantonakis and Nagy, 2001, Matz et al., 1999, Cormack et al., 1996{Shaner, 2004 #389, Gross et al., 2000, Mena et al., 2006).

Different fluorescent proteins such as EYFP, GFP or ECFP have been used in *M. pneumoniae* for endogenous protein localization (Kenri et al., 2004, Nakane et al., 2015, Jordan et al., 2001) and also to study the relationship of terminal organelle formation and gliding motility (Hasselbring et al., 2006b, Hasselbring et al., 2012, Seto and Miyata, 2003, Hasselbring and Krause, 2007b, Hasselbring and Krause, 2007a). However, the knowledge of the localization of terminal organelle proteins of *M. genitalium* is reduced to the proteins MG217 {Burgos, 2008 #23} and P32 (Garcia-Morales et al., 2016) which have been localized in the terminal organelle by TEM immunogold and epifluorescence microscopy.

To gain further knowledge about the terminal organelle of *M. genitalium* and their components, we have introduced a total of 15 proteins fused with the eYFP as a marker

position in a G37-P32mCherry background (Garcia-Morales et al., 2016), aiming to colocalize the target protein in basis a known point of reference.

4.2 Results

4.2.1 eYFP-tagged mutants in a P32-mCherry background

In order to localize the different proteins inside *M. genitalium* we have fused the target proteins with the eYFP (Hadjantonakis and Nagy, 2001). Therefore, different plasmids were engineered to deliver eYFP fusions into *M. genitalium* (see Appendix I: plasmid constructions, page 89). pMTnCat_eYGP:MGXXX is a minitransposon vector designed to carry the gene coding for the target protein fused with the eYFP at its N-ter domain while the pMTnCat_ MGXXX: eYGP is a minitransposon vector designed to carry the protein fused with the eYFP at its C-ter domain. In both cases a linker of 10 Asn residues is used to avoid steric impediments trying to maintain the proper folding of both proteins. Except the genes MG_191 and MG_192, coding for the P140 and P110 proteins respectively, all genes were cloned into one or both of these vectors as it is detailed in Table 0.1 and

Table 0.2. All this target genes are under the control of MG_438 promoter and were delivered by transposition into *M. genitalium* genome as an extra copy of the orginal gene. First, all genes were fused with the eYFP at its N-ter. For those fusions which cells exhibit an abnormal phenotype or did not show fluorescence, a C-ter fusion was tested.

Table 0.1. Protein fusions with eYFP at their N-ter.

Gene	Protein fusion	Plasmid name	Delivered by	Strain name
MG_217	eYFP - MG217	pMTnCat_eYFP:MG217	transposition	P32mCh YFP217
MG_218	eYFP - HMW2	pMTnCat_eYFP:MG218	transposition	P32mCh YFP218
MG_219	eYFP - MG219	pMTnCat_eYFP:MG219	transposition	P32mCh YFP219
MG_269	eYFP - MG269	pMTnCat_eYFP:MG269	transposition	P32mCh YFP269
MG_305	eYFP - DnaK	pMTnCat_eYFP:MG305	transposition	P32mCh YFP305
MG_312	eYFP - HMW1	pMTnCat_eYFP:MG312	transposition	P32mCh YFP312
MG_317	eYFP - HMW3	pMTnCat_eYFP:MG317	transposition	P32mCh YFP317
MG_491	eYFP -P41	pMTnCat_eYFP:MG491	transposition	P32mCh YFP491

Table 0.2. Protein fusions with eYFP at their C-ter.

Gene	Protein fusion	plasmid name	delivered by	strain name
MG_191	P140 - eYFP	pP140:eYFP	homologous recombination	P32mCh 191YFP
MG_192	P110 - eYFP	pP110:eYFP	homologous recombination	P32mCh 192YFP
MG_200	MG200 - eYFP	pMTnCat_MG200:eYFP	transposition	P32mCh 200YFP
MG_201	GrpE - eYFP	pMTnCat_MG201:eYFP	transposition	P32mCh 201YFP
MG_218	HMW2 - eYFP	pMTnCat_MG218:eYFP	transposition	P32mCh 218YFP
MG_239	Lon - eYFP	pMTnCat_MG239:eYFP	transposition	P32mCh 239YFP
MG_318	P32 - eYFP	pMTnCat_MG318:eYFP	transposition	P32mCh 318YFP
MG_386	MG386 - eYFP	pMTnCat_MG386:eYFP	transposition	P32mCh 386YFP

Since the MG_191 and MG_192 proteins form the nap complex in *M. genitalium* and are reciprocally stabilized (Scheffer et al., 2017, Burgos et al., 2006)the strategy was changed and the eYFP fusions were achieved by homologous recombination in order to maintain the protein levels required for the adhesion complex formation. In this case, each plasmid (see Appendix I: plasmid constructions, 89) contained two homology regions flanking the Asn_{10} linker, the eYFP gene and the *cat* gene. The left homology region (LHR) included 1 kb derived from the 3' end of the target gene (MG_191 or MG_192) excluding the stop codon, while the right homology region (RHR) included 1kb immediately downstream after the STOP codon. In this way, after a double cross recombination between the plasmid and the genome a C-ter fusion of the target protein with the eYFP separated with a Asn_{10} linker will be achieved (Figure 0.1).

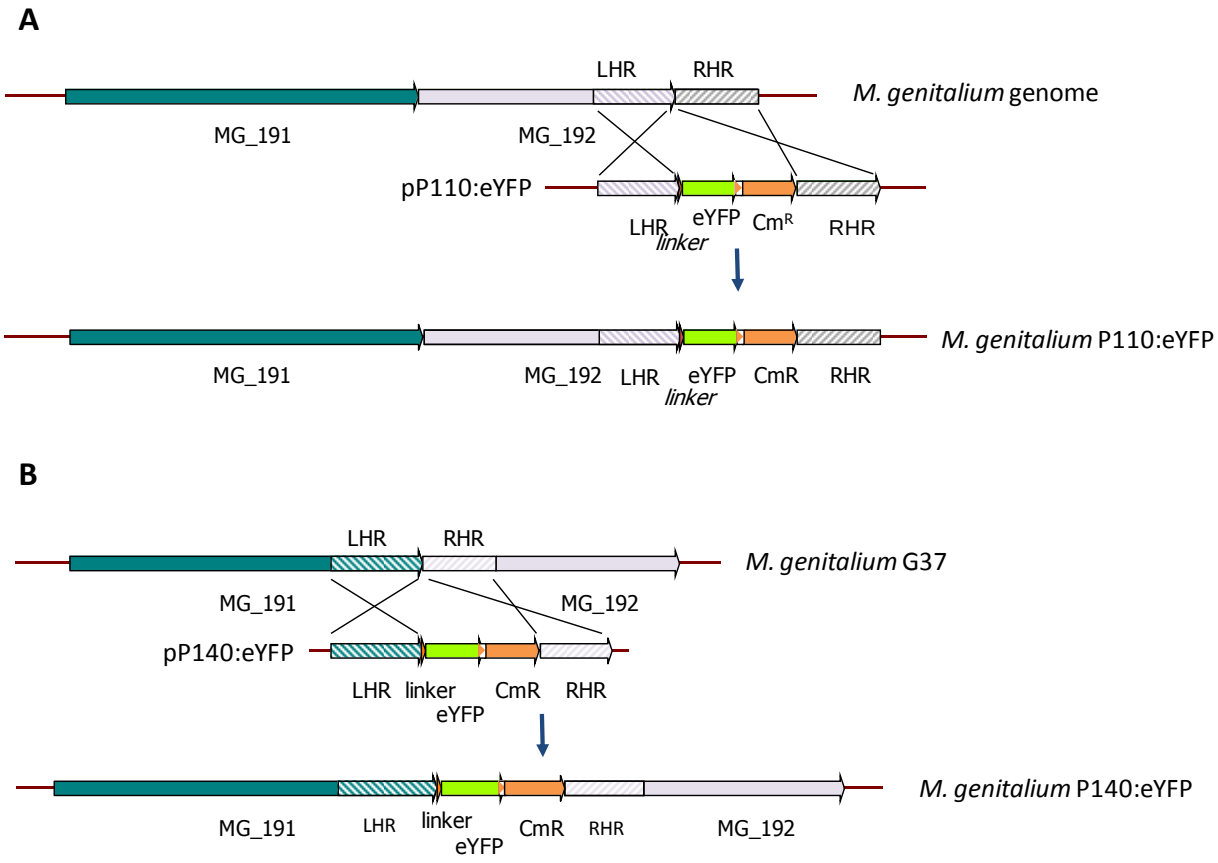

Figure 0.1. Homologous recombination scheme for MG_191 (A) and MG_192 (B) genes.

Chapter I: *Mycoplasma genitalium* terminal organelle proteins localized by eYFP tagging in a P32-mCherry background

In order to localize the different YFP-tagged proteins we have used the strain P32mCh (Garcia-Morales et al., 2016). This strain bears an extra copy of the P32 protein fused with the mCherry at its C-ter extreme. Since P32 protein has been localized in the terminal organelle (TO) we wanted to use it as a reference point comparing the position of the target proteins with P32 position (see point 4.2.2). Therefore, all plasmid constructions bearing the different protein fusions listed in Table 0.1 and

Table 0.2 were transformed in P32mCh strain.

Five independent clones of each transformation by transposition were recovered and their genomic DNAs were extracted. Clones that presented a non-adherent or semi-adherent phenotype (analyzed in the growing pattern at the cell-culture flasks) were discarded since this phenotype indicates an alteration of the proper cytoskeleton function. After Sanger sequencing of the insertion points, one clone of each transformation was selected for further analysis by fluorescence microscopy. The insertion points of each selected clone are detailed in Appendix III: Transposon localization of the selected clones bearing the different eYFP fusions, page 103. The criterion for selecting the clones with a less conflictive insertion point was performed following the subsequent directives:

(i) The insertion point is in a non-coding region
(ii) The insertion point is in a gene coding for a protein which is not expected to have any impact in cytoskeleton formation and structure.

The eYFP fusions with the main adhesins P110 and P140 were analyzed by PCR in order to determine that the fusion between the target protein and the eYFP by homologous recombination was achieved (Figure 0.2). A 1540 bp band is expected for the MG_191:eYFP fusion while a 2063 bp band is expected for the MG_192:eYFP fusion (Figure 0.2A). In both cases, one of the primers used in the PCR is annealing upstream of the LHR to confirm that the genetic fusion is correctly performed and enclosed the hole gene (Figure 0.2B). The clones P32mCh P140YFP c2 and P32mCh P110YFP c1 were selected for further analysis.

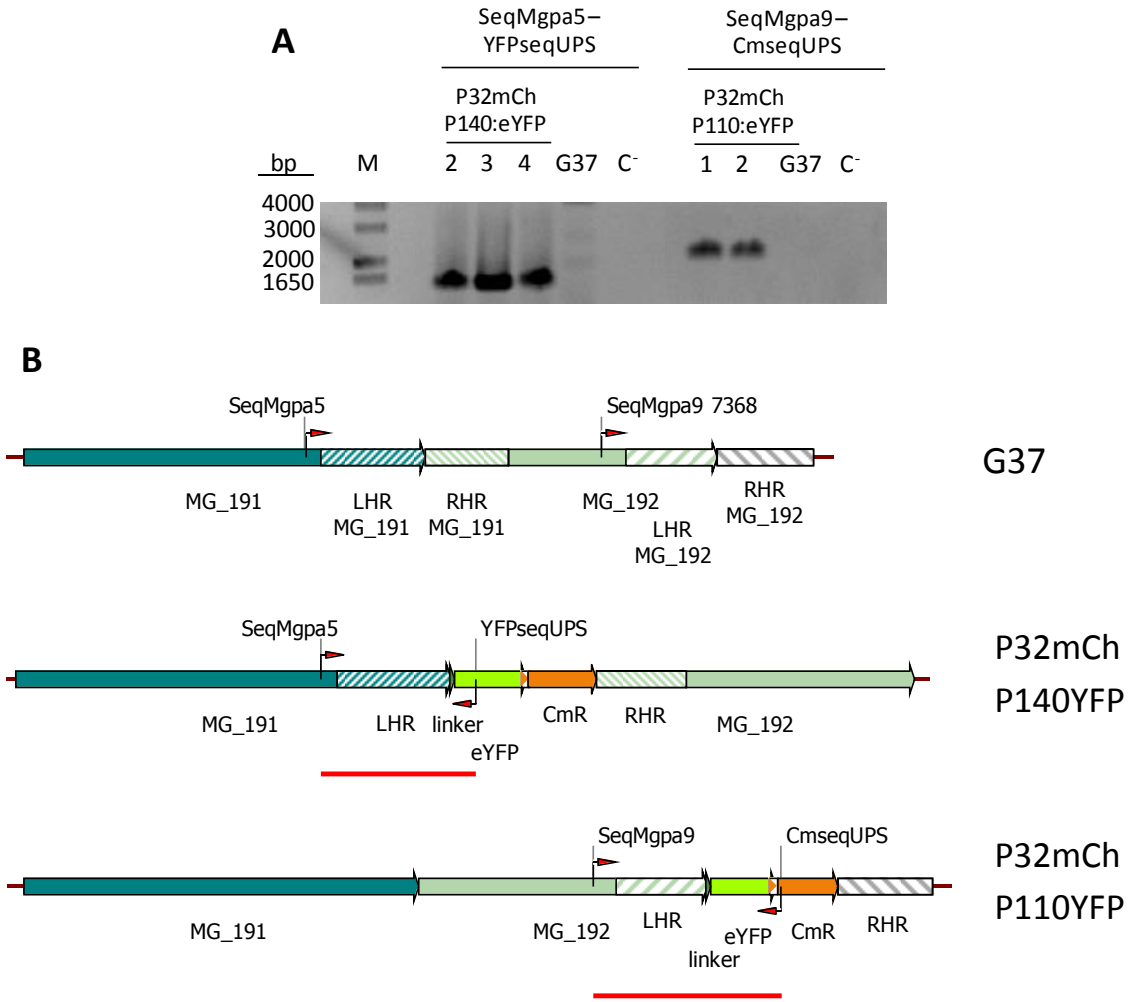

Figure 0.2. Confirmation of MG_191 and MG_192 fusions with eYFP. A. PCR amplification of the gDNA from the recovered clones using the primers SeqMgpa5 and YFPseqUPS for the MG_191:eYFP fusion and the primers SeqMgpa9 and CmseqUPS for the MG_192:eYFP fusion. gDNA from G37 strain was used as a negative control and also a negative control using mQ water as a template (C^-) was performed. **B.** Genetic scheme of the intended fusions in the different strains and the primers used for the PCR. The red line indicates the expected PCR band amplification (1540 bp for the P32mCh P140YFP strain and 2063 bp for the P32mCh P110YFP strain).

4.2.2 Localization of the different terminal organelle proteins by epifluorescence microscopy analysis

In order to determine the localization of the different proteins fused with the eYFP in a P32:mCherry background we used a epifluorescence microscopy approach. Cells from the different strains listed in Table 0.1 and

Table 0.2 were grown in SP4 medium in Mattek plates overnight. Different fixation protocols were tested in order to avoid complete cell lysis and cell autofluorescence due to the fixation treatment. The final fixation protocol with glutaraldehyde, DNA staining with Hoechst and image acquisition protocol are detailed in Materials and Methods, page 87. TetraSpeck microspheres (Sigma) were used for aligning the different fluorescent images acquired using a custom script in Matlab program (Michael Kunz, unpublished).

For each selected mutant, a minimum of 7 images containing between 40 and 350 cells were acquired. All the proteins localized in the terminal organelle shown a eYFP fluorescence polarized respect to the DNA (Figure 0.3). Comparing the eYFP position with the P32 protein marked with mCherry, the target proteins were assigned to the following substructures of the terminal organelle (an example of each localization assignation is shown in Figure 0.3):

(i) **Terminal button:** proteins assigned to this structure shown a eYFP fluorescence in the most apical region of the terminal organelle and the mCherry fluorescence behind the eYFP (Figure 0.3A). The proteins that have been localized in this position are MG217 and HMW3.

(ii) **Segmented paired plates:** the proteins that have been localized in this position are GrpE, HMW2, HMW1 and P32. The fluorescence images of the strains bearing this proteins fused with the eYFP shown an overlap in the fluorescence emitted by the eYFP and the mCherry (Figure 0.3B). As it was expected, the eYFP and mCherry fluorescence exhibited by the cells from the P32mCh 318YFP strain overlaped perfectly, suggesting there were not any difference

between the P32 fusion either with the eYFP or mCherry. The HMW2 was fused with the eYFP at its N-ter and C-ter regions. However, the images taken from the cells of these two strains (P32mCh YFP218 and P32mCh 218YFP respectively) apparently did not show any dramatic difference in the position of the HMW2 protein.

(iii) **Wheel complex:** proteins assigned to this structure shown eYFP fluorescence still polarized respect the stained DNA but behind the mCherry fluorescence (Figure 0.3C). The proteins that have been localized in this position are Lon, DnaK, MG219, MG386, MG200, MG269 and P41. The eYFP fluorescence in the strain P32mCh YFP491 (bearing the P41 fused to the eYFP) was partially overlapping with the mCherry fluorescence although its epicenter was found a little bit displaced. For this reason this protein was assigned to the wheel complex.

(iv) **Along all terminal organelle:** the proteins that have been localized in this position are P110 and P140. The eYFP fluorescence emitted by these fusion proteins included all the terminal organelle region showing a continuous fluorescence from the region before the P32 marker (terminal button) to the region behind the P32 (wheel complex). In these images the mCherry fluorescence corresponding to the P32 proteins was enclosed into eYFP fluorescence (Figure 0.3E).

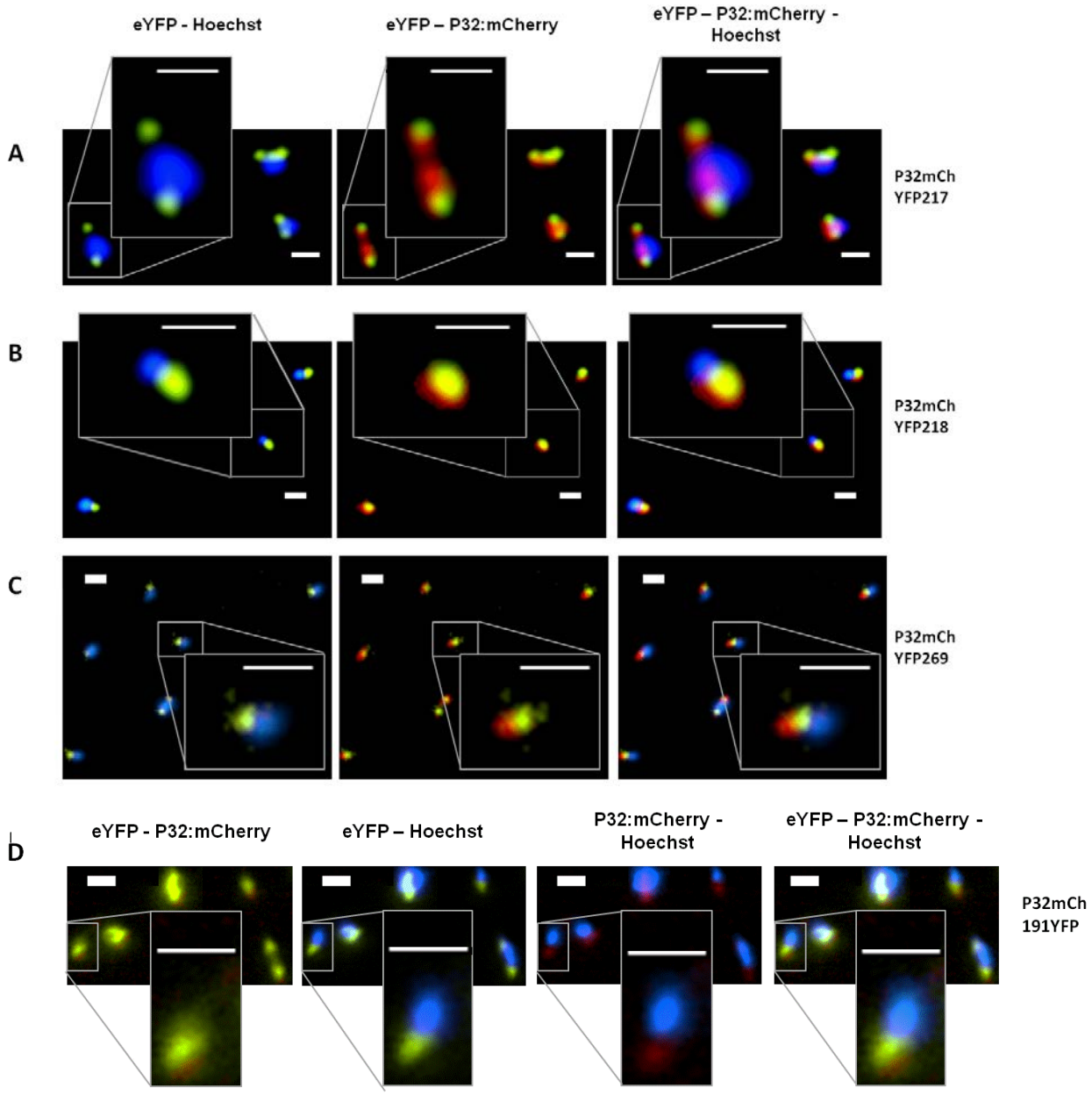

Figure 0.3. Epifluorescence images of cells from P32mCh YFP217 (A), P32mCh YFP218 (B), P32mCh YFP269 (C) and P32mCh191YFP (D) strains. The images for the different fluorescent channels (yellow for the eYFP fused with the target protein, red for the mCherry fused with the P32 protein and blue for the DNA stained with Hoechst) were merged as it is detailed in each column.

4.2.3 Localization of terminal organelle proteins quantitatively

The images acquired as explained in point 4.2.2 were analyzed to determine the distance between the three fluorescent foci: the target protein fused with the eYFP (in yellow), the P32 protein fused with mCherry (in red) and the DNA stained with Hoechst (in blue). Two different scripts based in Matlab (Michael Kunz, unpublished) were used to:

(i) Identify all the fluorescent focis in the three fluorescent images
(ii) Determine the three different fluorescent focis that belongs to each individual cell.
(iii) Determine the distance between the three focis: distance DNA-eYFP, DNA-P32, and P32-eYFP.

Aggregated cells, cells in division process and lysed cells were manually removed from the taken images in order to avoid problems with the software used. A minimum of 200 different cells for each strain were analyzed to determine the distances.

First of all, the distance between the P32 protein (marked with mCherry protein) and DNA (stained with Hoechst) was calculated in all the different strains generated in this work. The distance between the eYFP and the DNA in the mutant P32mCh 318YFP was also included in this analysis, since it was equivalent to the distance between the P32 protein (in this case fused with the eYFP) and the DNA. The mean of the calculated distance along the different mutants is 230 nm with a 3.3 nm standard error (SE). No significant statistical differences were observed among the distance between the different mutants (see Appendix IV: Statistical analysis of fluorescence distances, Distance between P32 protein and DNA, page 105).

Then, the distance between the DNA and the target protein marked with the eYFP was calculated following the same procedure. After statistical analyses of the calculated distances, the different proteins were assigned to different groups in function of their distance to DNA (Figure 0.4). The first group was formed by the proteins DnaK and MG219 (strains P32mCh YFP305 and P32mCh YFP219 respectively) which were localized in the most proximal part of the terminal organelle. The second group was

composed by the proteins MG239 and MG386 (strains P32mCh YFP239 and P32mCh 386YFP respectively). The third group comprised the proteins MG200 and MG269 (strains P32mCh 200YFP and P32mCh YFP269). All the proteins assigned from the first to the third groups shown a eYFP fluorescence between the DNA signal and the mCherry fluorescence. The fourth group comprised the proteins P140, P110, P41, MG201 and the HWM2 fused with eYFP at its C-ter extreme (strains P32mCh 191YFP, P32mCh 192YFP, P32mCh YFP491, P32mCh 201YFP and P32mCh 218YFP respectively). The fifth and sixth groups contained only one protein each: HMW1 and P32 respectively (strains P32mCh YFP312 and P32mCh 318YFP respectively) and shown a eYFP fluorescence that partially or totally overlapped with the mCherry fluorescence (corresponding to P32 protein). The last group contained the proteins in the most distal part of the terminal organelle: MG217, HMW2 fused with eYFP at its N-ter domain and HMW3 (strains P32mCh YFP217, P32mCh YFP218 and P32mCh YFP317.

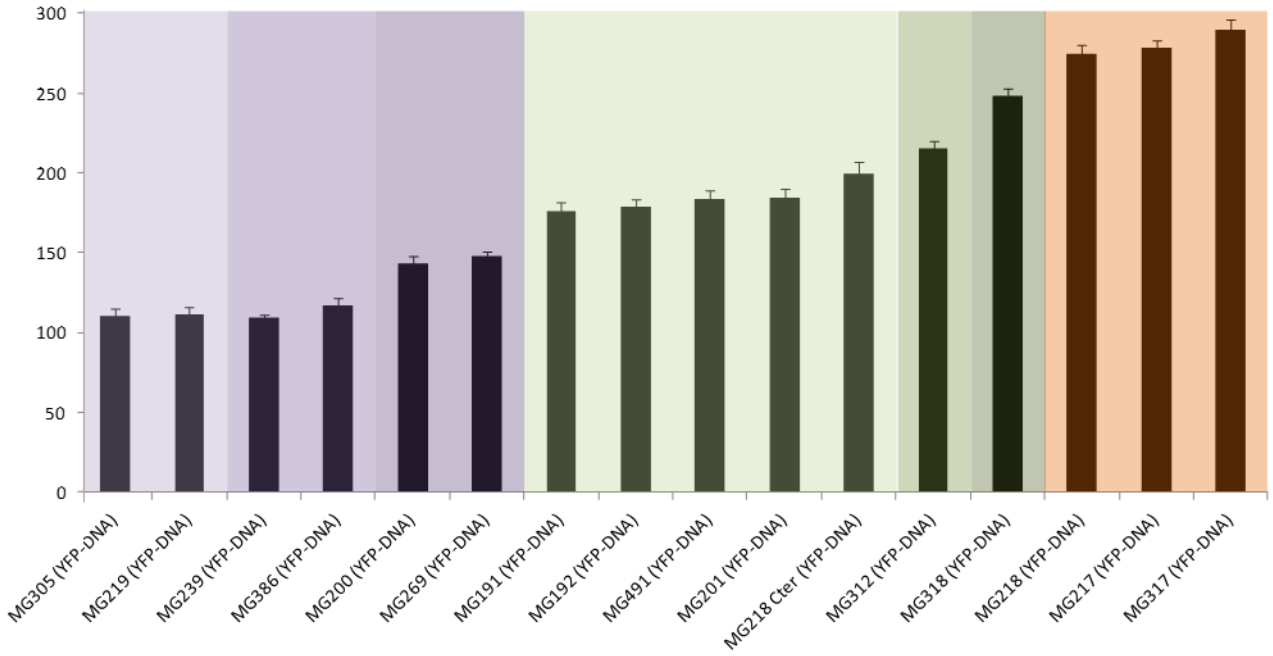

Figure 0.4. Measured distance between the eYFP (fused to the target protein) and stained DNA in the different strains. The mean of the distance between eYFP and DNA is plotted for each strain with its SE. In the x axis is represented each strain indicating the protein fused with the eYFP (MGXXX) and the distance calculated in brakets i.e. YFP-DNA. A Kruskal-Wallis test was performed and the homogenous subsets are represented in different colours (p-value < 0.05).

4.3 Discussion

Although multiple studies of cytadherence and motility proteins have been performed in *M. genitalium* (Burgos et al., 2006, Burgos et al., 2008, Burgos et al., 2007, Calisto et al., 2012, Garcia-Morales et al., 2016, Martinelli et al., 2015, Pich et al., 2008, Pich et al., 2006a, Pich et al., 2009), only MG217 and P32 have been previously localized (Burgos et al., 2008),(Garcia-Morales et al., 2016). In this work, a total of 13 proteins of *M. genitalium* have been localized by epifluorescence microscopy in the terminal organelle for the first time: MG200, MG219, MG269, MG386, DnaK, GrpE, Lon, HMW1, HMW2, HMW3, P41, P110 and P140.

Taking into account the previous studies of the terminal organelle, the fluorescence images analyzed qualitatively (Figure 0.3) and measuring the distance of the target protein to the DNA (Figure 0.4), the proteins can be assigned to the different structures of the terminal organelle (Figure 0.5, page 38).

The proteins P110 and P140 fused to the eYFP showed a fluorescence along all the terminal organelle (Figure 0.3E), as it has been described for their *M. pneumoniae* homologue proteins P1, P40 and P90 (Hahn et al., 1998, Seto et al., 2001, Seto and Miyata, 2003) (Table 0.3). This fluorescence distribution also correlates with their position along all the membrane surrounding the *M. genitalium* terminal organelle (Scheffer et al., 2017) as it can be seen in Figure 0.5. The measured distance for these two proteins (Figure 0.4) situates them in the middle of the terminal organelle although they are surrounding all the terminal organelle. However, this can be explained if we consider that the program gives the distance between the centers of the two foci.

Table 0.3. Equivalences between genes and proteins of *M. genitalium* and their homologues in *M. pneumoniae*. TO stands for terminal organelle, W for wheel complex, SPP for segmented paired plates, TB for terminal button, IF for inmunofluorescence and FM for epifluorescence microscopy.

M.genitalium			***M. pneumoniae***		
Gene	**Protein**	**Localization**	**Gene**	**Protein**	**Localization**
MG_191	P140	All TO	MPN_141	P1	Nap
MG_192	P110	All TO	MPN_142	P40, P90	Nap
MG_200	MG200	W	MPN_119	TopJ	W
MG_201	GrpE	SPP	MPN_120	GrpE	-
MG_217	MG217	TB	MPN_309	P65	TB
MG_218	HMW2	SPP	MPN_310	HMW2	SPP
MG_219	MG219	W	MPN_312	P24	W
MG_239	Lon	W	MPN_332	Lon	W
MG_269	MG269	W	MPN_387	MPN387	W
MG_301	GAPDH	CB	MPN_330	GAPDH	-
MG_305	DnaK	W	MPN_434	DnaK	-
MG_312	HMW1	SPP	MPN_447	HMW1	SPP
MG_317	HMW3	TB	MPN_452	HMW3	TB
MG_318	P32	TB	MPN_453	P30	TB, surface
MG_386	MG386	W	MPN_567	P200	W
MG_491	P41	W/SPP	MPN_311	P41	W

The proteins P32, MG217 and HMW3 are localized in the terminal button, the most apical region of the terminal organelle. Statistical analysis of the distance between the eYPF and the DNA grouped the MG217 and HMW3 at the most apical part and the P32 closer to the DNA (Figure 0.4). However, it must be stated that the proteins MG217 and HMW3 present the eYFP fused at its N-ter domain while the P32 has the eYFP at its C-ter domain so the difference observed can be due to the eYFP fusion instead of a real different positioning. This is also supported by the fact that the P32 seems to be anchoring the TO

cytoskeleton to the membrane (Gonzalez-Gonzalez, 2015) and the transmembrane region is found at its N-ter domain, suggesting that the P32 N-ter domain can be anchored to the membrane while the eYFP at its C-ter domain used for the localization is behind it, giving a larger distance. *M. pneumoniae* homologues of these three proteins (Table 0.3) were previously localized in the attachment organelle (Seto and Miyata, 2003) (Seto et al., 2001) (Kenri et al., 2004) and further studies have localized them more precisely in the terminal button (Nakane et al., 2015). In contrast to P32 intern localization by membrane shaving (Garcia-Morales, L. and González-González L., manuscript in preparation), P30 is located on the surface of the front end and is supposed to be exposed in the membrane (Nakane et al., 2015).

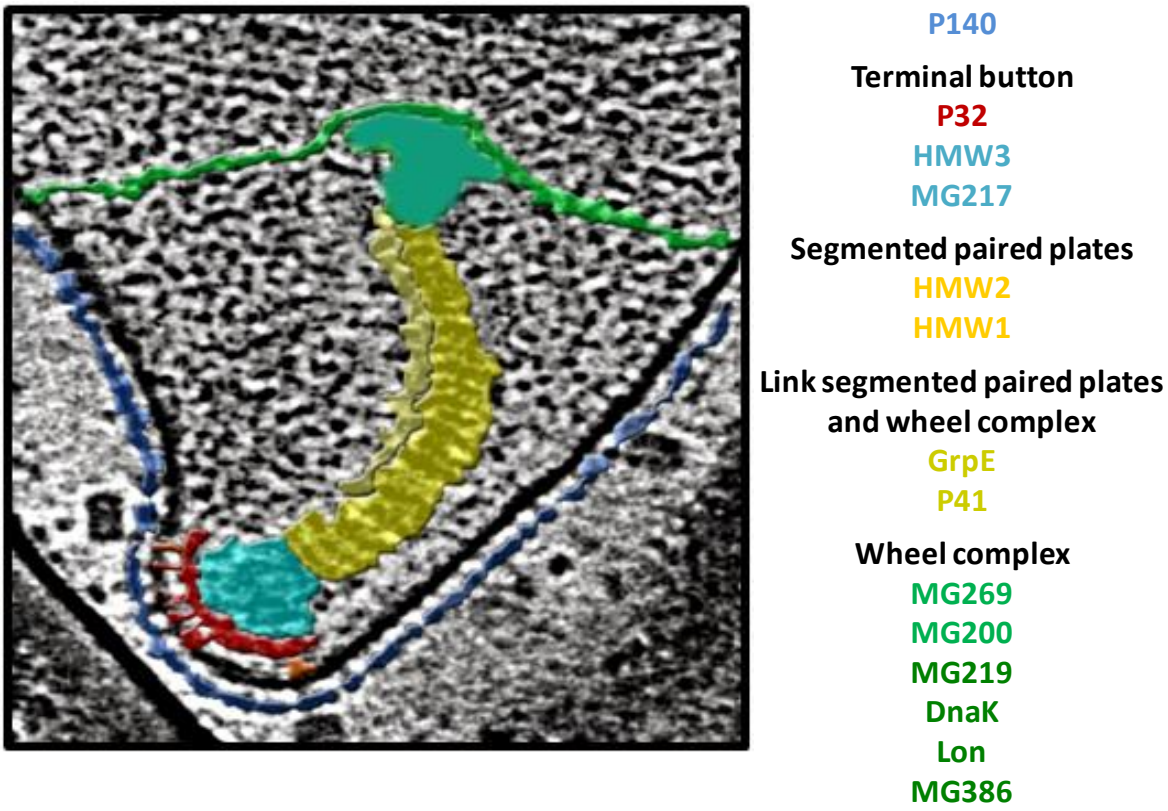

Figure 0.5. Schematic representation of the proteins localized in the terminal organelle of *M. genitalium*. Cryoelectron micrograph of the TO from G37 cells adapted from (Gonzalez-Gonzalez, 2015). The nap is shown in dark blue, the most apical region of the terminal button anchoring the TO to the membrane is shown in red, the terminal button is shown in light blue, the segmented paired plates are shown in yellow and the wheel complex is shown in green: light green for the wheel complex and dark green for the most proximal part of the wheel complex delimiting the electron-lucent area.

HMW1 and HMW2 proteins are localized in the segmented paired plates. The protein HWM2 has been fused with the eYFP at its C-ter and N-ter. Although qualitative analyses of the fluorescence images from these two strains did not show appreciable differences, the measurement of the distance between the eYFP and the DNA in these two strains is statistically significant different (Figure 0.4). This suggests that the N-ter domain of the HMW2 is placed in near to the terminal button while the C-ter domain is placed near to the wheel complex. This result is in agreement with the previous study performed in *M. pneumoniae* where the HMW2 shown a different localization depending of placement of the fluorescent protein fusion (Nakane et al., 2015). These two proteins, involved in cell adhesion and morphology (Burgos et al., 2007, Dhandayuthapani et al., 1999, Pich et al., 2008), are predicted to be a coiled coil proteins, which is in agreement with the hypothesis that they are organized as structured fibrils forming the segmented paired plates (Miyata, 2010).

The proteins GrpE and P41 are found after the HWM2 and HMW1. According to the measured distance between the eYFP fused to the target protein and the stained DNA (Figure 0.4) we can localize them between the segmented paired plates and the wheel complex. The role of P41 in gliding motility (the rod seems to be not directly essential for the movement) and their function anchoring the TO to the cell body (Garcia-Morales et al., 2016) suggests that it can be positioned in the most apical part of the wheel complex helping to transmit the force generated in the movement to the nap complex. Its *M. pneumoniae* homologue protein, although having a slight different function, has also been localized in the wheel complex (Nakane et al., 2015). The GrpE has been localized in the terminal organelle for the first time in the *mycoplasma* genus. This protein acts as a nucleotide exchange factor to promote the ADP dissociation from the nucleotide-binding cleft of DnaK protein, helping in this way to the folding pathway of the chaperones system DnaJ/DnaK/GrpE (Wu et al., 2012, Harrison, 2003, Grimshaw et al., 2001).

The proteins MG269, MG200, MG219, DnaK, Lon and MG386 are localized in the wheel complex (Figure 0.5). The proteins MG269 and MG200 are further positioned respect to the DNA than the proteins MG219, DnaK, Lon and MG386 that are in the most proximal

part of the wheel complex (Figure 0.4). Although statistical analyses of the measured DNA-eYFP distance (Figure 0.4) grouped the proteins DnaK and MG219 in one group, and Lon and MG386 in a different group, we cannot conclude that these differences are biologically relevant since the measured distances are quite similar and the statistic difference could rely on the distribution. Moreover, no other experimental studies are available to support this idea, so more experimental data will be needed to support it. As for the GrpE, this is the first time that DnaK has been localized in the terminal organelle of the genus *Mycoplasma*. The other *M. pneumoniae* homolog proteins MPN387, TopJ, P24 and P200 (Table 0.3) have been previously studied and linked to the terminal organelle (Jordan et al., 2007, Miyata, 2008, Kenri et al., 2004, Hasselbring and Krause, 2007b, Hasselbring and Krause, 2007a, Cloward and Krause, 2009, Hasselbring et al., 2006a) and more recently their position has been assigned to the wheel complex with the Lon protease (Nakane et al., 2015).

The proteins MG219, MG269 and MG386 play a role in gliding motility but they are not involved in cell adhesion (Gonzalez-Gonzalez, 2015), Lluc-Senar M., unpublished, (Pich et al., 2006a). Their *M. pneumoniae* homolog proteins have similar functions (Jordan et al., 2007, Hasselbring et al., 2006a) except for the P24, which even being involved in the gliding motility has different mechanistic roles (Hasselbring and Krause, 2007b, Gonzalez-Gonzalez, 2015). MG200 protein was previously related only to gliding motility (Pich et al., 2006a), but further studies has demonstrated that it is very similar to its homolog protein TopJ (Cloward and Krause, 2010, Cloward and Krause, 2011). MG200 presents a functional DnaJ domain at its N-ter domain which is essential for P110 and P140 stability. Therefore, this protein has a dual role: its C-ter domain is involved in gliding motility while its N-ter domain containing the DnaJ is indirectly involved in cell adhesion by stabilizing the main adhesins (Broto, 2014). Apart from proteins related to cell motility we can also found the Lon protease in this structure. It has been described for *Mesoplasma florum*, a *mycoplasma* specie, that the Lon protease is effectively degrading unfolded proteins (Gur and Sauer, 2008). Its position in the TO of *M. genitalium* suggests an important requirement of a protein quality control to ensure that the proteins conforming the TO are properly folded (or if not they are degraded) and can maintain their

functionality being a piece of a perfect machinery that allows the cell adhesion and motility.

Quantitative measurement of the distance between the eYFP fused tot the target protein and the DNA as a reference points gives a powerful tool to determine more precisely the protein localization in comparison to the qualitative method using the P32 marked with the mCherry as a reference point. However, all the data should be analyzed carefully and more than one method needs to be combined to contrast the information and avoid false localizations biased by the eYFP tagging. Therefore, taking all these data together, we can conclude the order of the different proteins studied in this work. The proteins DnaK, MG219, Lon and MG386 are found in the most proximal part of the terminal organelle. MG200 and MG269 are found after this set of proteins. After these two proteins we can find the proteins P41 and GrpE that can act as a link between the wheel complex and the segmented paired plates. The segmented paired plates comprise the proteins HMW1 and HMW2. After these two proteins we can found the proteins P32, MG217 and HMW3 in the terminal button, the most apical structure of the terminal organelle.

Four of the five genes overexpressed in heat shock response (Musatovova et al., 2006) have been localized in the terminal organelle: MG200, DnaK and Lon protease were found in the wheel complex and GrpE in the most apical part of this structure while the ClpB protein was localized in the cellular body (data not shown). The presence of the proteins DnaK, MG200 (which has a functional DnaJ domain) and GrpE in the terminal organelle is in agreement with the necessity of molecular chaperones to help the correct protein folding of the TO proteins. Most of the proteins conforming the TO are membrane proteins, present hydrophobic regions and high molecular weights (Parraga-Nino et al., 2012), so their folding could be addressed by this chaperone system (Schroder et al., 1993). However, it must be said that it is not a unique localization: the emitted fluorescence is directly proportional to the amount of protein so other molecules can be found in other cellular positions. Therefore, although it may seem that these proteins can be found in different positions (Figure 0.4), it does not exclude the possible interactions between them as it has been demonstrated in other organisms (Wu et al., 2012, Harrison et

al., 1997) (Grimshaw et al., 2001, Groemping et al., 2001). Moreover, the proteins DnaK and GrpE, in addition to their function as molecular chaperones, can be also playing a role in the gliding motility, since other studies have shown that can be involved in the motility processes such as being required for the flagellum formation (Shi et al., 1992). This hypothesis is also supported by the example of the protein MG200. This protein, apart from presenting a DnaJ domain which is involved in the P110 and P140 stability (Broto, 2014) is also gliding determinant (Pich et al., 2006a).

This study reinforces the current knowledge of terminal organelle composition and the localization of its main components in the different substructures. Interestingly, this important structure also contains proteins to help the proper folding (such as DnaK, GrpE and MG200 with a functional DnaJ domain) and the Lon protease to control the protein life and degrade the unfolded proteins. The precise localization of the different proteins involved in the adhesion and gliding supposes a small step to the understanding of this complex machinery that produces the adhesion and movement of this small microorganism.

5. Chapter II: All-in-one construct for genome engineering using Cre-lox technology in *Mycoplasma genitalium*

5.1 Introduction

Site specific recombination systems such as those based in Cre/lox from bacteriophage P1 (Sternberg et al., 1981, Sternberg and Hamilton, 1981), Xis/att from bacteriophage λ (Nash, 1977) or FLP/FRT from Sacharomyces cerivisiae (Broach et al., 1982) have been widely used for genome engineering in microorganisms, complex eukaryotic cells and mammals (Nagy, 2000, Yu and Bradley, 2001, Garcia-Otin and Guillou, 2006, Turan et al., 2011). In a first step, the modification including the recombinogenic sequences is introduced in the genome. In second transformation or transfection step, a recombinase coded in a suicide plasmid, a curable plasmid or any other delivery vector catalyzes a recombination between two site-specific recognition sites, thus generating the desired DNA integration, excision or inversion. It is also possible to have the recombinase as a transgene in the genome of the organism of study and introduce the recombinase by genetic crossing. However, this approach has to deal with the recombinase off-site effects and toxicity which have been broadly described (Loonstra et al., 2001, Huh et al., 2010, Schmidt et al., 2000). Among the different site specific recombination systems, the Cre-lox shows a remarkable plasticity. Cre recombinase recognizes multiple loxP sites (Sternberg et al., 1981, Sternberg and Hamilton, 1981) allowing the design of variant sites such as lox66, lox2272, lox71, loxN, loxLE or loxRE (Albert et al., 1995, Lee and Saito, 1998, Gueldener et al., 2002, Langer et al., 2002, Livet et al., 2007). All these variant lox sites have been tested for compatibility and recombination efficiency.

Many genetic tools well established for other microorganisms are not available in mycoplasmas (Halbedel and Stulke, 2007). Furthermore, most of the tools available, such as transposons, mini-transposons, replicative plasmids and suicide vectors for gene

replacement rely on the incorporation of selective markers. These markers may interfere with the cell metabolism and their use is a limiting factor for genome engineering given the low number of selection markers available. To circumvent these problems, we were aimed to implement the Cre-lox technology in *M. genitalium* by two different approaches. First, we used a suicide vector bearing Cre recombinase gene under the control of a constitutive promoter following similar procedures to those used in others organisms (Duret et al., 2005). Finally, we implemented a time-saving method based on TetR repressor by engineering the inducible Pxyl/$TetO_2$ promoter previously used in *Mycoplasma agalactie* (Breton et al., 2010). This modified promoter tightly controls the expression of the Cre recombinase gene, which allows the introduction of both the desired mutation and Cre recombinase in a single step.

5.2 Results

5.2.1 Stability of suicide vectors in M. genitalium

Since no replicative vectors are available in *M. genitalium*, we tested whether a suicide plasmid delivered by electroporation and bearing a gentamicin resistance gene marker could remain inside the cells for limited periods of time. To this end, the plasmid pGmRS was engineered (see Appendix I: plasmid constructions) and transformed into *M. genitalium* G37 WT cells. These cells were then incubated in the presence of gentamicin for 24, 48, 72, 96 and 168 hours and were finally plated in SP4-agar in the absence of antibiotic to quantify the number of viable cfus remaining after the gentamicin treatment. As a control G37 WT cells were electroporated without any plasmid and treated in the same way (Figure 5.1).

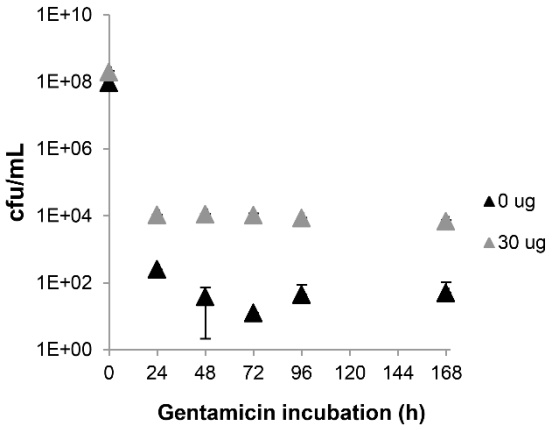

Figure 5.1. Persistence of a suicide vector inside M. genitalium cells. G37 strain was electroporated with 30 or 0 µg of pGmR (grey or black triangles respectively) and cells were incubated with gentamicin 100 µg · mL^{-1} for 24, 48, 72, 96 and 168 hours. Cells were then plated in SP4-agar medium and colonies were scored. Three independent repeats for each condition were performed and the mean with its standard error (SE) are plotted.

About 10^4 colonies were recovered from cells electroporated with pGmRS, with no appreciable differences between the different gentamicin incubation times tested. In contrast, only a few colonies were recovered from non-electroporated control cells. These results suggest that 10^4 cells incorporate the pGmRS plasmid when delivered by electroporation, gentamicin marker remains functional inside these cells at least for several days and gentamicin is killing most of the plasmid-free cells.

5.2.2 Evaluation of the Cre-Lox system

To evaluate the feasibility of Cre-lox system in *M. genitalium*, first a mutant strain including an antibiotic marker gene flanked by two lox66 sequences was designed. To this purpose we engineered the minitransposon pMTnTc66Cat66 which carries the tetracycline resistance gene and also the chloramphenicol acetyltransferase gene (*cat*), which was flanked by two lox66 sequences (see Appendix I: plasmid constructions). This minitransposon was transformed on *M. genitalium* cells and several recovered colonies were grown in liquid culture and their DNAs were extracted and analyzed by direct genome sequencing to confirm the presence of the minitransposon and to determine the

genomic insertion points. One of the clones recovered was named TcloxCm and selected for further studies. On the other hand, we also constructed the suicide plasmid pGmRSCre bearing the Cre recombinase gene under the control of MG_438 constitutive promoter (see Appendix I: plasmid constructions). This construct was expected to promote the expression of Cre recombinase once introduced to *M. genitalium* cells. Plasmid pMTnTc66Cat66 was designed to easily detect the *cat* cassette excision in TcloxCm mutants both by plating cells in a selective medium and by PCR amplification (Figure 5.2).

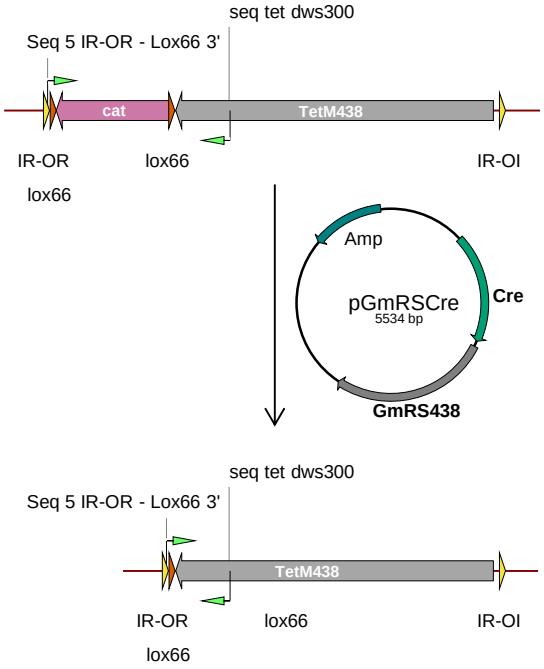

Figure 5.2. Suicide vector strategy scheme. Green arrows indicate the primers used for screening the cat gene presence or absence: Seq 5 IR-OR – Lox66 3' and seq tet dws300. cat indicates the chloramphenicol resistance gene under the control of MG_438 promoter, TetM438 indicates tetracycline resistance gene under the control of MG_438 promoter, IR-OR and IR-OI indicates the inverted repeats recognized by the transposase, lox66 indicates the lox66 sequences, Amp indicates the ampicillin resistance gene, Cre indicates the gene coding for the Cre recombinase, GmRS438 indicates the gentamycin resistance gene under the control of MG_438 promoter.

Encouraged by the apparent stability of suicide vectors inside *M. genitalium* cells, we transformed a TcloxCm mutant with and without the pGmRSCre plasmid and resulting cells were further incubated for 48, 72 and 168 hours in the presence of gentamicin (Figure 5.3). TcloxCm viable cells remaining after the different gentamicin incubation times were

also quantified, with results similar as those obtained when using pGmRS plasmid (Figure 5.2 and Figure 5.3).

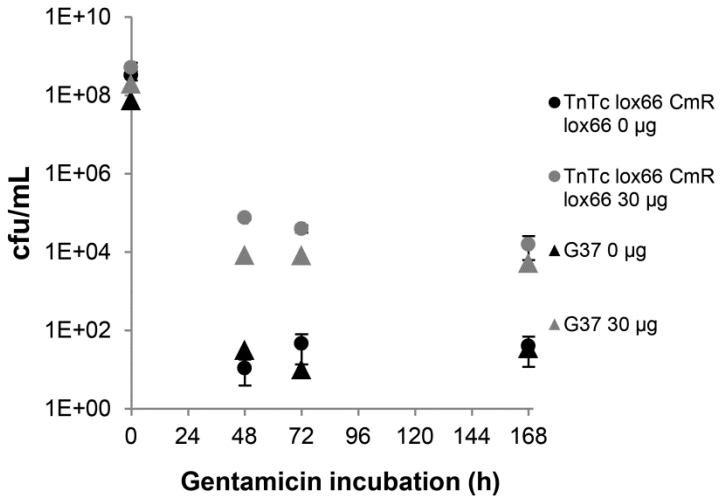

Figure 5.3. Persistence of pGmRSCre vector inside G37 and TcloxCm cells. G37 and TcloxCm strains were transformed with 30 or 0µg of pGmRCre (grey and black respectively) and cells were incubated in SP4 medium containing gentamicin 100 $\mu g \cdot mL^{-1}$ for 48, 72 and 168 hours. Cells were then plated in SP4-agar medium and colonies were scored. Three independent repeats and two technical replicates were performed for each strain and condition and the mean values with its standard error (SE) are plotted.

To assess the excision of cat cassette, five clones recovered from each experimental condition were checked by PCR. After 48 hours of gentamicin incubation, all recovered clones showed an 1118-bp PCR band consistent with the presence of the *cat* gene flanked by two lox66 sequences. Fortunately, after 72 and 168 hours of gentamicin incubation all recovered clones exhibited a single 246-bp PCR band consistent with the excision of *cat* cassette (Figure 5.4). These clones were able to grow in SP4 medium but no growth was observed when they were cultured in SP4 medium supplemented with chloramphenicol, confirming also the absence of *cat* gene. None of the few clones recovered from control TcloxCm cells electroporated in the absence of pGmRSCre plasmid and incubated with gentamicin showed the excision of the marker cassette (Figure 5.4).

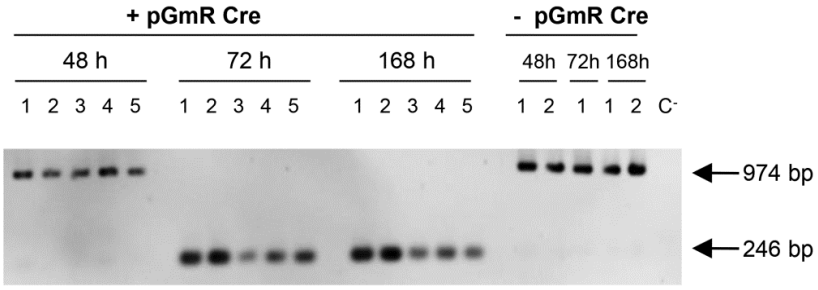

Figure 5.4. PCR screening for cat gene presence. Colonies from TcloxCm strain electroporated with or without pGmRSCre and incubated in SP4 medium containing gentamicin 100 µg·mL^{-1} for 48, 72 and 168 hours were recovered and expanded to isolate genomic DNAs. Genomic DNAs were amplified by PCR with the primers Seq_tet_DWS300 and Seq_5_IR-OR-Lox66_3. A 1118-bp PCR band is expected from genomic DNAs bearing the cat gene (1118 bp) and a 246-bp PCR band is expected in those genomes with a excision of this selectable marker.

All these results indicate that Cre recombinase expression directed by pGmRSCre plasmid has no noticeable toxic effects in *M. genitalium* cells and this enzyme efficiently excises sequences flanked by lox in this microorganism.

5.2.3 Cre expression under the control of an inducible promoter

Genome engineering in a minimal cell model like *M. genitalium* would be greatly benefited from the existence of working constructs bearing an inducible Cre recombinase gene by providing a simple way to genetically modify cells in a single transformation step. As proof of concept, we chose to obtain an unmarked deletion of MG_217 gene, which has been previously shown to be easily deleted by homologous gene replacement (Burgos et al., 2008). First we designed the plasmid pΔMG_217Cre (see Appendix I: plasmid constructions) containing a cassette including (a) the TetR repressor gene under the control of spiralin promoter (Breton et al., 2010), (b) the Cre recombinase gene under the control of a tailored version of the inducible Pxyl/TetO_2 promoter from pMT85-XTST (Breton et al., 2010) (named Pxyl/TetO_2mod) and (c) the *cat* gene as the selectable marker. Pxyl/tetO_2mod is the result of engineering the Pxyl/TetO_2 promoter to minimize the transcriptional leakage exhibited by this promoter simply by removing the sequence including the ribosome binding site at the 3' end of this DNA fragment (see Appendix V:

pXyl/TetO$_2$mod promoter). With this modification we expected a strong decrease in translation efficiency of Cre recombinase, greatly reducing the expression of this enzyme in the absence of inducer. This whole cassette, which was named Cre-cat cassette, was flanked by two lox66 sequences and enclosed by the same flanking regions previously used to obtain the MG_217 null mutant (Burgos et al., 2008). A double cross-over recombination event between plasmid pΔMG_217Cre and the *M. genitalium* genome is expected to promote the deletion from bases 60 to 980 of the MG_217 gene (82.2% of the coding region) and the replacement of this region by the cassette flanked by lox66 sequences (Figure 5.5A).

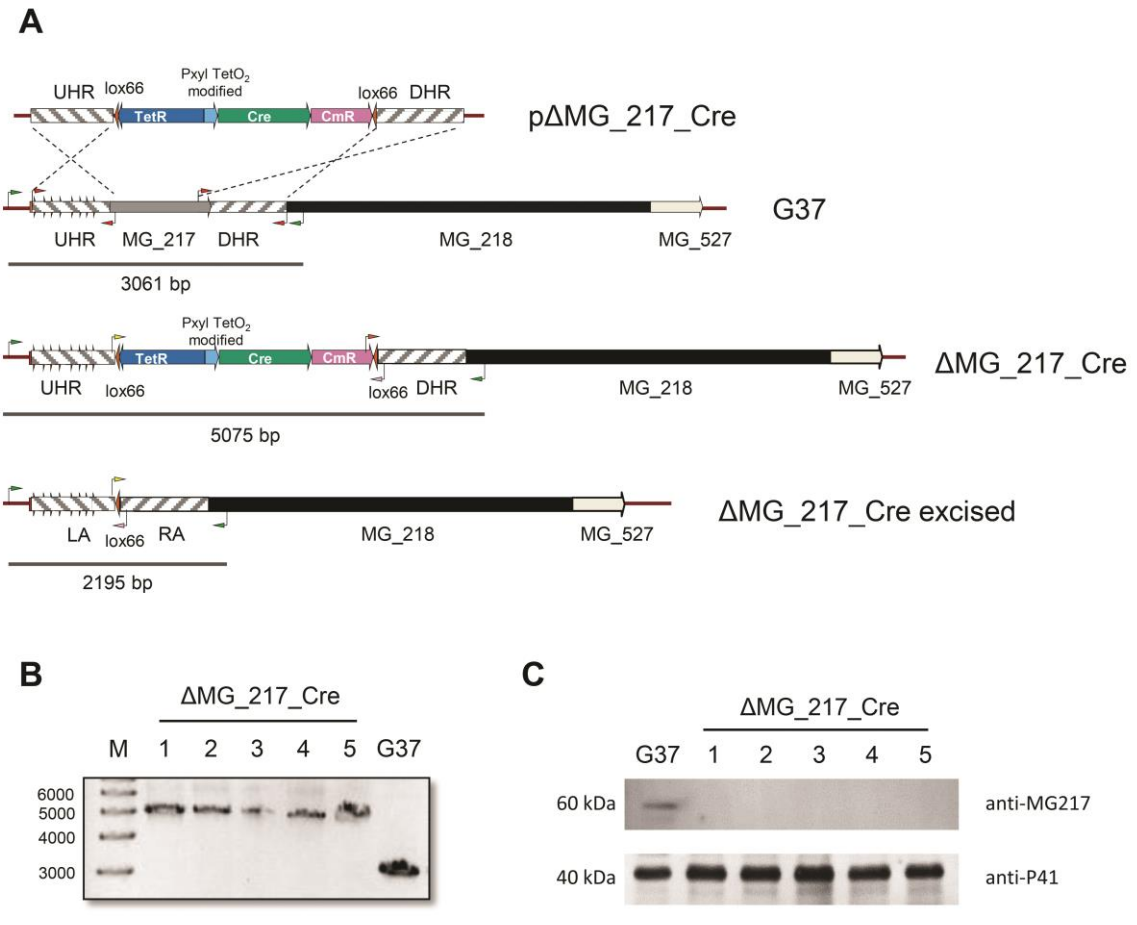

Figure 5.5. Obtaining ΔMG_217_Cre mutant. (A). Schematic representation of recombination events between the pΔMG_217Cre suicide vector and the MG_217 gene in G37 strain. PCR bands expected when using 5 screening D217 and 3 screening D217 primers to amplify G37, ΔMG_217_Cre and ΔMG_217_Cre genomic DNAs are also indicated. Primers are shown as colored arrows in each strain: green for 5 screening D217 and 3 screening D217 primers; yellow

for qPCR 217BE_DWS primer; orange for qPCR CmDWS primer; pink for qPCR 217BD_UPS primer and red for 5 XhoI SacI BE mg217, 3 SpeI AscI BE mg217, 5 ApaI BD mg217 and 3 BamHI NotI BD mg217 primers. **(B).** Genomic DNAs from G37 and ΔMG_217_Cre strains were amplified by PCR using 5 screening D217 and 3 screening D217 primers (green)**. C.** Western-Blot analyses of protein extracts from G37 and ΔMG_217_Cre strains. MG_217 protein was detected using a mouse anti-MG_217 polyclonal antibodies and a rabbit polyclonal antiserum anti-P41 was used as a loading control.

To obtain the ΔMG_217Cre strain, WT cells were electroporated with pΔMG_217Cre plasmid and transformant colonies were isolated on SP4 medium containing chloramphenicol. Several colonies were expanded and their genomic DNAs were analyzed by PCR to check the presence of the intended replacement. All clones recovered showed a 5075-bp band consistent with the deletion of MG_217 gene and its replacement by Cre-cat cassette (Figure 5.5B). To further confirm the deletion of MG_217 gene, a Western blot was performed using the mouse polyclonal anti-MG217 antibodies. A 60 kDa band corresponding to MG217 protein was detected in G37 wild type strain but it was not present in any of the recovered clones (Figure 5.5C).

Several independent clones of ΔMG_217_Cre strain were grown for 72 h at different tetracycline concentrations to induce Cre expression. These induced cultures were then plated in SP4 agar to quantify all viable cells and also in chloramphenicol-SP4 agar plates to quantify the viable cells still bearing the *cat* gene. In the presence of the lowest inductor concentration tested 70 % of cells could grow in the presence of chloramphenicol and only around a 10 % of cells incubated with the highest tetracycline concentrations were still found resistant to chloramphenicol (Figure 5.6A). The excision of the Cre-cat cassette was also quantified by qPCR (Figure 5.6B), obtaining similar results and indicating that more than 90% of the cell population excised this cassette when incubated with tetracycline at concentrations higher than 1 ng mL^{-1}. No statistically significant differences were found in the frequency of genomes with excised cassettes upon inducing Cre expression at 1, 10 or 100 ng mL^{-1} tetracycline (Figure 5.6).

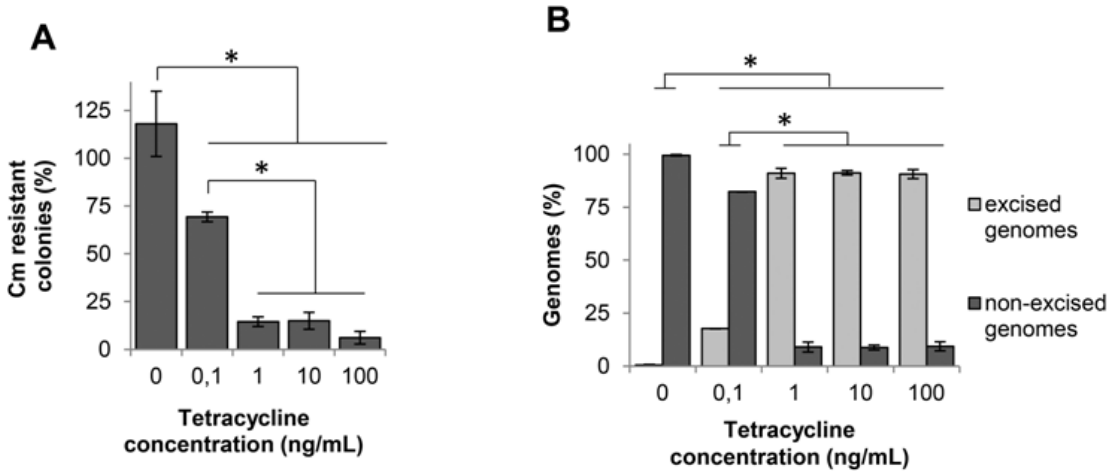

Figure 5.6. Cre recombinase expression tests. (A) Cell cultures containing several isolates of ΔMG_217Cre strain were grown with 0, 0,1, 1, 10 or 100 ng/mL tetracycline for 72 h and plated in SP4 agar plates and in SP4 agar plates supplemented with 34 µg/mL chloramphenicol. For each condition 3 independent biological replicates and 4 technical repeats were performed. The frequency of chloramphenicol resistant cfus was plotted for each condition with standard error bars. By a * symbol are indicated statistical significant differences with a p-value < 0.05. **(B)** Genomic DNAs from cell cultures in panel A were analyzed by qPCR to quantify the Cre-cat cassette excision using primers qPCR CmDWS – qPCR 217BD_UPS and qPCR 217BE_DWS - qPCR 217BD_UPS. The frequency of the three biological repeats is plotted with its respective standard error bars. By a * symbol are indicated statistical significant differences with a p-value < 0.05.

The presence of genomes with excised cassettes was finally checked by PCR in five isolated clones recovered after incubating with 10 ng mL^{-1} tetracycline for 72 h the clone ΔMG_217_Cre_c1. These clones showed a 2195-bp PCR band consistent with the excision of Cre-cat cassette (Figure 5.7). We also determined the sequence of the excised cassettes by direct Sanger sequencing of genomic DNAs from these clones. Sequence analyses demonstrated that all the clones analyzed have the same DNA sequence inside the excised cassettes (data not shown). All these data taken together indicate that Cre expression is efficiently induced in the presence of tetracycline and the amounts of recombinase produced are enough to precisely excise DNA regions flanked by lox66 sequences.

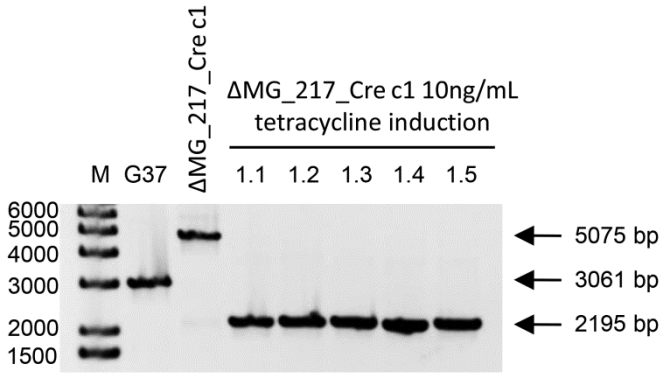

Figure 5.7. Cre-cat cassette excision detected by PCR. ΔMG_217_Cre_c1 mutant was grown in SP4 medium containing 10 ng mL-1 tetracycline for 72 h and cells were plated in SP4-agar medium. Five colonies were recovered and expanded to isolate their genomic DNAs. Cre-cat cassette excision was inspected by PCR using primers 5 screening D217 and 3 screening D217. Outline and expected bands are shown in Figure 5.5A.

5.2.4 Stability of lox66 cassettes in long term uninduced cultures

Some applications using the Cre-lox technology may require a strict control on Cre recombinase expression. To obtain quantitative data about the transcriptional leakage of Pxyl/TetO_2mod promoter in ΔMG_217Cre strain, the stability of Cre-cat cassette in this strain was tested after one, six and eleven serial culture passages in the absence of inducer and chloramphenicol. Cells from these culture passages were plated in SP4 agar and chloramphenicol-SP4 agar and no statistically significant differences in the number of viable cells plated in both conditions were observed at the different culture passages (Figure 5.8A). A more precise quantification of the genomes with excised Cre-cat cassettes was made by qPCR. Only a 0.53 % of the cell genomes isolated after the first culture passage exhibited excised cassettes. The number of excised cassettes slightly increased in the cell genomes isolated after six and eleven serial passages, showing frequencies of 1.36% and 4.50% respectively (Figure 5.8B) and indicating that Cre expression in ΔMG_217Cre cells is strongly repressed in the absence of inducer.

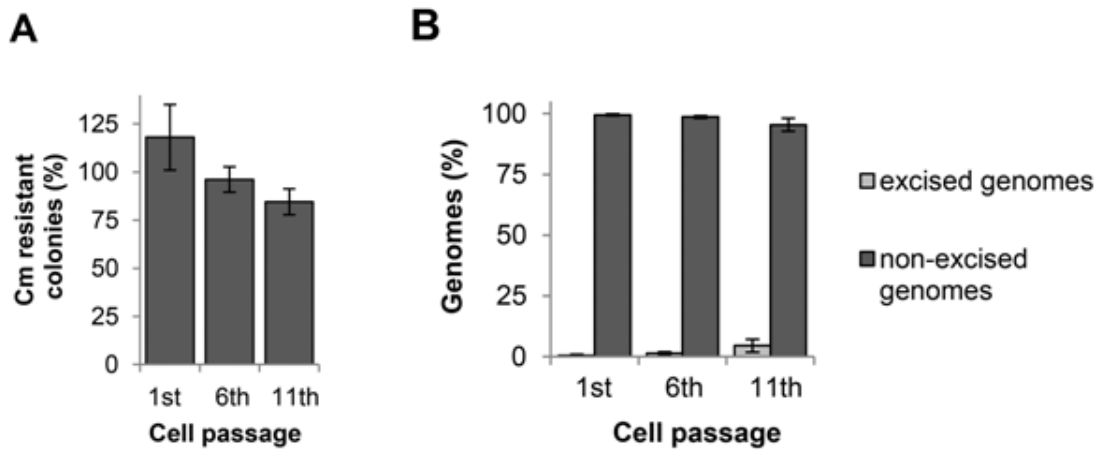

Figure 5.8. Stability of lox66 cassettes in long term uninduced cultures. (A) ΔMG_217Cre strain was subjected up to eleven serial culture passages in the absence of tetracycline inducer and chloramphenicol. Each passage was started using 1% of cells of the previous passage. At passages 1, 6 and 11 cell samples were plated in SP4-agar medium and SP4-agar medium supplemented with chloramphenicol 34 µg mL-1. For each passage, 3 independent biological replicates and 4 technical repeats were analyzed. The frequency of chloramphenicol resistant cfus in the analyzed passages is plotted with standard error bars. **(B)** Genomic DNAs from cell cultures in panel A were analyzed by qPCR to quantify the Cre-catcassette excision using primers qPCR CmDWS – qPCR 217BD_UPS and qPCR 217BE_DWS - qPCR 217BD_UPS.

5.3 Discussion

Mycoplasmas are widely used for synthetic biology studies including modified genome transplantations (Glass et al., 2006a, Glass, 2012, Gibson et al., 2010, Gibson et al., 2008b, Karr et al., 2012). Although their genomes can be synthesized chemically with the desired mutations and then assembled in yeast cells (Gibson et al., 2008b, Gibson et al., 2008a), this is a difficult and time consuming process that may not apply for high-throughput studies. Furthermore, transposition or gene replacement is nowadays a quicker, easier and cheaper way to obtain genetic modifications. Since Cre-lox technology is not currently available in mycoplasmas, we chose to adapt this friendly-user technology as a new genetic tool for working with these microorganisms. Among multiple benefits, the Cre-lox system makes possible the removal of marker genes, allowing multiple rounds of genome editions. In this way, combining Cre technology and either homologous gene replacement

or transposition may allow in minimal genome studies to introduce sequential gene deletions after removing the marker genes.

As the first step to implement the Cre-lox technology in *M. genitalium* we tested the Cre expression when delivered by suicide plasmid (Beare et al., 2012) and demonstrated that cells transformed by a suicide plasmid remain viable in the presence of a selective medium for several days (Figure 5.3). Our data also indicate that more than 99% of viable cells recovered in the presence of a selective medium were transformed with the suicide plasmid, suggesting that the background of these experiments was very low, being the frequency of spontaneous gentamicin resistant cells lower than 1% of viable cells. This suicide plasmid was also proved a very effective way to promote the Cre recombinase expression inside mycoplasma cells since all examined clones showed the excision of a lox66 cassette 48 h after plasmid delivering (Figure 1C). Since no excision of this cassette was detected in the absence of the suicide vector, we can discard the presence of intrinsic Cre-like recombinases in *M. genitalium*.

Once it was demonstrated the Cre recombinase function in *M. genitalium*, we developed an all-in-one vector to introduce in a single transformation step both a genome modification and an inducible version Cre recombinase gene. This saving-time technology would be especially interesting for those microorganisms with slow growing rates like mycoplasmas. To this end, a Cre-cat cassette was designed to include a Pxyl/TetO2 tetracycline-inducible system (Breton et al., 2010) which was modified to improve the control on Cre expression. The presence of Cre-cat cassette did not interfere in the gene replacement experiments and the ΔMG_217Cre mutant was obtained with a transformation efficiency of $2 \cdot 10^{-7}$ per viable cell, virtually the same transformation efficiency that was described in a previous report (Burgos et al., 2008). In addition, this mutant exhibited the same phenotype as previously described (data not shown) suggesting that the presence of Cre-cat cassette is not toxic for mycoplasma cells and no polar effects are produced on MG_217 flanking genes. We also tested the effect of different tetracycline concentrations when inducing Cre expression by quantifying the frequency of the cassette excisions in genomes of ΔMG_217Cre cells. Cre expression was detected at tetracycline concentrations as low as

0.1 ng mL^{-1} and the maximum expression rate was reached at concentrations close to 1 ng mL^{-1}, which is 200 times below the minimal inhibitory concentration of this antibiotic in *M. genitalium* (Pich et al., 2006b). When using Cre-cat cassette in microorganisms very sensitive to tetracycline, this antibiotic might be replaced by anhydrotetracycline, a less toxic tetracycline analog (Rasmussen et al., 1991) that can also be used to induce Tet promoters.

Implementing the Cre-lox system in mycoplasmas opens a new horizon in the study of these minimal microorganisms. With this technology a huge variety of genome modifications, such as insertions, deletions, translocations and inversions at specific sites, can be achieved now in mycoplasmas. Once demonstrated that lox66 sequences and Cre recombinase are functional in *M. genitalium*, it seems feasible to use a combination of lox66 and lox71 sequences. Recombination between these two lox sites generates an inert lox72 sequence, which presents extremely reduced recombination efficiency (Albert et al., 1995). Although a huge repertory of non-compatible lox sequences is currently available (Albert et al., 1995, Lee and Saito, 1998, Langer et al., 2002, Lanza et al., 2012) the lox72 seems the most suitable sequence to obtain an unlimited number of genetic modifications without interferences between different lox sequence (Albert et al., 1995).

The RBS sequence at the 3' end of Pxyl/TetO2 was removed to obtain a promoter with an improved control on the expression of target genes. The leakage of the modified version of this promoter was tested using a very sensitive assay. This assay was designed to detect and quantify by qPCR the frequency of excised Cre-cat cassettes in serial passage cultures of ΔMG_217Cre cells in the absence of inducer. After eleven serial passages, i.e. more than a month of continuous cell culture, only 4.5 % of the total cell population underwent a cassette excision. As only four molecules of Cre recombinase are needed to perform a site-specific recombination (Van Duyne, 2001), our results suggest that Cre expression is tightly controlled. In addition, if the Cre-cat cassette is wanted to be strictly maintained, the addition chloramphenicol to the culture medium would kill those cells bearing excised the cassettes, resulting in a negligible cell mortality rate at every passage. Finally, the modifications introduced in Pxyl/TetO2 also make this inducible promoter a promising

tool for other molecular applications. A tight control of the expressed genes is essential to develop conditional knock-out mutants to study the function of essential genes, the introduction of inducible counterselectable markers and the evaluation of mutant phenotypes after inducing the expression of target genes in time-course experiments.

6. Chapter III: Implementation of iCRISPR for gene knock-down in *Mycoplasma pneumoniae*

6.1 Introduction

Some bacteria use the Clustered Regularly Interspaced Short Parlindriomic Repeats (CRISPR) and CRISPR-associated proteins (Cas) systems to fight against bacteriophage infections, acting as an adaptive immune system (Mojica et al., 2005, Pourcel et al., 2005, Barrangou et al., 2007). Among these different systems, Type II CRISPR-Cas has been adapted for targeted genome modifications in eukaryotic cells (Cong et al., 2013, Mali et al., 2013), some bacteria (Yang et al., 2016, Zheng, 2017, Su et al., 2016) and also in some Archaea (Gophna, 2017). This extensive use regards in the simplicity of the system: it only requires the protein Cas9 and a sgRNA to perform a double stranded break (DSB) in the exact genome position targeted by the sequence of the sgRNA (Figure 6.1a).

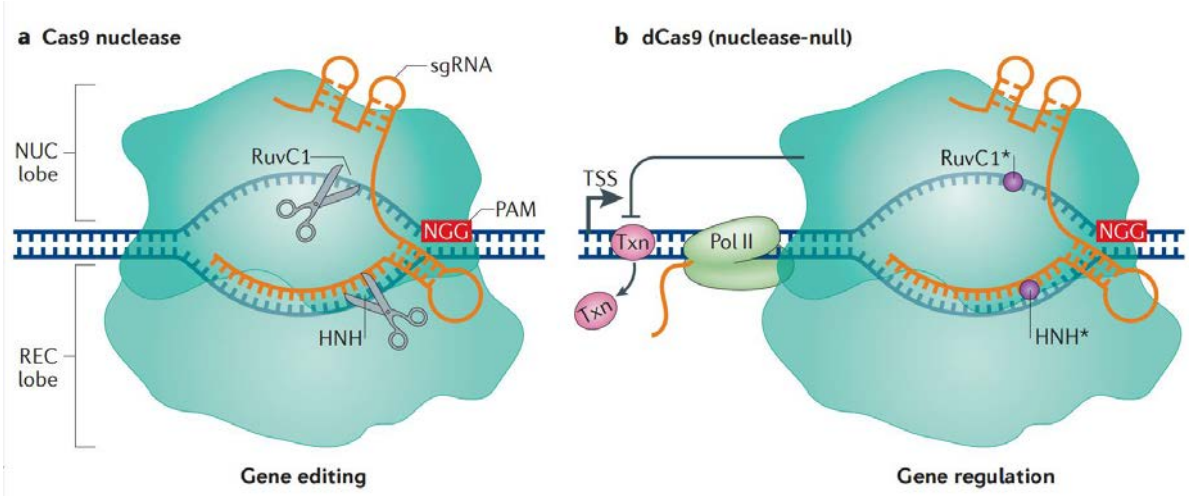

Figure 6.1. Cas9 and sgRNA drawing for gene editing (a) and dCas9 drawing for gene regulation (b). Image from (Dominguez et al., 2016)

It has been reported that specific mutations in RuvC1 and HNH domains of Cas9 protein leads to a suppression of its nuclease activity. The resulting nuclease-deficient protein, called dCas9, is unable to cleave DNA but retains the ability to specifically be bound to

DNA when guided by a sgRNA (Qi et al., 2013). Therefore, a sgRNA - dCas9 complex will be able to bind at a specific region of DNA and block the RNA pol advance, allowing a direct manipulation of the transcription process without genetically altering its DNA sequence (Qi et al., 2013) (Figure 6.1b).

Currently, the only useful genetic tool available to modify *M. pneumoniae* genomes is the mini-transposon mini-Tn4001. Although it has been used in a wide number of different studies from the study of essential genes (Lluch-Senar et al., 2015) to the isolation of mutant strains with a gene randomly truncated by the transposon insertion (Hasselbring, 2006), the randomness insertion is not suitable for isolating specific mutants. Therefore, one of the most important handicaps when trying to study the gene function in *M. pneumoniae* is the absence of a directed method to suppress the contribution of the gene of interest to the microorganism phenotype. To solve this gap in the study of *M. pneumoniae,* here, we deliver the dCas9 and a sgRNA targeting Venus fluorescent protein gene to determine that CRISPR-dCas9 is a useful system that can be used in *M. pneumoniae*, adding a new tool for targeted studies in this minimal cell. The combination of this new technique with an inducible promoter previously reported (Mariscal et al., 2016) opens the possibility to study essential genes and knock-down specific genes, which were not possible with the genetic tools available up to date.

6.2 Results

6.2.1 Introducing dCas9 in *M. pneumoniae* cells bearing the Venus fluorescent protein

To test the specific RNA interference directed by the dCas9 protein we aimed to downregulate the Venus fluorescent protein expression. Therefore, we used a *M. pneumoniae* M129 mutant that bears the gene coding for the Venus fluorescent protein (Nagai et al., 2002) and confers gentamicin antibiotic resistance (Yus, E. unpublished). The Venus gene is under the control of the mp200 promoter and small fragment of mp200

ORF, coding for a 29 amino acid cysteine-rich peptide, is fused at the 5' end of the *Venus* gene to stabilize the fusion protein (Zimmerman and Herrmann, 2005). Cells from this mutant were pooled and named V pool. Cells from this pool exhibited a strong fluorescence along the whole cell body (Figure 6.2) despite each individual cell was bearing a copy of Venus gene in a random position of its genome.

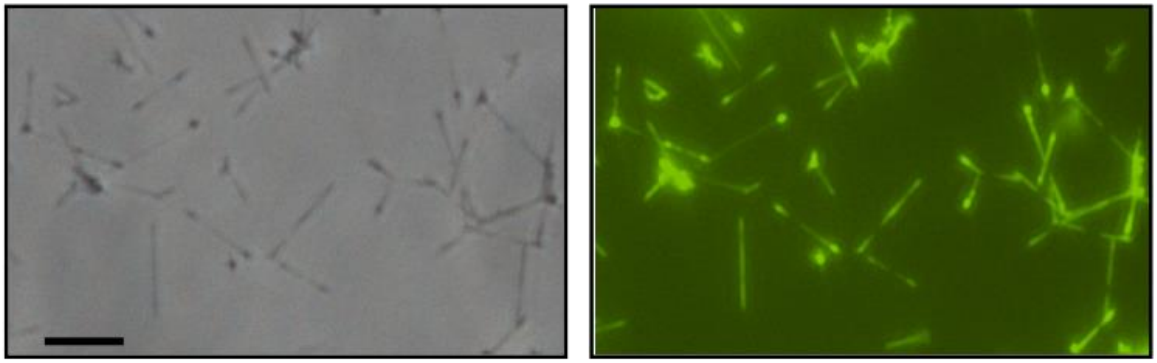

Figure 6.2. Single cell analysis of Venus fluorescence from V pool. Cells were grown in SP-4 medium and analyzed by phase contrast and epifluorescence microscopy. Scale bar: 5 μm

These cells were transformed again either with TnPac_dCas9cons or TnPac_dCas9ind constructs and all cells from each transformation experiment were also recovered and pooled. The minitransposon vectors TnPac_dCas9cons and TnPac_dCas9ind (see Appendix I: plasmid constructions, 96) bear the *pac* gene, the sgRNA targeting the *Venus* gene and the *dCas9* gene under the control of the constitutive promoter MG_438 or the inducible promoter Pxyl/TetO2mod respectively. In the case of the TnPac_dCas9ind, this vector also bears the TetR repressor to repress the dCas9 expression upon induction. The sequence of the sgRNA targeting the *Venus* gene was based in the sgRNA targeting GFP gene previously described (Qi et al., 2013). This sequence was enclosed between the MG_438 constitutive promoter and the *Streptococcus pyogenes* terminator (Figure 6.3).

>p438sgRNA_sequence

GACGTCTAGTATTTAGAATTAATAAAGT**GACCAGGATGGGCACCACCC**GTTTTAGA
GCTAGAAATAGCAAGTTAAAATAAGGCTAGTCCGTTATCAACTTGAAAAAGTGGCA
CCGAGTCGGTGCTTTTTTTCGCCGGCG

Figure 6.3. Sequence of the synthetic sgRNA targeting Venus gene. MG_438 promoter is highlighted in blue. sgRNA targeting Venus gene is displayed in red with the sequence pairing with Venus gene highlighted in bold. *S. pyogenes* terminator is displayed in black. MreI and AatII restriction enzymes sequences are underlined.

Therefore, these new cell pools contained, in addition to the previous copy of the *Venus* gene, a copy of the sequence coding for sgRNA targeting *Venus* gene and the *dCas9* gene either under the control of a constitutive promoter (3) (V-dCas9cons pool) or under the control of the pXyl/TetO_2mod inducible promoter (V-dCas9ind pool) (10) in another random location of its genome.

6.2.2 Down regulation of *Venus* expression in *M. pneumoniae* dCas9 cells

To obtain data about the down regulation of *Venus* expression, the amount of Venus transcript in the different cell pools obtained was analyzed by qPCR. While Venus expression in cells from V-dCas9ind pool showed no significant differences with cells from V pool, a significant decrease of *Venus* expression in V-dCas9cons cells (78.5 %) was observed (Figure 6.4). This result suggests that coexpression of dCas9 and the sgRNA targeting *Venus* is leading to a functional dCas9 – sgRNA complex. This complex can efficiently block transcription in the *Venus* gene, which results in a reduction of *Venus* gene expression.

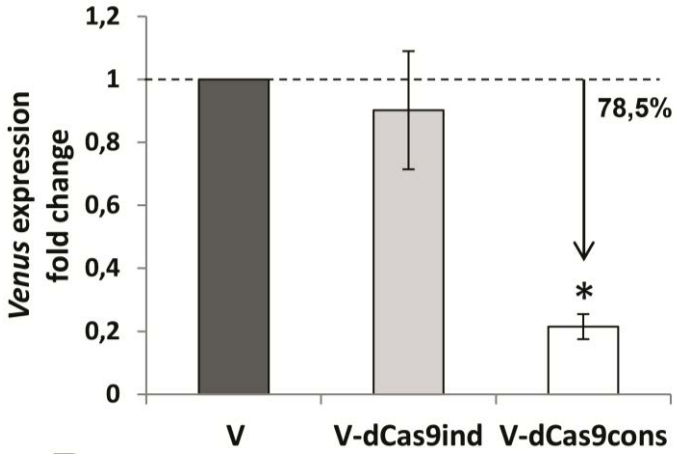

Figure 6.4. Analysis of *Venus* expression by RT-qPCR in *M. pneumoniae* cells. Fold-change of *Venus* expression in the different cell pools obtained. *Venus* expression in V-dCas9ind and V-dCas9cons pools was normalized using the values from V pool as reference. Cell pools were grown in SP-4 medium in the absence of tetracycline. Mean of three independent biological repeats with its standard error bars are plotted for each condition. Statistically significant differences with a p-value < 0.05 are indicated with a * symbol. In % is indicated the decrease of the Venus expression.

The expression of dCas9 under the control of an inducible promoter may be desirable when using the iCRSPR system to down-regulate the expression of genes essential for mycoplasma growth. In this way, we tested whether dCas9 expression under the control of pXyl/TetO_2mod inducible promoter (previously described in chapter II) can also promote down regulation of *Venus* gene. Cells from V-dCas9ind pool were grown for 66 h in the presence of 10 ng·mL^{-1} tetracycline and showed nearly a100 fold decrease (97.2 %) in *Venus* expression when compared to uninduced cells (Figure 6.5). In addition, no significant differences were observed in *Venus* expression between non induced V-dCas9ind cells and cells from V pool, suggesting that dCas9 expressión is tightly repressed in the absence of inducer (Figure 6.4 and Figure 6.5). We also investigated if tetracycline itself might be promoting down regulation of Venus reporter in V cells. In these cells no significant differences in Venus expresion were found in the presence and in the absence of tetracycline (Figure 6.5), indicating that down-regulation of the reporter in induced V-dCas9ind cells is only at the consequence of dCas9 expression.

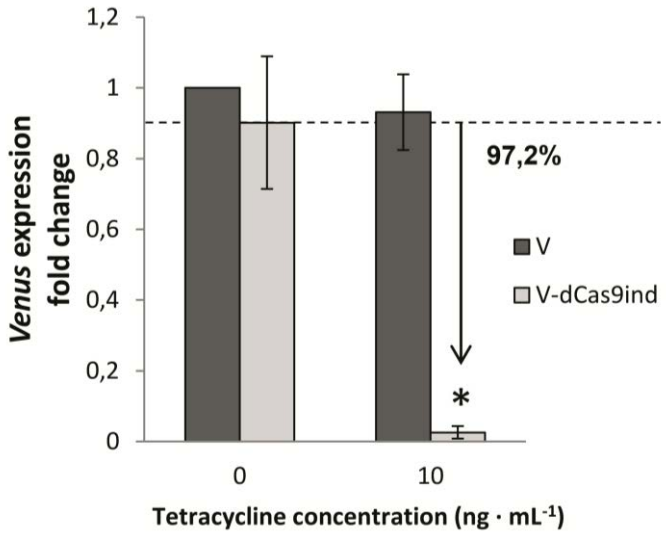

Figure 6.5. Analysis of *Venus* expression by RT-qPCR in *M. pneumoniae* cells treated with tetracycline. Fold-change of Venus expression in cells from V and V-dCas9ind pools grown in SP-4 medium in the absence of tetracycline and in the presence of 10 ng·mL-1 of this antibiotic. *Venus* expression in V and V-dCas9ind pools was normalized using the values from V pool without antibiotic treatment as reference. Mean of three independent biological repeats with its standard error bars are plotted for each condition. Statistically significant differences with a p-value < 0.05 are indicated with a * symbol. In % is indicated the decrease of the Venus expression

6.2.3 Analysis of Venus by epifluorescence microscopy

To demonstrate whether RNA transcription decrease correlates with protein reduction, Venus expression was analyzed by epifluorescence microscopy. All cells from V strain showed a strong fluorescence along the cell body (Figure 6.6A). In contrast, only a few cells from V-dCas9cons strain exhibited a detectable fluorescence. However, these fluorescent cells were as bright as cells from V pool (Figure 6.4.B).

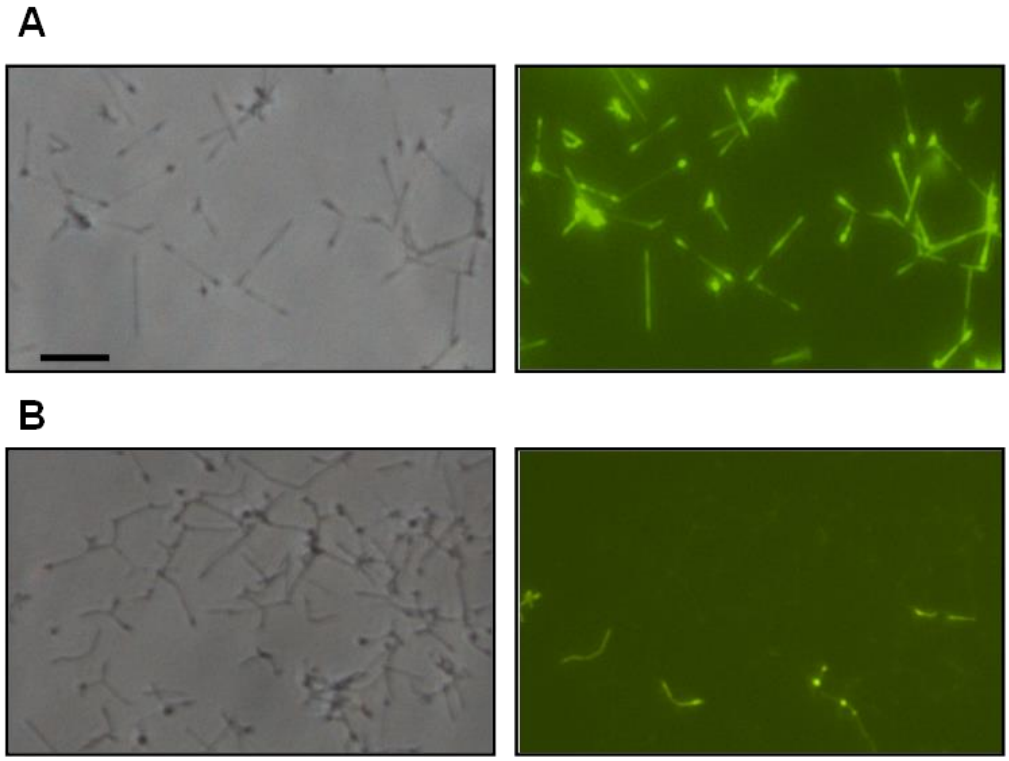

Figure 6.6. Single cell analysis of Venus fluorescence. A. V cell pool. **B.** V-dCas9cons cell pool. Cells from V and V-dCas9cons pools were grown for 66h in SP-4 medium and analyzed by phase contrast and epifluorescence microscopy. All images are shown at the same magnification. Scale bar: 5 µm

Cells from V-dCas9ind pool and V pool were grown with or without tetracycline and Venus fluorescence was monitored at 24, 48 and 66 hours of growth. In the absence of tetracycline, the number of fluorescent cells and the fluorescence intensity of individual cells were very similar in both pools (Figure 6.7 and Figure 6.8, upper panels). This is in agreement with the results above suggesting that dCas9 expression is tightly repressed in V-dCas9ind cells growing in the absence of inducer (Figure 6.4). According with qPCR data (Figure 6.5), fluorescence analysis of cells from V pool revealed that Venus expression was not affected with 10 $ng \cdot mL^{-1}$ tetracycline at any incubation time (Figure 6.7). In the presence of tetracycline, Venus fluorescence from cells of V-dCas9ind pool exhibited a strong decay after 24 h and no fluorescent cells could be detected after 48 h and 66 h, supporting also that Venus expression was strongly blocked by dCas9–sgRNA complex (Figure 6.8).

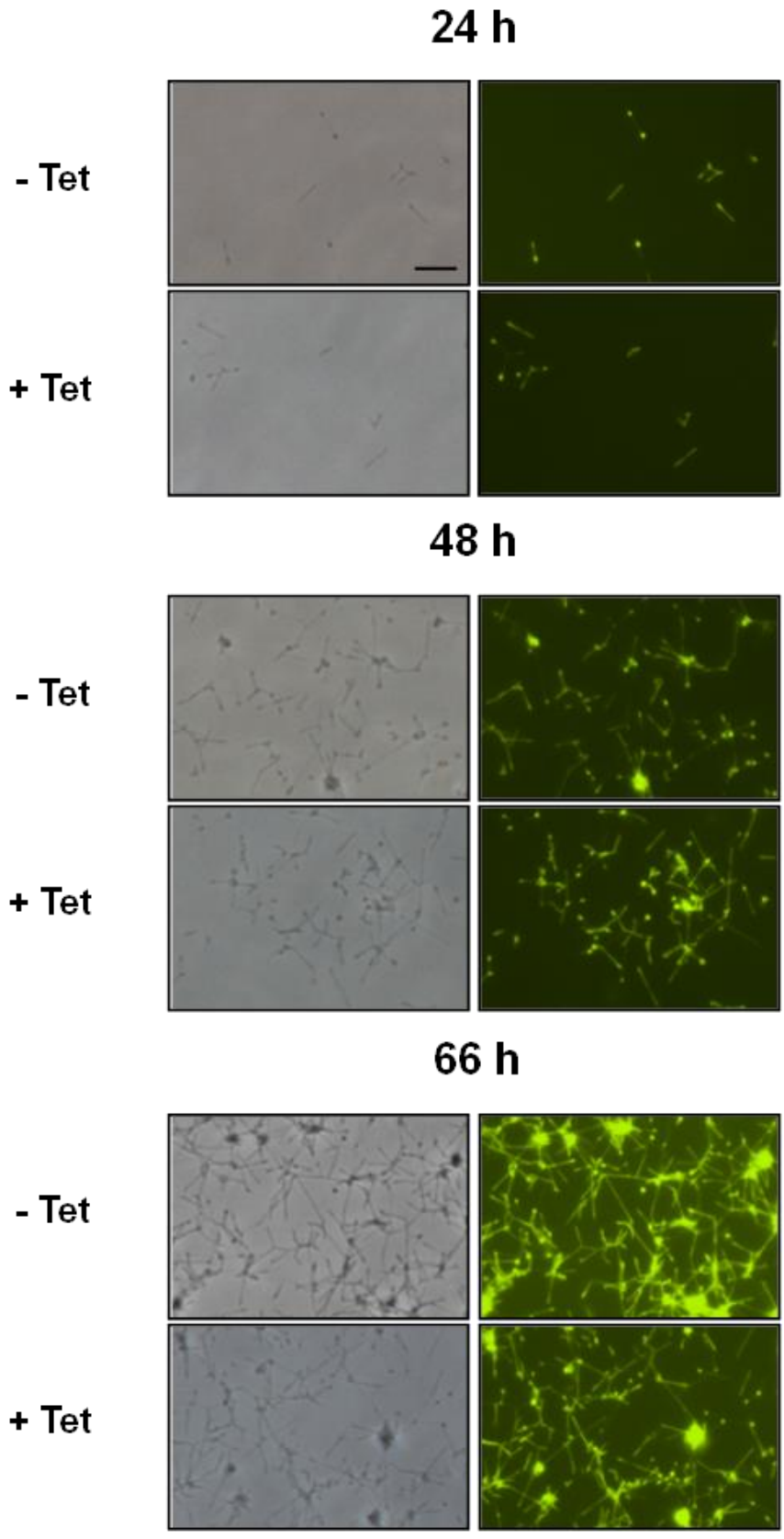

Figure 6.7. Time-course fluorescence analysis of cells from V pool. Cells from V pool were grown for 66 h in SP-4 medium in the absence of tetracycline and supplemented with 10 ng·mL-1 tetracycline (–Tet and +Tet, respectively) and analyzed by phase contrast and epifluorescence microscopy after 24, 48 or 66 h of growing. All images are shown at the same magnification. Scale bar: 5 μm

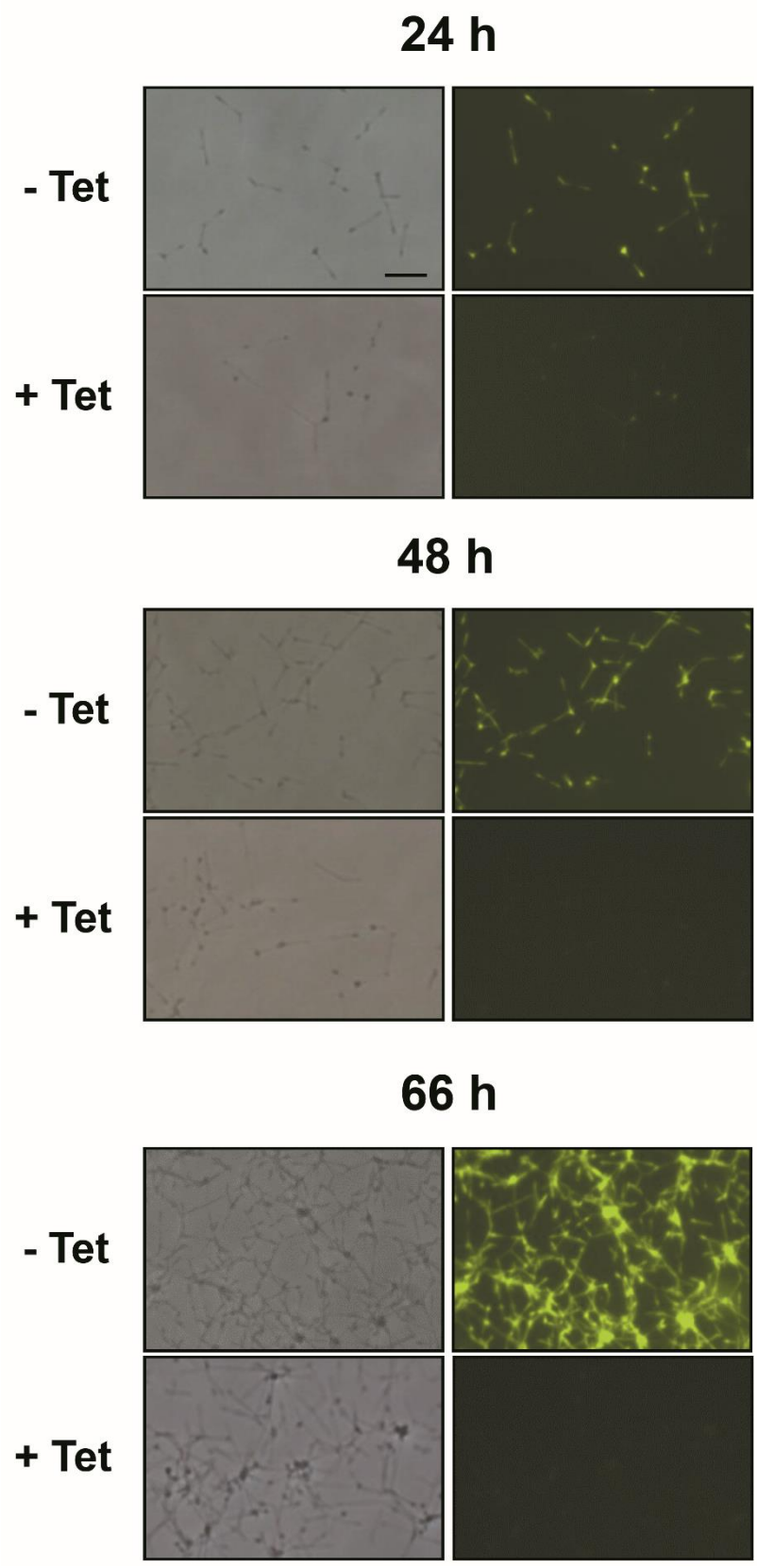

Figure 6.8. Time-course fluorescence analysis of cells from V-dCas9ind pool. Cells from V-dCas9ind pool were grown for 66 h in SP-4 medium in the absence of tetracycline and supplemented with 10 ng·mL-1 tetracycline (–Tet and +Tet, respectively) and analyzed by phase contrast and epifluorescence microscopy after 24, 48 or 66 h of growing. All images are shown at the same magnification. Scale bar: 5 µm.

6.3 Discussion

Mycoplasmas are appealing models of minimal cells and their limited genetic repertory make these microorganisms especially well-suited for systems biology studies and genome engineering technologies. However, many routine tools for genetic analysis are still missing in mycoplasmas, particularly those addressed to the work with essential genes. Neither conditional mutants nor other common methods to deal with these genes have been previously reported. Based on the recent advances in iCRSPR techonology which allow the silencing of gene expression by dCas9 engineered variant (Jinek et al., 2012), we have developed several vectors and methods to down-regulate gene expression in mycoplasmas. Here we show that inducible versions of dCas9 and different sgRNAs can be easily introduced and expressed in these minimal cells, decreasing in a reproducible way up to 100 fold the expression of target genes.

To test the iCRISPR system in this microorganism we chose a variant of Venus fluorescent protein fused to a 29 aminoacid peptide of mp200 ORF to improve protein stability and provide an ubiquitous cell distribution (Zimmerman and Herrmann, 2005). The reporter gene was also under the control of the promoter sequences from mp200 since this ORF is strongly expressed at both transcriptional and translational levels. When the construct containing the Venus reporter was delivered by transposition to *M. pneumoniae* cells, all the transformant cells exhibited a strong fluorescence along the whole cell body, irrespective of the particular transposon location in each transformant cell (Figure 6.2). Transformant cells were maintained as a cell pool in order to test if the Venus reporter gene could be effectively knocked down by the iCRISPR system in different genome locations and in the presence of very heterogeneous genetic environments (Guell et al., 2009).

Coexpression of dCas9 and a sgRNA targeting *Venus* gene, both under the control of MG438 constitutive promoter (Pich et al., 2006b), led to a 78 % *Venus* gene down-regulation in *M. pneumoniae* V-dCas9cons cells (Figure 6.4). These results indicate that dCas9 is properly expressed, bounds to the specific sgRNA and blocks the RNA

polymerase in the target gene as it has been previously described for other microorganisms (Qi et al., 2013). This reduction in the Venus RNA levels also correlates with the reduced fluorescence exhibited by V-dCas9cons cells (Figure 6.6), and demonstrates that iCRISPR system is functional in *M. pneumoniae*. However, some cells remained fluorescent after delivering dCas9cons construct by transposition, indicating that Venus expression was not effectively blocked in these cells. Probably, the transcriptional activity MG438 constitutive promoter might not suffice to generate an effective amount of dCas9-sgRNA complex to block the transcription of Venus reporter when this gene is located in some particular genome sites. In contrast, when dCas9 was under the control of the inducible promoter pXyl/TetO_2mod, *Venus* down-regulation was 97% and virtually all transformant cells were non fluorescent when cultured for 48 h in the presence of inducer (Figure 6.5 and Figure 6.8). This highlights the importance to select a strong, inducible promoter to control the expression of *dCas9*.

Tetracycline was used as inducer of dCas9 expression in the V-dCas9ind cell pool. Previous works have reported that certain antibiotics at low, subinhibitory concentrations modulate bacterial transcription patterns and the expression of some genes might be altered (Knudsen et al., 2012). We tested the effect of tetracycline in *Venus* expression by incubating the cells from V pool in the presence of this antibiotic and discarded any direct effect of tetracycline in the down regulation of the reporter gene (Figure 6.5). In addition, uninduced cells from V-dCas9ind pool showed no significant differences in *Venus* expression when compared to cells from V pool (Figure 6.4). This data is in agreement with previous findings confirming Pxyl/TetO2mod promoter exhibits no detectable leakage in the absence of inducer (Mariscal et al., 2016). However, this promoter is strongly induced in the presence of tetracycline and near a 100 fold decrease was observed when quantifying Venus transcript (Figure 6.5). Also in the presence of inducer, time-course fluorescence analyses revealed the presence of some fluorescent cells at the shortest incubation time, but virtually no fluorescent cells at the longest incubation times were detected (Figure 6.8). This suggests that the Venus reporter used is a very stable protein and has a long shelf life when expressed in *M. pneumoniae*. Despite the very long incubation times upon the continuous synthesis of dCas9 required to clear out the Venus

fluorescence, no noticeable toxic effects were detected. All these results taken together suggest that the iCRISPR system designed is particularly well suited to address the knocking down of *M. pneumonaie* genes, even though if these genes are strongly transcribed or coding for very stable proteins with extended shelf lives.

The presence of off-targets when using both Cas9 and dCas9 has been widely reported elsewhere and cannot be excluded when using CRISPR systems in mycoplasma cells. The presence of off-targets could be a problem when analyzing the phenotype of knocked-down cells. The origin of off-targets is mainly related to sgRNAs partially annealing to genes other than the target gene and could be also the result of a metabolic stress when inducing the expression of the dCas9 enzyme. Using a re-engineered version of dCas9 with a lower DNA affinity (Kleinstiver et al., 2016) together with a carefully design of different sgRNA (Doench et al., 2016) may contribute to ameliorate the off-target problem.

However, sgRNAs and dCas9 is a fast and reliable a method to conditionally express essential mycoplasma genes. In addition, in many mycoplasma species refractory to be transformed by homologous recombination, sgRNAs and dCas9 is the single method available to characterize the role of essential genes.

We have shown that iCRISPR system is functional in *M. pneumoniae*, suggesting that this system can be easily expanded to other mycoplasmas. Implementation of this new technique provides a powerful tool for targeted gene regulation in minimal cells such as *M. pneumoniae* or the synthetic minimal cell syn3.0 (Hutchison et al., 2016).

7. General discussion

M. genitalium G37 and *M. pneumoniae* M129 with only 515 and 729 annotated proteins respectively (NCBI, 2017, Lluch-Senar et al., 2016) are among the smallest free-living organisms. Their reduced genomes make these organisms appealing models for synthetic biology studies and also to determine the minimal genes essential for life. However, most of the genetic tools used in other microorganisms are not available for the modification of mycoplasmas, complicating in this way the manipulation and studies of these bacteria. Here, we have described the implementation of three useful techniques that can open and facilitate the study of these minimal cells: the use of fluorescent proteins as markers for protein localization, the engineering of an inducible promoter to reduce the transcriptional leakage and the use of this tuned inducible promoter to control the Cre expression and the dCas9 expression, two molecular techniques to manipulate the genome and the transcriptome respectively.

Determine the exact position of target proteins of *M. genitalium* represents a challenge objective due to the small size of these cells and the photobleaching and photostability of fluorescent proteins (FP). However, the combination of a quantitative determination of the distance between the DNA and the target protein (fused with a FP) with the use of a reference point (a known protein marked with a FP and the target protein with a different FP) has been proved to be a suitable method to determine the position of an unlocalized protein. The measuring of the distance in lots of cells ($n > 200$) together with a statistical analysis permits the augmentation of the resolution of an optical microscope, allowing a more precise localization in these minimal cells.

As it has been reported before (Hasselbring et al., 2012, Seto and Miyata, 2003, Balish et al., 2003, Nakane et al., 2015), fluorescent proteins in *M. pneumoniae* show a higher intensity than those exhibited in *M. genitalium*. This difference can be due to the size of the cells and also to a different protein life in those microorganisms. However, the use of the Venus fluorescent protein in *M. pneumoniae* reveals a really high and bright fluorescence, maybe due to the improvement of this fluorescent protein respect its relative eYFP. Moreover, this enhanced fluorescence exhibited by the Venus fluorescent protein in

M. pneumoniae cells can be also due to the fusion of a cystein-rich 29-aminoacid peptide that have been proved to improve the protein stability (Zimmerman and Herrmann, 2005). These results encourage the use of the Venus protein in future experiments with mycoplasma species instead of the eYFP.

Inducible promoters are widely extended and with multiple options in different microorganisms. However, only one inducible system has been reported for the *Mollicutes* (Breton et al., 2010). In this work, we have engineered this inducible promoter in order to reduce the transcriptional leakage since for some proteins, such as Cre recombinase, a tightly control of its expression is required. For example, only 4 molecules of Cre recombinase are able to perform an excision of the sequence between the lox sequences. Therefore, since we are delivering the marker gene and the Cre recombinase (under the control of the inducible promoter) both in the same vector and between the lox sequences, a small transcriptional leakage will drastically reduce the recovered transformant cells. To our knowledge, this is the first time that the Cre recombinase and the intended mutation are delivered in the same vector in one transformation step. This achievement has a special importance for its application in mycoplasma cells since it represents a considerable gain of time for the study of these slow-growing microorganisms. Moreover, the application *per se* of Cre-lox technology in mycoplasmas opens new possibilities to study these microorganisms that were not possible before such as the deletion/insertion of multiple genes in the same strain. This procedure was limited up to four deletions/insertions in total since only 4 marker genes are available for mutant selection, but with the Cre-lox technique the marker genes can be excised and the modifications in the same strain are unlimited.

The study of essential genes can be performed using an inducible promoter: first delivering an extra copy of the essential gene under the control of the inducible promoter and then deleting the essential gene from the genome while inducing the expression of the extra copy of this gene previously delivered. Once the strain is obtained the phenotype can be studied switching-off the induction of the system controlling the target gene. However, this is a complicated and time-consuming methodology that can be substituted by the iCRISPR-dCas9 system. Here, we have demonstrated that *Venus* expression can be

specifically downregulated using the dCas9 in *M. pneumoniae* cells. The combination of dCas9 with the previous engineered inducible promoter leads to a 100-fold decrease in *Venus* expression upon induction and with no appreciable differences in non-induced cultures. Therefore, this is a promising tool for the study of targeted genes including essential genes and their implication in mycoplasmas. Moreover, the simplicity of dCas9 system that only relies on a specific sgRNA makes this tool a very versatile technique that can be easily used for massive studies.

In this work we have implemented up-to-date tools, such as Cre-lox system or iCRISPR, which were not available for mycoplasmas. In this way, we provide new methods for modifying mycoplasma cells that allows the study of these minimal cells in a simplier way. Moreover, the implementation of these techniques in mycoplasma allows new type of studies that were not possible before, opening the possibilities to understand better these minimal microorganisms and the essentiality of life.

8. Conclusions

Chapter I: Mycoplasma genitalium terminal organelle proteins localized by eYFP tagging in a P32-mCherry background

- A total of 16 different mutants bearing a *M. genitalium* protein fused with the eYFP in a P32-mCherry background have been obtained.
- The proteins HMW1, HMW2, HMW3, MG200, MG217, MG219, MG269, MG386, P110, P140, P32, P41 and Lon have been localized in *M. genitalium* cells, confirming its position in the terminal organelle as it has been described in other mycoplasmas.
- DnaK and GrpE proteins have been localized in the terminal organelle structure for the first time in the *mycoplasma* genus.
- The position of each protein has been assigned to the different substructures of the terminal organelle combining the qualitative analyses using the P32 as a reference point with the quantitative analyses.
    - Proteins P32, MG217 and HMW3 have been localized in the terminal button.
    - Proteins HMW1 and HMW2 have been localized in the segmented paired plates.
    - Proteins P41, GrpE, MG200, MG269, DnaK, MG219, Lon and MG386 have been localized in the wheel complex. The measurement of the distance between the eYFP fused to the target protein and the DNA have permitted to determine the order of the proteins. From the most apical to the most proximal part we can separate the proteins in three different groups: (i) P41 and GrpE, (ii) MG200 and MG269 and (iii) DnaK, MG219, Lon and MG386.
    - Proteins P110 and P140 have been localized along all the terminal organelle.

~ The protein HMW2, located in the segmented paired plates, is disposed with its N-ter domain near to the terminal button and its C-ter domain near to the wheel complex as it has been also described for its *M. pneumoniae* homologue.

Chapter II: All-in-one construct for genome engineering using Cre-lox technology

- It has been determined that a suicide plasmid can be used to express a protein temporarily in *M. genitalium* cells up to one week.
- A highly tight inducible promoter with very few leakages has been obtained.
- It has been demonstrated that Cre-lox system is fully functional in *M. genitalium* cells.
- Induction of Cre expression with 1 $ng \cdot mL^{-1}$ leads to a 90% of excised cassettes flanked by lox sequences.
- To our knowledge this is the first time that a genome modification involving Cre recombinase can be achieved in one transformation step.

Chapter III: Implementation of iCRISPR for gene knock-down in *Mycoplasma pneumoniae*

~ A *M. pneumoniae* strain expressing the Venus fluorescent protein has been obtained and all cells exhibit a strong and stable fluorescence along all the cell body.

~ Constitutively expressed dCas9 from *S. pyogenes* and a sgRNA targeting *Venus* gene leads to 78 % *Venus* gene down-regulation in *M. pneumoniae* cells.

~ Uninduced cells from V-dCas9ind show no significant differences in *Venus* gene expression with cells from Venus derivative supporting the few leakage associated with the engineered inducible promoter Pxyl/$TetO_2$mod.

~ Induction of dCas9 expression with 1 $ng \cdot mL^{-1}$ leads to a 100-fold decrease of *Venus* gene expression.

- The decrease in *Venus* gene expression due to the binding of dCas9-sgRNA correlates with a reduction of protein amounts.
- dCas9/CRISPR system provides a powerful tool for targeted gene regulation in *M. pneumoniae* and the combination of this system with a tightly regulated inducible promoter is a promising method for the study essential genes.

9. Materials and Methods

9.1 Bacterial growth and strains

9.1.1 E. coli strains culture

E. coli XL1 Blue was the strain used for cloning procedures as it presents a high transformation efficiency and is deficient for recombination. Presence of F' factor allows α-complementation, M13 phage infection and lac repressor superproduction (*lac*I^q). Its genotype is: *sup*E44 *hsd*R17 *rec*A1 *end*A1 *gyr*A46 *thi rel*A1 *lac*$^-$*F*$^-$[*pro*AB^+ *lac*I^q *lacZ*ΔM15 Tn*10*(tet^r)]

E. coli XL1 Blue was grown in LB medium (Luria-Bertani medium). This is a rich culture medium composed by: 10 g/L tryptone (Sharlau microbiology), 5 g/L yeast extract (Sharlau microbiology), 10 g/L NaCl (Fluka) and 15 g/L agar (Sharlau microbiology) if solid medium is desired. Autoclave 15 min at 121 ^oC

Liquid cultures were inoculated in a laminar flux cabin (Telsar, model AV-100) and grown overnight at 37^oC and 250 rpm in an orbital shaking incubator (Braun, model Centromat H). A maximum proportion of 1:5 (culture volume vs total recipient volume) were used for a correct aeration. Inoculums for 3 mL cultures were an isolated colony recovered from a solid medium or 2 to 10 µL from a working stock. For large volume cultures a 1% inoculum from a preculture grown until A_{600}~1 was used.

Solid cultures were inoculated in a laminar flow cabinet (Telsar, model AV-100) and used for individual colonies isolation. A *Digralsky* spreader or an inoculation loop were used to spread all the cells after transformation or for streaking a small volume from a liquid culture respectively. Plates were incubated at 37^oC overnight in an incubator (Memmert). Isolated colonies were recovered with a sterile wood stick and expanded in liquid medium.

E. coli strains were conserved in 15 % glycerol at -80^oC. Obtainment of *E. coli* XL1Blue competent cells were performed using inoue ((Sambrook et al., 2006)). Heat shock transformation were performed as described ((Sambrook et al., 2006))

Antibiotics and supplements used:

- Ampicillin (Roche): stocks were prepared at 200 mg mL^{-1} in H_2O MilliQ and sterilized by filtering the solution through a 0.22 filter (Millipore). Aliquots of 1 mL were stored at – 20°C. Working concentration for strains carrying high copy number pDNA is 100 µg mL^{-1}.
- Tetracycline (Fluka): stocks were prepared at 5 mg mL^{-1} in 70% ethanol sterilized by filtering the solution through a 0.22 filter (Millipore). Aliquots of 1 mL were stored at – 20°C. Working concentration for XL1Blue strain is 10 µg mL^{-1}. Avoid light exposure as it is a photosensitive compound.
- Isopropyl β-D-1-thiogalactopyranoside, IPTG (Sigma): stocks were prepared at 1M in H_2O MilliQ. Aliquots of 1 mL were stored at – 20°C. IPTG was used for gene expression induction of those genes under the control of lactose promoter. Working concentration usually was 1mM.
- 5-bromo-4-chloro-3-indolyl-β-D-galactopyranoside or X-gal (VWR): used in LB plates for recombinant plasmids selection (for clonings based in LacZ). 20 mg were dissolved in 1 mL of N,N-dimethylformamide and added to 500 mL of LB agar.

9.1.2 *M. genitalium* strains culture

9.1.2.1 Medium and component preparation

The medium used for growing *M. genitalium* was SP4 (Spiroplasma Medium 4). It was prepared in two steps. First 1.75 g PPLO Broth (BD, Becton Dickinson), 5 g Bactotryptone (BD, Becton Dickinson), 2.65 g Bactopeptone and 2.5 g glucose (Sigma) were dissolved in H_2O MilliQ up to 312 mL. pH was adjusted to 7.8 with NaOH 2 M. If solid medium was desired 3.5 g Bactoagar (BD, Becton Dickinson) were added before autoclaving process at 121°C for 15 min. Then, the following components were added to this base: 50 mL of Yestolate 2%, 6 mL of Phenol red 0.1% pH7.0, 17.5 mL of yeast extract (see the preparation below), 25 mL of CMRL (LifeTechnologies), 85 mL of Fetal Bovine Serum, 1.71 mL of Glutamine 29.2 mg mL^{-1} (Sigma) and 250 µL of ampicillin 200 mg mL^{-1}. Then, pH were readjusted again to 7.8 with NaOH 2 M.

Components and antibiotics used:

- Yestolate 2%: 20 g of Yestolate (BD, Becton Dickinson) were dissolved in 1 L H_2O MilliQ water, autoclavated at 121 ^oC for 15 min and stored at 4 ^oC.
- Phenol Red 0.1% pH 7.0: 0.5 g of Phenol Red (Sigma) were dissolved in 500 mL H_2O MilliQ water and pH was carefully adjusted to 7.0. Stored at 4 ^oC after sterilization by autoclaving at 121 ^oC for 15 min.
- Yeast extract 25% (w/v): 250 g of fresh yeast were dissolved in 1L of distilled water and autoclaved at 115 ^oC for 10 min. Then, it was centrifuged at 400 g for 10 min at 4 ^oC and the supernatant was autoclaved at 115 ^oC for 10 min. Then it was aliquoted in a laminar flow cabinet and 20 mL aliquots were stored at -20 ^oC.
- Fetal Bovine Serum (FBS): Fetal Bovine Serum (LifeTechnologies) was heated to 56 ^oC for 30 min in order to inactivate the complement system. Then it was aliquoted in a laminar flow cabinet and 45 mL aliquots were stored at -20 ^oC.
- Ampicillin (Roche): stocks were prepared at 200 mg mL^{-1} in H_2O MilliQ and sterilized by filtering the solution through a 0.22 filter (Millipore). Aliquots of 1 mL were stored at – 20^oC. Working concentration was 100 µg mL^{-1} in order to prevent bacterial contamination.
- Tetracycline (Fluka): stocks were prepared at 5 mg mL^{-1} in 70% ethanol sterilized by filtering the solution through a 0.22 filter (Millipore). Aliquots of 1 mL were stored at – 20^oC. Working concentration for strains carrying the marker gene *tet*M438 (pich et al 2006a) was 2 µg mL^{-1}. Avoid light exposure as it is a photosensitive compound.
- Chloramphenicol (Roche): stocks were prepared at 34 mg mL^{-1} in 70% ethanol sterilized by filtering the solution through a 0.22 filter (Millipore). Aliquots of 1 mL were stored at – 20^oC. Working concentration for strains carrying the marker gene *cat*M438 (calisto 2012) was 34 µg mL^{-1}.
- Gentamicin solution 50 mg mL^{-1} (LifeTechnologies): used for selection of strains carrying *aac(6')-aph(2'')* resistance gene (pich et al 2006a). Working concentration was 100 µg mL^{-1}.

9.1.2.2 *M. genitalium* cultures

All *M. genitalium* cultures were inoculated in a laminar flow ClassII biosafety cabinet (Telsar, model BIO-II-A) and incubated at 37^{o}C in a 5% CO_2 atmosphere (Jouan, models EG 110 IR and 160-150).

Solid cultures were performed to isolate individual colonies in SP4 agar plates, prepared the same day or stored at 4 ^{o}C up to 5 days (about 7 mL of SP4 medium in 50 mm petri dishes). Between 10 and 200 µL of a cellular suspension were plated in SP4 solid medium and left about 15 min until it was absorbed. Individual colonies were observed between 7 and 15 days after inoculation with a stereomicroscope (Wild Heerbrugg Leitz Plan) and recovered with sterile microtips.

Liquid cultures were inoculated with 35, 100 or 150 µL of a working stock in 25, 75 or 150 cm^2 flasks (TPP) with 5, 20 or 35 mL of SP4 medium respectively. For adherent strains, medium was aspirated and cells were recovered in the desired solution with a scraper (TPP). For semi-adherent or non-adherent strains, cells were scraped in the culture medium and centrifuged 30 min at 4000 g and 4 ^{o}C. Supernatant was discarded and cells were resuspended in the desired solution.

G37 *M. genitalium* working stocks were prepared as follows. 100 µL of a master stock (in a 2nd cell passage) were inoculated in 75 cm^2 flasks (TTP) with 20 mL SP4. After 72 h, old medium was aspirated and cells were resuspended in 10 mL of fresh SP4 medium. Aliquots of 100 µL were stored at -80 ^{o}C.

Individual colonies were recovered with sterile microtips and propagated in 25 cm^2 flasks (TTP) with 5 mL SP4. When the cultures were grown, between 8 and 20 days depending on the mutant strain generated, cells were resuspended in 1 mL of fresh SP4 medium and stored at -80 ^{o}C. Working stocks were prepared inoculating 35 µL of this master stock in 25 cm^2 flasks (TTP) with 5 mL SP4 and, when the cultures were grown, cells were resuspended in 1 mL of fresh SP4 medium and stored at -80 ^{o}C. No glycerol addition was needed to conserve cells at -80 ^{o}C due to the high FBS concentration in SP4 medium.

9.1.2.3 *M. genitalium* transformation

M. genitalium was transformed by electroporation. The protocol used was based in *M. penumoniae* transformation (Hedreyda et al 1993) and adapted to *M. genitalium* transformation (Reddy et al 1996). It was slightly modified in Jaume Piñol's laboratory. Briefly:

- 100 µL of a working stock were inoculated in a 75 cm^2 flask (TTP) with 20 mL SP4.
- After 72 h, 10 mL of old medium were discarded and cells were scraped in the resting medium (10 mL).
- This cell suspension was disaggregated through a 0.45 µm filter (Millipore) and reinoculated into a 150 cm^2 flask (TTP) with 20 mL of fresh SP4.
- Next day, medium was aspirated and cells were washed for three times with electroporation buffer (8 mM HEPES, 272 mM sucrose pH 7.4).
- After three washes, cells were scraped in 1 mL of electroporation buffer (approximately $1 \cdot 10^9$ cfu mL^{-1}).
- 10 or 30 µg of pDNA (for transposition or homologous recombination respectively) were mixed with 100 µL of cell suspension. It was incubated in an electroporation cuvette 0.2 cm gap width (VWR) in ice for 15 min.
- Electroporation was performed at 2.5 kV, 250 Ω and 25 mF with an electroporation system (ECM 630 BTX) and immediately cuvettes were incubated in ice for 15 min.
- 900 µL of SP4 were added to each cuvette and electroporated cells were transferred to a sterile microcentrifuge tube. It was incubated for 2-3h at 37 ^oC in order to allow resistance marker gene expression.
- Finally cells were plated in SP4 agar plates supplemented with the corresponding antibiotic. As control title, viable cells and spontaneous mutants were also plated.

9.2 DNA manipulations and molecular cloning

9.2.1 Plasmid DNA extraction

pDNA extraction were carried out with the commercial kit Fast Plasmid Miniprep Kit (5 Prime) under manufacturer's instructions. If a high purity was needed (i.e. molecular cloning) the commercial kit GeneJET Plasmid Miniprep (Fermentas) was used following manufacturer's instructions. For higher amounts of pDNA GenElute^{TM} HP Plasmid Midiprep Kit (Sigma) was used under manufacture instructions. Plasmid DNA precipitation was performed with one volume of isopropanol in the presence of 0.3 M ammonium acetate. After centrifugation at 16000 g at 4oC for 10 min, the pellet was washed with 70% ethanol two times. Once the pellet was completely dried in a vacuum chamber it was resuspended in electroporation buffer.

9.2.2 Genomic DNA extraction from *M. genitalium* cultures

Late exponential phase cultures grown in 75 cm^2 flasks were washed three times with PBS 1x (Roche). Cells were scraped in 1 mL of PBS, centrifuged for 15 min at 16000 g at 4 ^oC and resuspended in 500 µL of solution I (0.1 M Tris-HCl pH 8.0, 0.5 M NaCl, 10 mM EDTA). Cells were lysed with 10 µL of SDS 20% and treated with one volume of phenol-chloroform-isoamyl alcohol (25:24:1) inverting carefully the tubes to mix gently the phases. This mixture was centrifuged at 16000 g for 20 min and the aqueous phase was recovered carefully. A second treatment with one volume of phenol-chloroform-isoamyl alcohol (25:24:1) were performed. Genomic DNA, placed in the aqueous phase recovered, was precipitated with 2.5 volumes of absolute ethanol. After carefully inverting the microcentrifuge tube it was centrifuged at 16000 g for 15 min and the pellet was washed two times with 70 % ethanol centrifuging each time at 16000 g for 10 min. Finally the pellet was completely dried in a vacuum chamber and resuspended in 50 µL of TE (10 mM Tris-HCl pH 8.0, 1 mM EDTA pH 8.0) with RNAse (concentracion!!). If this gDNA was wanted for Sanger sequencing it was suspended in 0.2x TE to avoid polymerase inhibition by the presence of EDTA.

9.2.3 DNA quantification

DNA quantification was performed using a NanoDrop 1000 Spectrophotometer (Thermo Scientific) following the manufacturer's instructions.

9.2.4 DNA sequencing

Sequencing reactions were performed with the commercial kit Big Dye 3.0 Terminator Kit (Applied Biosystems) and analysed with an ABI 3100 Genetic Analyzer (Applied Biosystems) following the manufacturer's instructions. All the reactions were performed by Servei de Genòmica i Bioinformàtica de la UAB.

9.2.5 DNA restriction

DNA restrictions were performed using restriction enzymes from Roche or Fermentas following the manufacturer's instructions.

9.2.6 DNA ligation

All ligations were performed using T4 DNA ligase (Roche) following the manufacturer's instructions.

9.2.7 DNA agarose electrophoresis

Agarose (SeaKem LE Agarose) was dissolved between 0.6 and 2.0 % w/v in TAE (40 mM Tris-HCl pH 7.6, 20 mM acetic acid, 1 mM EDTA pH 8.0). DNA electrophoresis was performed with Bio-rad electrophoresis equipment at 60-70 V for preparative electrophoresis or 80-90 V for analytic electrophoresis. Commercial 1 kb Plus DNA Ladder (Life Technologies) was used to estimate the molecular length of the DNA fragments. After electrophoresis, agarose gels were stained for 15 min with 0.5 $\mu g\ mL^{-1}$ EtBr. Bands were detected under UV irradiator (refs) and photographed with Gel Doc XR (BioRad) using QuantityOne 4.6 software.

DNA agarose bands were purified using the kit NucleoSpin Gel and PCR Clean-Up (Macherey-Nagel) according to manufacturer's instructions.

9.2.8 DNA PCR amplification

DNA amplification for cloning processes was performed with Phusion^{TM} polymerase (Sigma) according to manufacturer's instructions as it presents proof-reading activity. For screening PCRs GoTaq polymerase (Promega bio-tek) was used. dNTPs used were purchased from Sigma.

All oligonucleotides used (Appendix II: oligonucleotides) were purchased from Invitrogen or Sigma.

9.3 RNA extraction and qPCR analyses

Total RNA extraction was performed using the commercial kit RNAqueous (Ambion). Late exponential phase cultures grown in 75 cm^2 flasks were washed three times with PBS 1x (Sigma). Cells were scraped in 1 mL of PBS, centrifuged for 15 min at 16000 g at 4 ^oC and resuspended in 500 µL of lysis solution from RNAqueous kit (LifeTechnologies). Next steps for total RNA extraction were performed following manufacter's instructions. Then, the extracted RNA was treated with Turbo DNA-free kit (LifeTechnologies) in order to remove the remaining genomic DNA and quantified using NanoDrop.

9.4 SDS-PAGE and Western blotting

9.4.1 Protein extraction and quantification

Total protein extraction from *M. genitalium* cells was performed as follows. Late exponential phase cultures grown in 75 cm^2 flasks were washed three times with PBS 1x (Roche) and cells were resuspended in 75 µL of PBS (cells were centrifuged for 15 min at 16000 g at 4 ^oC when needed). Cells were lysed using protein loading buffer prepared according to "Molecular Cloning: A Laboratory Manual" (Sambrook et al., 2001). If needed, protein extraction was quantified using the commercial kit Protein Quantification Assay (Macherey-Nagel).

9.4.2 SDS-PAGE (Sodium Dodecyl Sulfate Polyacrylamide Gel Electrophoresis)

SDS-PAGE gel preparation and all the solutions needed was performed following the standard protocol described in "Molecular Cloning: A Laboratory Manual" (Sambrook et al., 2001). Acrylamide gels were prepared with a 40 % acrylamide:bis-acrylamide solution (37.5:1) (Bio-Rad). For the stacking gel a 4 % acrylamide:bis-acrylamide mix was used, while for the running gel the percentage used was between 7 and 15 %, depending on the molecular range wanted to be better resolved. For each gel 5 µL of a molecular weight marker were included (BenchMark™ Protein Ladder from LifeTechnologies). For Western Blotting 10 µL of a pre-stained molecular weight marker were included (BenchMark™ Pre-stained Protein Ladder from LifeTechnologies or Precision Plus Protein™ Dual Xtra Standards from Bio-Rad). Gels were run at 15-20 mA until the bromophenol blue front, present in the samples, began to migrate out of the gel.

9.4.3 Gel Staining

After protein electrophoresis, gels were washed with H_2O MilliQ to remove SDS and stained with 0.1 % (w/v) Commassie Brilliant Blue R (Sigma-Aldrich) dissolved in methanol:acetic acid:water (5:2:5) for 15-30 min with slow agitation. Then, gels were unstained in 10 % acetic acid with a sponge that captures blue staining and accelerates the unstaining process. Once the bands were blue and the gel transparent, it was photographed with GS-800 Calibrated Densitometer (Bio-Rad) and analysed with Quantity One 4.6 software (Bio-Rad).

Alternatively, a more sensitive protein staining based in Colloidal Coomassie G-250 was used. After protein electrophoresis, gels were washed three times with H_2O MilliQ to remove SDS and stained with colloidal staining solution for 1-12 h. Gels were unstained with 10% (v/v) ethanol and 2 % (v/v) orthophosphoric acid.

Colloidal staining solution was prepared in the order as follows:

1. 100 g of aluminium sulphate was dissolved in Milli-Q water.
2. 200 mL of absolute ethanol were added.

3. 0.4 g of CBB G-250G (Sigma-Aldrich) were added to the solution and mixed.
4. As recently as the solution is completely dissolved, phosphoric acid was added. The incorporation of the acid to the alcoholic media lets the Coomassie molecules aggregate into their colloidal state.
5. Finally fill up with Milli-Q water

Changes in the order of preparation would lead to a more violet-bluish solution that is less sensitive.

Protein detection limit with Commassie staining is about 0.3-1 μg/band while for Colloidal staining the detection limit decreases to 4-8 ng protein/band.

9.4.4 Western Blot

SDS-PAGE gels, protein transfer to a PVDF membrane and all of the necessary solutions were prepared following the standard protocols described in "Molecular Cloning: A Laboratory Manual" (Sambrook et al. 2001). Mini Trans-Blot equipment (Bio-Rad) was used for protein transfer to PVDF membrane (Millipore). PVDF was activated with methanol and equilibrated in transfer buffer following manufacturer's instructions. To identify the size of the bands detected in the PVDF membrane a pre-stained molecular weight marker was used. Transfer was performed at 100 V for 1 h and membranes were incubated 1 h at room temperature with Blocking Buffer (5 % BSA (Sigma) dissolved in PBS with 0.05 % (v/v) Tween20).

Polyclonal anti-MG217 obtained in mice (Burgos et al., 2008) was used for protein detection at 1:1000 dilution in Blocking Buffer. Secondary antibodies (dil 1/5000 in Blocking Buffer) against the constant region of mouse antibodies used in the first step were used for reveal the membrane using a bioluminescence reaction catalyzed by the HRP conjugated to the secondary antibody in the presence of a specific substrate (Luminata Forte, Millipore). Bioluminescence reactions were detected using VersaDoc (Bio-Rad) and analyzed with QuantityOne software (Bio-Rad)

9.5 Epifluorescence microscopy

For fluorescence image acquisition *M. genitalium* cells were grown in 35 mm glass bottom MATTEK plates (Mattek Cooperation, PA) under standard conditions overnight. SP-4 medium was aspirated and cells were fixed with PFA 1% diluted in PBS with calcium and magnesium (PBSCM). After 10 minutes of incubation, fixation solution was removed and cells were washed with SP-4 medium and incubated for 10 minutes in SP-4. After 4 washes with PBSCM, 3 mL of PBSCM with Hoechst 33342 at 10 μg mL^{-1} and 1.2 μL of TetraSpeck (Sigma) was added to the cells. Hoechst dye was used for staining the DNA and the TetraSpeck microspheres were used to align the different fluorescent images. MATTEK plates were spun at 200 g for 10 minutes to deposit the TetraSpeck microspheres. After that, fixed cells were analyzed in an inverted microscope Nikon Eclipse TE 2000-E and image acquisition was performed using a Nikon Digital Sight DS-SMC camera controlled by NIS-Elements BR software. A set of five frames were acquired for each image: phase contrast, fluorescence image for eYFP (excited at 500 nm and collected 542 nm with an exposure time of 1700 ms), an image of the Hoechst 33342 fluorescence (excited at 387 nm and collected at 447 nm with an exposure time of 800 ms), a fluorescence image to mCherry (excited at 560 nm and collected at 630 nm with an exposure time of 4000 ms) and a final phase contrast image to verify that during acquisition cells or visual camp was not changed. Acquired images were aligned using a matlab script (Mihael Kunz, unpublished) and the distance between the different foci of each cell were measured using also a matlab script (Mihael Kunz, unpublished).

10. Appendices

10.1 Appendix I: plasmid constructions

All the primers used for constructing these plasmids are listed in Appendix II: oligonucleotides and split according to the chapter in which were used. All the constructs below were screened by restriction analysis and confirmed by Sanger sequencing.

10.1.1 Plasmids used in Chapter I

10.1.1.1 Minitransposons with eYFP

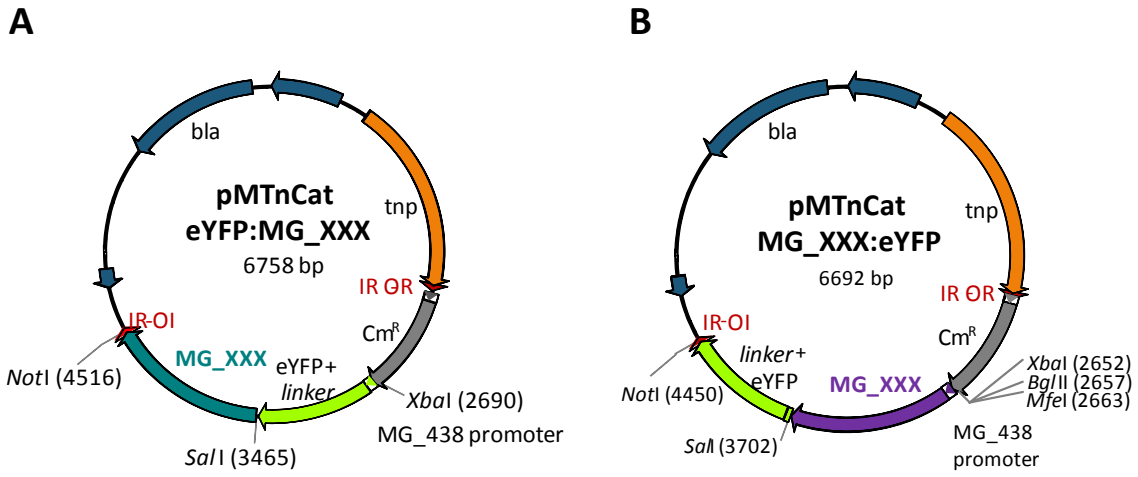

Figure 10.1. Minitransposons with eYFP fusions at N-ter or C-ter (A and B respectively) scheme. Restriction sites important for construct generation are indicated. bla indicates the ampicillin resistance gene, indicates transposase gene, IR-OR and IR-OI indicates the inverted repeats recognized by the transposase, CmR indicates the *cat* gene under the MG_438 promoter, eYFP indicates the gene coding for the eYFP, the linker is a DNA fragment coding for 10 Asn, MG_XXX indicates the place where the different genes coding for the target proteins will be ligated.

10.1.1.2 pP140:eYFP

pP140:eYFP (Figure 10.2) was constructed as follows. Left homology region (LHR) was amplified by PCR using G37 genomic DNA as a template and the primers "5 XbaI mg191 BE" and "3 XhoI mg191 BE" which incorporates the sequence recognized by XbaI and XhoI restriction enzymes respectively. The linker plus the eYFP gene were amplified by PCR from pMTnCat_eYFP_Ct (Figure 10.1B) using the oligonucleotides "5YFP-Met-Val-XhoI+linker" and "3YFPstop-MfeI" which incorporates the sequence recognized by XhoI and MfeI restriction enzymes respectively. *cat* gene under the control of MG_438 promoter was amplified from pMTnCat_eYFP_Ct (Figure 10.1B) using the oligonucleotides "5 Mfe + pM438 CmR" and "3 BamHI CmR" which incorporates the sequence recognized by MfeI and BamHI restriction enzymes respectively. Right homology region (RHR) was amplified by PCR using G37 genomic DNA as a template and the primers "5 BamHI mg191 BD" and "3 ApaI mg191 BD" which incorporates the sequence recognized by BamHI and ApaI restriction enzymes respectively. All PCR products were digested with the corresponding restriction enzymes and ligated into a pBSK previously digested with XbaI and ApaI restriction enzymes.

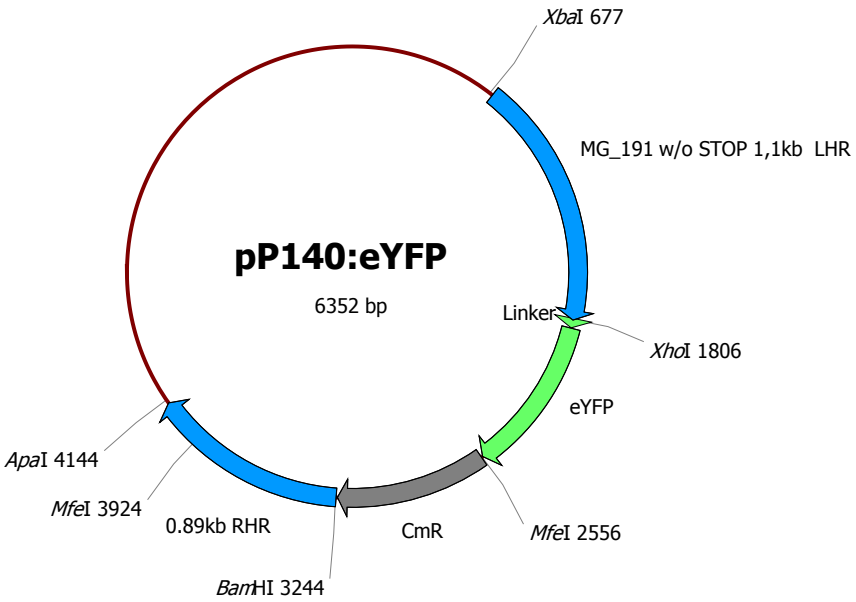

Figure 10.2. pP140:eYFP schematic representation. Restriction sites important for construct generation are indicated. LHR indicates left homology region including the last 1,1kb without the STOP codon of MG_191, linker indicates the sequence coding for 10 Asn, eYFP indicates de gene coding for the eYFP, CmR indicates the *cat* gene under the MG_438 promoter and RHR indicates the right homology region (0.89 kb).

10.1.1.3 pP110:eYFP

pP110:eYFP (Figure 10.3) was constructed as follows. Left homology region (LHR) was amplified by PCR using G37 genomic DNA as a template and the primers "5 XbaI mg192 BE" and "3 XhoI mg192 BE" which incorporates the sequence recognized by XbaI and XhoI restriction enzymes respectively. The linker plus the eYFP gene were amplified by PCR from pMTnCat_eYFP_Ct (Figure 10.1B) using the oligonucleotides "5YFP-Met-Val-XhoI+linker" and "3YFPstop-MfeI" which incorporates the sequence recognized by XhoI and MfeI restriction enzymes respectively. *cat* gene under the control of MG_438 promoter was amplified from pMTnCat_eYFP_Ct (Figure 10.1B) using the oligonucleotides "5 Mfe + pM438 CmR" and "3 BamHI CmR" which incorporates the sequence recognized by MfeI and BamHI restriction enzymes respectively. Right homology region (RHR) was amplified by PCR using G37 genomic DNA as a template and the primers "5 BamHI mg192 BD" and "3 ApaI mg192 BD" which incorporates the sequence recognized by BamHI and ApaI restriction enzymes respectively. All PCR products were digested with the corresponding restriction enzymes and ligated into a pBSK previously digested with XbaI and ApaI restriction enzymes.

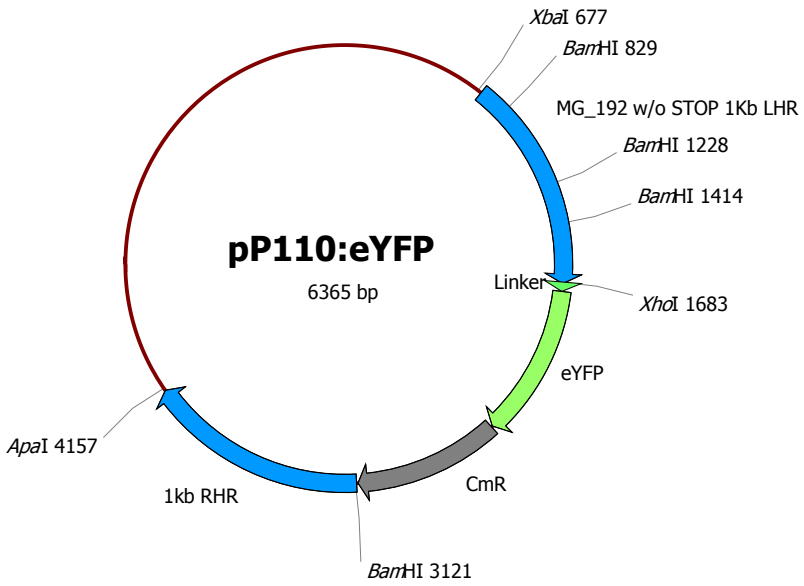

Figure 10.3. pP110:eYFP schematic representation. Restriction sites important for construct generation are indicated. LHR indicates left homology region including the last 1 kb without the STOP codon of MG_192, linker indicates the sequence coding for 10 Asn, eYFP indicates de gene coding for the eYFP, CmR indicates the *cat* gene under the MG_438 promoter and RHR indicates the right homology region (1 kb).

10.1.2 Plasmids used in Chapter II

10.1.2.1 pGmRS

pGmRS (Figure 10.4) was constructed as follows. The *aac(6')-aph(2")* gene that confers gentamycin resistance was amplified by PCR from pMTnGm (REF) using the primers 5_BamHI_pM438-GmRshort and 3_BamHI_GmR_short. The amplification with these primers only include the ORF region (excluding the inverted repeats flanking the *aac(6')-aph(2")* gene) and incorporate the MG_438 promoter at the 5'-end. This PCR product was digested with BamHI digested and ligated to a BamHI digested pBSK.

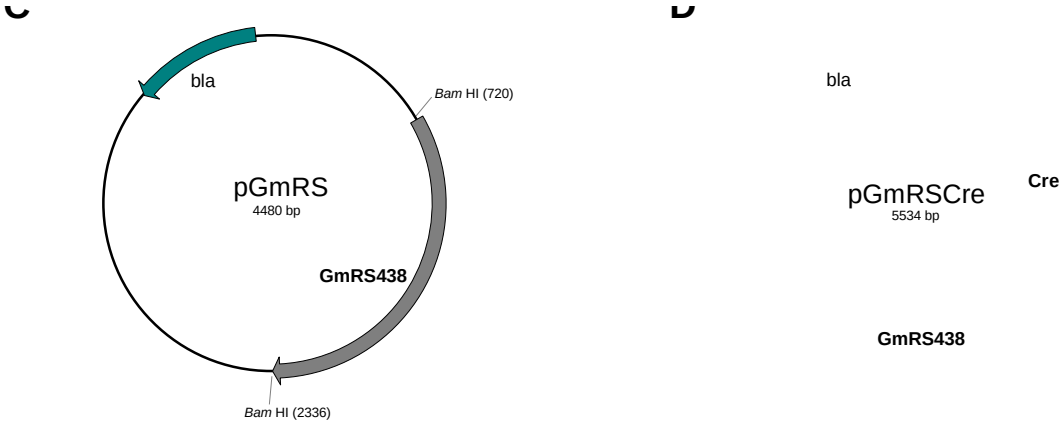

Figure 10.4: pGmRS schematic representation. Restriction sites important for construct generation are indicated. bla indicates the ampicillin resistance gene, GmRS438 indicates the aac(6′)-aph(2″) gene under the MG_438 promoter.

10.1.2.2 pMTnTc66Cat66

pMTnTc66Cat66 (Figure 10.5) was constructed as follows. *cat* gene was amplified by PCR from pMTnCat (REF) using the primers 5_SpeI_lox66_PstI_pmg438_CmR and 3_ApaI_lox66_SalI_CmR. The first one incorporates the sequence of lox66 between SpeI and PstI restriction sites, while the second primer incorporates the lox66 sequence between ApaI and SalI restriction sites. This PCR product was digested with SpeI and ApaI restriction enzymes, mixed with EcoRI-SpeI digested tetracycline resistance gene excised from pMTnTetM438 (Pich et al., 2006b) and ligated to the vector pMTn4001 (Pich et al., 2006b) previously digested with EcoRI and ApaI.

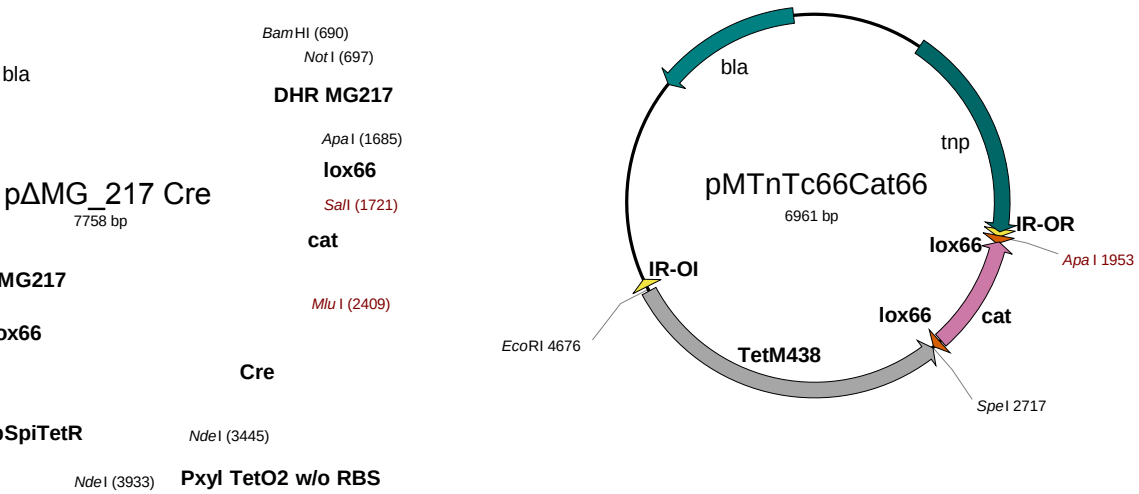

Figure 10.5. pMTnTc66Cat66 schematic representation. Restriction sites important for construct generation are indicated. Unique restriction sites are shown in red. bla indicates the ampicillin resistance gene, tnp indicates transposase gene, IR-OR and IR-OI indicates the inverted repeats recognized by the transposase, lox66 indicates the lox66 sequences, cat indicates the chloramphenicol resistance gene under the control of MG_438 promoter, TetM438 indicates tetracycline resistance gene under the control of MG_438 promoter.

10.1.2.3 pGmRSCre

pGmRCre (Figure 10.6) was constructed as follows. Cre recombinase gene was amplified by PCR from pSH62 (Gueldener et al., 2002) using the primers 3_MluI_Cre and 5_pM438Cre, which incorporates the sequence of MG_438 promoter. The PCR product was then ligated to vector pGmR previously digested with EcoRV.

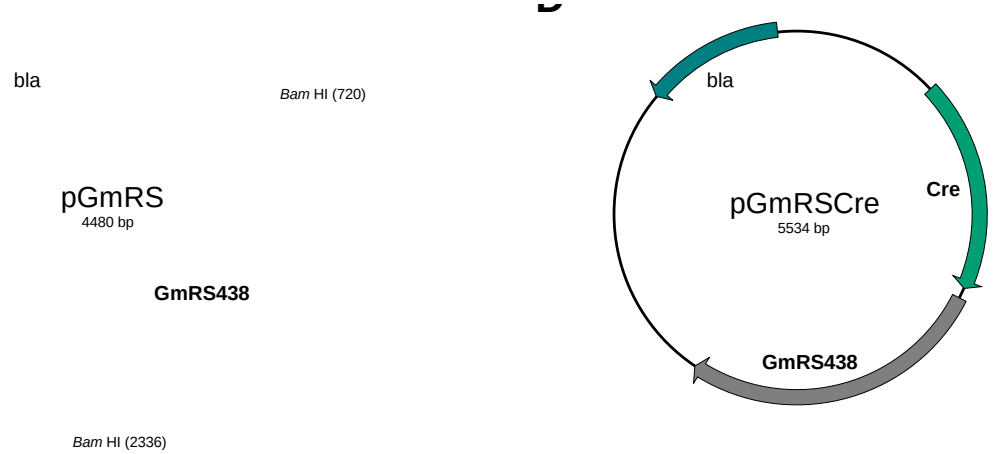

Figure 10.6. pGmRSCre schematic representation. bla indicates the ampicillin resistance gene, Cre indicates the Cre recombinase coding gene under the control of MG_438 promoter and GmRS438 indicates the aac(6′)-aph(2″) gene under the MG_438 promoter.

10.1.2.4 pΔMG_217Cre

pΔMG_217Cre (Figure 10.7) was constructed as follows. First, TetR repressor under spiralin promoter control was amplified by PCR from pMT85-XTST (Breton et al., 2010) using the primers 5 KpnI Pspi-TetR and 3 SpeI lox 66 PstI TetR, which incorporates the lox66 sequence between SpeI and PstI restriction sites. This PCR fragment was then digested with SpeI and KpnI to generate cohesive ends. Xylose promoter including TetO regions (Pxyl/$TetO_2$) was amplified using the primers 5_KpnI_Pxyl/TetO2 and 3_NcoI_Pxyl/TetO2 from pMT85-XTST. This PCR product was KpnI – NcoI digested and ligated into a Litmus28 vector restricted with the same enzymes. Then, an ExSite mutagenesis PCR (Williams et al., 2007) was performed using the primers 5_NdeI_TetO2 and 3_NdeI_Litmus28 in order to modify the inducible promoter by deleting the region from nt 7200 to nt 7276 of pMT85-XTST, which includes the RBS sequence, obtaining in this way the Pxyl/$TetO_2$mod promoter cassette (see Appendix V: pXyl/$TetO_2$mod promoter). Cre recombinase was amplified by PCR from pSH62 (Gueldener et al., 2002) using the primers 5_NdeI_Cre and 3_MluI_Cre and digested with NdeI and MluI. *cat* gene was amplified from pMTnCat (Calisto et al., 2012) using the primers 5_MluI_pmg438_CmR and 3_ApaI_lox66_SalI_CmR, which incorporate the sequence of lox66 between the ApaI and SalI restriction sites. This PCR fragment was then digested with MluI and ApaI. Pxyl/$TetO_2$mod was excised from Litmus28 using the NdeI and MluI sites, mixed with the digested PCR products and ligated into a pBSK previously digested with SpeI and ApaI restriction enzymes. The resulting plasmid was named pBSK-TetR-Pxyl/TetO-Cre-cat. In a second step, a 919-bp PCR fragment containing the upstream homology region (UHR) and 60 bp of the 5' end of MG_217 was amplified by using the primers 5_XhoI_SacI_BE_mg217 and 3_SpeI_AscI_BE_mg217. The resulting PCR fragment was digested with XhoI and SpeI. Another 976 bp PCR fragment containing the last 139 bp of MG_217 and the corresponding downstream homology region (DHR) was amplified using the primers 5_ApaI_BD_mg217 and 3_BamHI_NotI_BD_mg217 and further digested with ApaI and BamHI. Finally, both PCR fragments were mixed with the 2.9 kb SpeI-ApaI fragment from pBSK-TetR-Pxyl/TetO-Cre-cat and ligated to a pBSK previously digested with XhoI and BamHI.

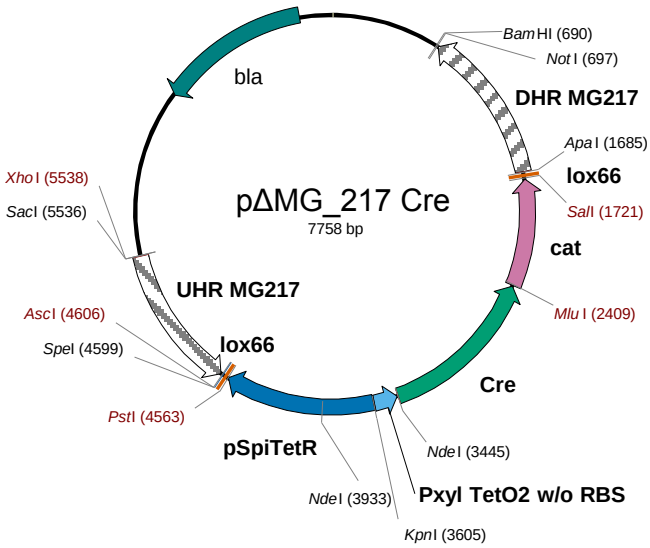

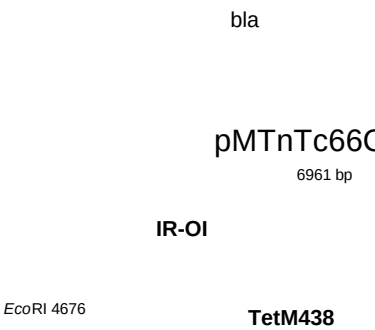

Figure 10.7. pΔMG_217Cre schematic representation. Restriction sites important for construct generation are indicated. Unique restriction sites are shown in red. bla indicates the ampicillin resistance gene, DHR indicates downstream homology region, cat indicates the *cat* gene under the MG_438 promoter, Cre indicates *Cre* gene, PxylTetO2 w/o RBS indicates the Pxyl$TetO_2$mod promoter (see Appendix V: pXyl/TetO2mod promoter), pSpiTetR indicates the TetR repressor under the control of the spiralin promoter and UHR indicates the upstream homology region.

10.1.3 Plasmids used in Chapter III

10.1.3.1 TnPac_dCas9ind

TnPac_dCas9ind was constructed as follows. A synthetic version of Cas9 gene from *Streptococcus pyogenes* codon optimized for expression in *M. pneumoniae* was purchased to GenScript. Nuclease activity of Cas9 was abolished by introducing D10A and H840A mutations (8). First, Cas9 was amplified using 5_BamHI_pxyl_dCas9 and 3_SalI_dCas9 oligonucleotides including BamHI and SalI sites and introducing the D10A mutation. Then, a second Cas9 fragment was amplified using 5_SalI_dCas9_H840A and 3_AatII_Cas9 oligonucleotides including SalI and AatII sites and introducing mutation H840A. Both PCR products were purified and digested with the corresponding restriction enzymes. A third DNA fragment including the sequence coding for the sgRNA targeting Venus gene under the control of MG_438 constitutive promoter (3) was synthesized by GenScrip. This fragment was flanked by AatII and MreI sites and the sgRNA sequence was based in the sgRNA targeting GFP gene previously described (9). An additional DNA fragment containing the TetR repressor and pXyl/TetO2mod promoter was obtained by digesting plasmid pΔMG_217Cre (10) with PstI and BamHI. All these fragments were finally ligated into a modified TnPac minitransposon (10) previously digested with PstI and MreI.

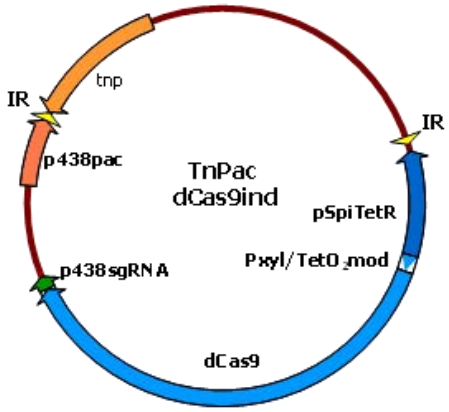

Figure 10.8. TnPacdCas9ind schematic representation. tnp indicates transposase gene, IR indicates the inverted repeats recognized by the transposase, dCas9 indicates *dCas9* gene, PxylTetO$_2$mod indicates the PxylTetO$_2$mod promoter (see Appendix V: pXyl/TetO2mod promoter), pSpiTetR indicates the TetR repressor under the control of the spiralin promoter, p438sgRNA indicates the sgRNA targeting the Venus gene under the control of the MG_438 promoter (see Figure 6.3) and p438pac indicates the gene coding for puromycin resistance gene under the control of MG_438 promoter,.

10.1.3.2 TnPac_dCas9cons

To obtain the TnPac_dCas9cons construct, first dCas9 was amplified from TnPac_dCas9ind using the primer 5_PstI_p438_Cas9, which includes MG_438 constitutive promoter and a PstI site, and primer 3_AatII_Cas9, which includes an AatII site. The PCR product was purified and PstI – AatII digested. A second DNA fragment containing the sgRNA targeting Venus gene was obtained by digesting plasmid *miniTnPac_dCas9ind* with AatII and MreI. Both fragments were ligated into a modified TnPac minitransposon (10) previously digested with PstI and MreI.

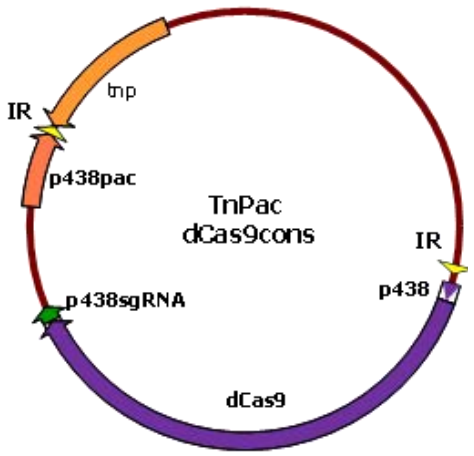

Figure 10.9. TnPac dCas9cons schematic representation. tnp indicates transposase gene, IR indicates the inverted repeats recognized by the transposase, dCas9 indicates *dCas9* gene under the control of MG_438 promoter, p438sgRNA indicates the sgRNA targeting the Venus gene under the control of the MG_438 promoter (see Figure 6.3) and p438pac indicates the gene coding for puromycin resistance gene under the control of MG_438 promoter.

10.2 Appendix II: oligonucleotides

10.2.1 Oligonucleotides used in Chapter I

A. eYFP N-ter fusions (transposition)

Name	Sequence	Tm
5mg200-ATG-Sal	gctactgtcgacGCTGAACAGAAACGTGATTATTATGAAGTG	63.78
3mg200-Not	gctactgcggccgcCTAACTAATGGGTTCTTGGGAGAGGTATTG	64.63
5mg217-ATG-Sal	tacctagtcgacGAAAAAAATAGATCAGCTTTTCAACAAAAC	61.61
3mg217-Not	tacctagcggccgcTTATTCATAGAAGTCATCACGGTAACC	59.55
5mg218-ATG-Sal	gctactgtcgacAAACCATTTGATAAAAAACCTTCGCTG	63.99
3mg218-Not	gctactgcggccgcTTATTTACTTGCTGCTTTTTGGGCAATC	65.62
5mg219-ATG-Sal	gctactgtcgacAATAGTGATAGTGATCTAAAACTCCAAAAG	58.04
3mg219-Not	attggcggccgcTTAAGATCTGGTTTTTTTATTGC	53.47
5mg269-ATG-Sal	gctactgtcgacAATAATTTTGATTACTATAGAGACTTTGATG	55.73
3mg269-Not	gctactgcggccgcTTAATCAATTAATTTACTAACCCTGTTAATAG	56.73
5mg301-ATG-Sal	gctactgtcgacGCAGCAAAGAATAGAACCATTAAGG	60.28
3mg301-Not	gctactgcggccgcTTAGAGCTTAGCACAATAGCTAACTACTCTC	59.64
5mg305-ATG-Sal	gctactgtcgacAGTGCAGACAATGGTTTAATTATTG	57.34
3mg305-Not	gctactgcggccgcTTATTTTGCTTGTGGACCTTGTTC	60.20
5mg312-ATG-Sal	gctactgtcgacGCTAAAAACAAGCAATCGGTTTTTGAAG	65.37
3mg312-Not	gctactgcggccgcTTAATAATCAAGGCTAAAATCACCACTGCTTTC	66.25
5mg317-ATG-Sal	gctactgtcgacAACGATAAACAGAAAGCTAAAATAAACAAAG	60.63
3mg317-Not	gctactgcggccgcTTAAAAGTCCTTAGATCAATATGATCTTGATG	61.13
5mg386-ATG-Sal	gctactgtcgacCCAAAAACAACAAAGAATAAAAACAAAAAC	61.95
3mg386-Not	gctactgcggccgcCTATTTTTTATCATTACTGCCAAAAACATC	60.42
5mg353-ATG-Sal	gctactgtcgacGAAAAAACATCAAATACAAGTAAGCCAC	60.31
3mg353-Not	gctactgcggccgcTTAGTCTGCGTACTTTCAACGCAC	61.50
5mg451-ATG-Sal	gctactgtcgacGCAAGAGAGAAATTTGACCGTTC	60.07
3mg451-Not	gctactgcggccgcCTATTCTAGAACTTCTGTTACAGTGCCTG	60.09

B. eYFP C-ter fusions (transposition)

Name	Sequence	Tm
5mg200-MfeI+pM438	gctactcaattg*tagtatttagaattaataaagt*ATGGCTGAACAGAAACGTG	65.55
3mg200 w/o STOP SalI	gctactgtcgacACTAATGGGTTCTTGGGAGAG	64.55

5mg201-BglII+pMG438	gctactagatct*tagtatttagaattaataaagt*ATGTGTGAAAAATCACAAACAATTAAAGAG	61.56
3mg201- w/o STOP SalI	gctactgtcgacTGATTTTTTATTACCTTTGCTGACAAATAC	60.81
5mg239-MfeI+pMG438	gctactcaattg*tagtatttagaattaataaagt*ATGCCCGTTACGAAGAAAAGTC	60.30
3mg239 w/o STOP SalI	gctactgtcgacACTGAAAAGCTTGTTGTAGATATCACTGTATTC	62.21
5mg301-Xba+BglII +MfeIpMG438	gctacttctagagatctcaattg*tagtatttagaattaataaagt*ATGGCAGCAAAGAATAGAACCATTAAG	62.55
3mg301-STOP-Sal	gctactgtcgacGAGCTTAGCACAATAGCTAACTACTCTCACTAG	61.78
5mg386-BglII+pMG438	gctactagatct**c***tagtatttagaattaataaagt*ATGCCAAAAACAACAAAGAATAAAAAC	60.57
3-Nter-mg386-MfeI	gctacCAATTGTTTCTGGTTCAAAAGCAG	60.79
5-Cter-mg386-MfeI	gctacCAATTGAAACCCAATTAGAACCTAG	58.13
3-cter-mg386-STOP-Sal	gctactgtcgacTTTTTTATCATTACTGCCAAAAACATC	59.55
5mg355-BglII+pMG438	gctactagatct*tagtatttagaattaataaagt*ATGAATATTAATTTCACACCTGCTGGTG	63.00
3mg355 w/o STOP SalI	gctactgtcgacAGACTTATTATTTTGTGTAATGGTAATATTGTCTTTAACAAC	63.91
5YFP-Met-Val-Sal+**linker**	gctactgtcgac**aacaataacaacaataataataataac**AGCAAGGGCGAGGAGCTGTTC	65.96
3YFPstop-NotI	gctactgcggccgcCTACTTGTACAGCTCGTCAATGCCGAG	66.74

C. P110 eYFP C-ter fusion (homologous recombination)

Name	**Sequence**	**Tm**
5 XbaI mg192 BE	gctacttctagaACCAAGCCATGATGGTAAACAAACTCCTGTC	70.35
3 XhoI mg192 BE	gctactctcgagACTTTTGGTTTCTTCTGACTTAACTTCAACAGCTTTTTGTTC	71.47
5YFP-Met-Val-XhoI+**linker**	gctactctcgagAACAATAACAACAATAATAATAATAATAACAGCAAG	59.80
3YFPstop-MfeI	gctactgaattcCTACTTGTACAGCTCGTCAATGCCGAG	66.74
5 Mfe + pM438 CmR	gctactgaattc*tagtatttagaattaataaagt*ATGGAGAAAAAAATCACTGGATATACCAC	62.36
3 BamHI CmR	gctacggatccTTACGCCCCGCCCTGCCAC	71.17

5 BamHI mg192 BD	gctacggatccTTTTTAACCTTTCAATAACCTAAAACACAATCTTTAAAAC	65.66
3 ApaI mg192 BD	gctactgggcccTATTGTTACCTTGTTTGCGATACCCAG	63.23

D. P140 eYFP C-ter fusion (homologous recombination)

Name	Sequence	Tm
5 XbaI mg191 BE	gctactTCTAGACAGTGATGGTACCCCTAAATCACTG	65.91
3 XhoI mg191 BE	gctactctcgagTTGTTTTACTGGAGGTTTTGGTGGGGTTTTAG	69.57
5 BamHI mg191 BD	gctactggatccGATGAAAACAATGAGAAAACAGATTTATAAAAAAG	63.09
3 ApaI mg191 BD	gctactgggcccATAATAGAGTTGGGTGATAACATTTCTTGGG	63,97

E. Oligonucleotides for sequencing reactions

Name	Sequence	Tm
YFPseqUPS	GCGAAGCACTGCAGGCCGTAGCCGAAGGTGGTCACGAGG	87.30
SeqTnp3	GATTCATGATTATATCGATCAAC	51.60
Fup-17	GTAAAACGACGGCCAGT	52.81
Rup-17	GGAAACAGCTATGACCATG	52.31
CmseqUPS	CAACGGTGGTATATCCAG	50.32
CmseqDWS	ATGAATTACAACAGTACTG	40.72
SeqMgpa5	TAATCAATGACACCAGCTTTGGGTT	63.49
SeqMgpa9	CCTAACCCAGTGATGAGTGGTAAG	59.76
SeqMgpa9.1Rev	TCCACCGCACTCTCAGCAGCTGTG	71.78

10.2.2 Oligonucleotides used in Chapter II

Name	Sequence	Use
5 BamHI **pM438**-GmRshort	gctactggatcc**tagtatttagaattaataaagt**ATGAATATAGTTGAAAATGAAATATGTATAAG	Cloning
3 BamHI GmR short	gctactggatccCTATTTAATACTAATGTCTTTTATAATAGCTTTTC	Cloning
5 XhoI SacI BE mg217	gctactctcgaggagctcGGCCTGGAGCTGCAACC	Cloning
3 SpeI AscI BE mg217	gctactactagtggcgcgccGTTAAAAGGTTGGTTTGATGC	Cloning
5 KpnI Pspi-TetR	gctactggtaccAATTAAAAGTTAGTGAACAAGAAAACAGTG	Cloning
3 SpeI **lox 66** PstI TetR	gctactactagt**taccgttcgtataatgtatgctatacgaagttat**ctgcagTTAAGACCCACTTTCACATTTAAGTTG	Cloning
5 NdeI TetO2	gctactcatatgCTCTATCAATGATAGAGGATCCCGTTAATTATACTC	Exsite
3 NdeI Litmus28	gctactcatatgAAGCTTCGTGGATCCAGATATCCTG	Exsite
5 **pM438** Cre	**tagtatttagaattaataaagt**ATGTCCAATTTACTGACCGTACAC	Cloning
5 NdeI Cre	gctactcatATGTCCAATTTACTGACCGTACACCAAAATTTG	Cloning
3 MluI Cre	gctactacgcgtCTAATCGCCATCTTCCAGCAG	Cloning
5 MluI **pmg438** CmR	gctactacgcgtTAGTATTTAGAATTAATAAAGTATGGAGAAAAAAATC	Cloning
5 SpeI **lox66** PstI **pmg438** CmR	gctactactagt**taccgttcgtataatgtatgctatacgaagttat**ctgcag**tagtatttagaattaataaagt**ATGGAGAAAAAAATCACTGGATATACCAC	Cloning
3 ApaI **lox66** SalI CmR	gctactgggccc**ataacttcgtatagcatacattatacgaacggta**gtcgacTTACGCCCCGC	Cloning
5 PstI **pM438**-CmR	gctactctgcag**tagtatttagaattaataaagt**ATGGAGAAAAAAATCACTGGATATACCAC	Cloning
3 SalI CmR	gctactgtcgacTTACGCCCCGCCCTGCCAC	Cloning
5 ApaI BD mg217	gctactgggcccTTTATTGAGAACTACATTACCC	Cloning
3 BamHI NotI BD mg217	gctactggatccgcggccgcTTATCAACTAACTCTTGTTTGG	Cloning
qPCR CmDWS	tatacgcaaggcgacaaggt	qPCR
qPCR 217BD_UPS	ggggttgagggggtaatgta	qPCR
qPCR 217BE_DWS	ttcatattaaagcgcatggaaa	qPCR
qPCR 216 F	GGGTGATTTGGGCCTTGAAA	qPCR
qPCR 216 R	CCACTAGCAGTTTCCCCACT	qPCR
3 screening D217	GCATTTTGCTTGGTAATACCATC	Screening
5 screening D217	ATGGTGATTTAGAAAAACTCAAACAG	Screening
Seq Cre UPS	AACATCTTCAGGTTCTGCGGGAAACCATTTC	Sequence
Seq Cre DWS	GAGTTTCAATACCGGAGATC	Sequence
Seq 5 IR-OR - Lox66 3'	TAAAAGGGCCCATAACTTCG	Sequence
Seq tet DWS	AGAAATCCCTGCTCGGTGTA	Sequence

10.2.3 Oligonucleotides used in Chapter III

Name	Sequence	Use
5_PstI_**p438**_Cas9	attcccctgcag**tagtatttagaattaataaagt**ATGGATAAGAAATACTCAATAGGCTTAG	Cloning
5_BamHI_pxyl_dCas9	attcccggatcctctatcattgatagagcatATGGATAAGAAATACTCAATAGGCTTAGcTATCGGCACAAATAGCGTCGGATGG	Cloning
3_SalI_dCas9	attcccgTCGACATCATAATCACTTAAACGATTAATATCTAATTCTTG	Cloning
5_SalI_dCas9_H840A	attcccgTCGACgctATTGTTCCACAAAGTTTCCTTAAAGACGATTC	Cloning
3_AatII_Cas9	attcccgacgtcTTAGTCACCTCCTAGCTGACTCAAATCAATG	Cloning
5_AatII_**p438**_guidedvenus	attcccgacgtc**TAGTATTTAGAATTAATAAAGT**GACCAGGATGG	Cloning
3_MreI_guidedvenus	attccccgccggcgAAAAAAAGCACCGACTCGGTGCC	Cloning
Seq_Pxyl_Down	taccaattccagagtctccatatatg	Sequencing
seq_cas9mut_SalI_Down	caattgcaaaatgaaaagctctatctc	Sequencing
seq_cas9mut_SalI_Up	cttggaacgttatccgatttacc	Sequencing
seq_cas9_Down	tgatacaacaattgatcgtaaacg	Sequencing
5 qPCR Venus	GAGCGCACCATCTTCTTCA	qPCR
3 qPCR Venus	ATGCCGTTCTTCTGCTTGTC	qPCR
5 qPCR mpn617	TTCGCGGCAAGAATAAAGTT	qPCR
3 qPCR mpn617	AGACCAGTTTGTCGGATTGTTT	qPCR
5 qPCR mpn208	ATCGCTAAACGGGTTGATGT	qPCR
3 qPCR mpn208	CGCCAAAGAACTTCTCCAAG	qPCR
5 qPCR mpn515	GACTACCGCAAGGGGAAGAT	qPCR
3 qPCR mpn515	TTAGCCTTCCGTAACGCATC	qPCR

10.3 Appendix III: Transposon localization of the selected clones bearing the different eYFP fusions

Mutant	Protein fused to eYFP	Transposon localization			
		Truncated gene	Description of the protein truncated	Insertion point	% truncation
P32ch eYFP:MG_217 c5	MG217	Intergenic region	-	158315	-
P32ch eYFP:MG_218 c1	HMW2	Intergenic region	-	168342	-
P32ch eYFP:MG_219 c2	P24	Intergenic region	-	349211	-
P32ch eYFP:MG_269 c5	MG269	MG_140	Hypothetical protein (*hot spot*)	178396	22,4
P32ch eYFP:MG_305 c1	DnaK	MG_226	Membrane permease (APC transporter)	272302	68,7
P32ch eYFP:MG_312 c4	HMW1	MG_226	Membrane permease (APC transporter)	273055	17,79
P32ch eYFP:MG_317 c1	HMW3	MG_140	Hypothetical protein (*hot spot*)	178237	27,21
P32ch eYFP:MG_353 c2	HU	MG_285	Hypothetical protein (*hot spot*)	347895	34,80

P32ch eYFP:MG_451 c2	EF-Tu	MG_414	Hypothetical protein (*hot spot*)	518435	70,42
P32ch MG_191:eYFP c2	P140	-	-	-	-
P32ch MG_192:eYFP c1	P110	-	-	-	-
P32ch MG_200:eYFP c8	MG200	R1-R2 box	-	313325	-
P32ch MG_201:eYFP c1	GrpE	Intergenic region	-	174834	-
P32ch MG_239:eYFP c2	Lon	Intergenic region	-	555637	-
P32ch MG_355:eYFP c1	ClpB	MG_226	Membrane permease (APC transporter)	272131	80,31
P32ch MG_386:eYFP c2	MG386	Intergenic region	-	313875	

10.4 Appendix IV: Statistical analysis of fluorescence distances

10.4.1 Distance between P32 protein and DNA

Hypothesis Test Summary

	Null Hypothesis	Test	Sig.	Decision
1	The distribution of Distance is the same across categories of Mutant.	Independent-Samples Jonckheere-Terpstra Test for Ordered Alternatives	,065	Retain the null hypothesis.

Asymptotic significances are displayed. The significance level is ,05.

Independent-Samples Jonckheere-Terpstra Test for Ordered Alternatives

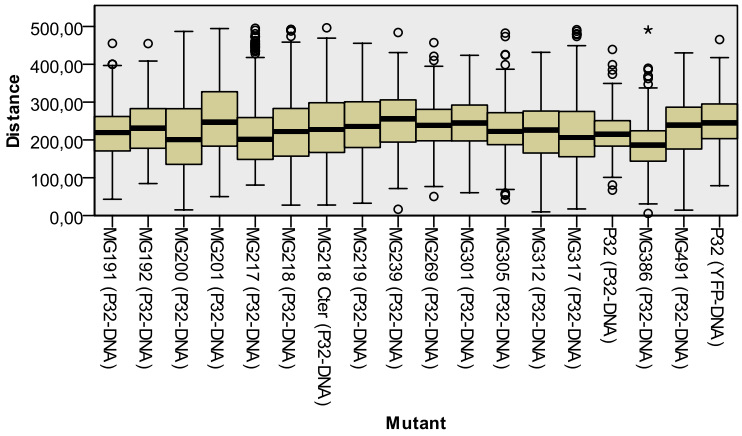

Total N	4.799
Test Statistic	5.515.553,000
Standard Error	55.307,600
Standardized Test Statistic	1,846
Asymptotic Sig. (2-sided test)	,065

1. Multiple comparisons are not performed because the overall test does not show significant differences across samples.

10.4.2 Distance between target protein fused with eYFP and DNA

Hypothesis Test Summary

	Null Hypothesis	Test	Sig.	Decision
1	The distribution of Distance is the same across categories of Mutant.	Independent-Samples Jonckheere-Terpstra Test for Ordered Alternatives	,000	Reject the null hypothesis.

Asymptotic significances are displayed. The significance level is ,05.

Independent-Samples Jonckheere-Terpstra Test for Ordered Alternatives

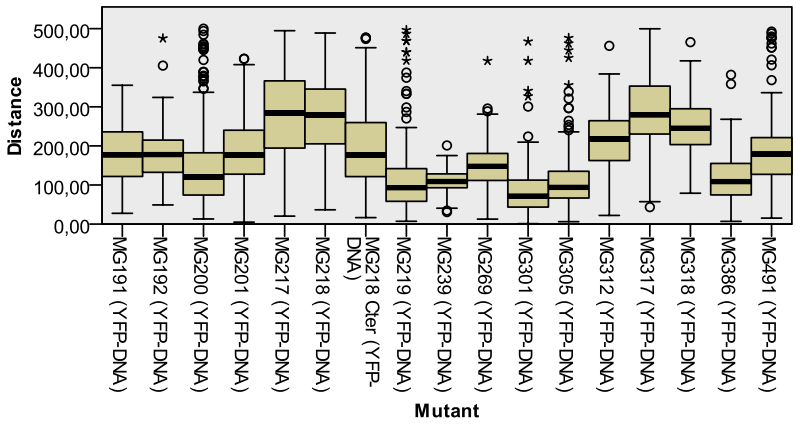

Total N	4.589
Test Statistic	4.730.416,000
Standard Error	51.687,199
Standardized Test Statistic	-3,622
Asymptotic Sig. (2-sided test)	,000

10.5 Appendix V: pXyl/TetO$_2$mod promoter

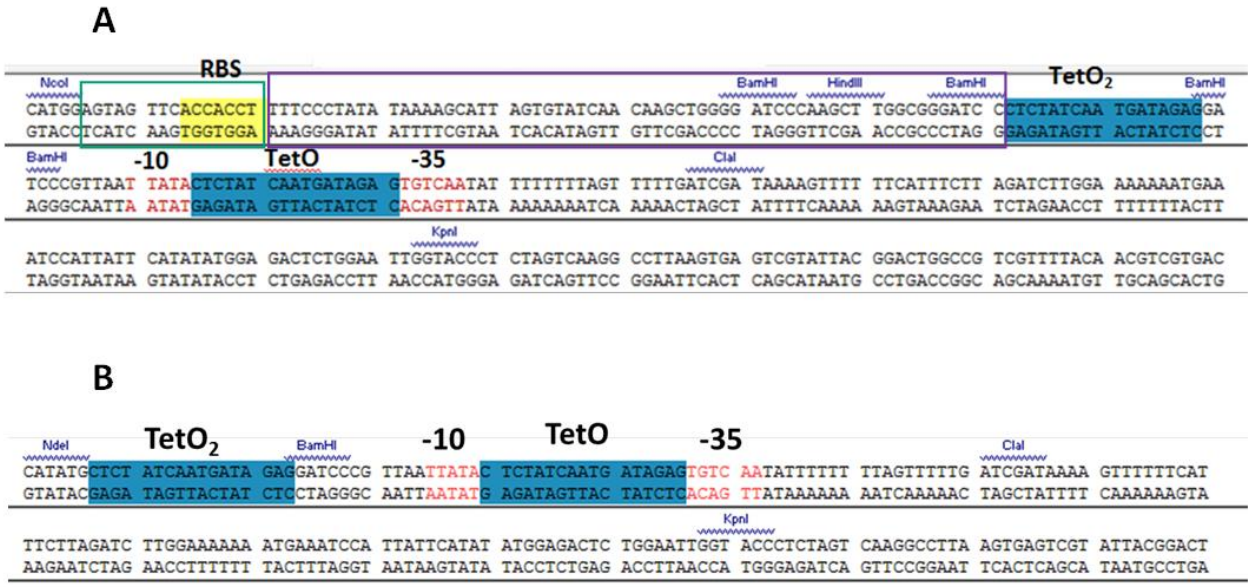

Figure 10.10. Structure of Pxyl/TetO$_2$ and Pxyl/TetO$_2$mod promoters. A. Sequence of Pxyl/TetO$_2$ promoter from pMT85-XTST (Breton et al., 2010). **B.** Sequence of Pxyl/TetO$_2$mod promoter generated in this work. Sequence highlighted in yellow corresponds to RBS, blue highlighted sequence corresponds to TetO operator region, red sequences correspond to -35 and -10 boxes. The sequence enclosed in the green rectangle including the RBS and the sequence enclosed in the purple rectangle (apparently non-functional in pMT85-XTST) were removed to create Pxyl/TetO$_2$mod promoter.

11. Bibliography

ALBERT, H., DALE, E. C., LEE, E. & OW, D. W. 1995. Site-specific integration of DNA into wild-type and mutant lox sites placed in the plant genome. *Plant J,* 7**,** 649-59.

ALGIRE, M. A., LARTIGUE, C., THOMAS, D. W., ASSAD-GARCIA, N., GLASS, J. I. & MERRYMAN, C. 2009. New selectable marker for manipulating the simple genomes of Mycoplasma species. *Antimicrob Agents Chemother,* 53**,** 4429-32.

BALASUBRAMANIAN, S., KANNAN, T. R. & BASEMAN, J. B. 2008. The surface-exposed carboxyl region of Mycoplasma pneumoniae elongation factor Tu interacts with fibronectin. *Infect Immun,* 76**,** 3116-23.

BALISH, M. F. 2014. Mycoplasma pneumoniae, an Underutilized Model for Bacterial Cell Biology. *Journal of Bacteriology,* 196**,** 3675-3682.

BALISH, M. F., HAHN, T. W., POPHAM, P. L. & KRAUSE, D. C. 2001. Stability of Mycoplasma pneumoniae cytadherence-accessory protein HMW1 correlates with its association with the triton shell. *Journal of Bacteriology,* 183**,** 3680-3688.

BALISH, M. F., SANTURRI, R. T., RICCI, A. M., LEE, K. K. & KRAUSE, D. C. 2003. Localization of Mycoplasma pneumoniae cytadherence-associated protein HMW2 by fusion with green fluorescent protein: implications for attachment organelle structure. *Mol Microbiol,* 47**,** 49-60.

BEARE, P. A., LARSON, C. L., GILK, S. D. & HEINZEN, R. A. 2012. Two systems for targeted gene deletion in Coxiella burnetii. *Appl Environ Microbiol,* 78**,** 4580-9.

BLAYLOCK, M. W., MUSATOVOVA, O., BASEMAN, J. G. & BASEMAN, J. B. 2004. Determination of infectious load of Mycoplasma genitalium in clinical samples of human vaginal cells. *J Clin Microbiol,* 42**,** 746-52.

BRETON, M., SAGNE, E., DURET, S., BEVEN, L., CITTI, C. & RENAUDIN, J. 2010. First report of a tetracycline-inducible gene expression system for mollicutes. *Microbiology,* 156**,** 198-205.

BROACH, J. R., GUARASCIO, V. R. & JAYARAM, M. 1982. Recombination within the yeast plasmid 2mu circle is site-specific. *Cell,* 29**,** 227-34.

BROTO, A. 2014. *Anàlisi funcional de dominis de proteïnes implicades en la motilitat de Mycoplasma genitalium* . Universitat Autònoma de Barcelona.

BURGOS, R., PICH, O. Q., FERRER-NAVARRO, M., BASEMAN, J. B., QUEROL, E. & PINOL, J. 2006. Mycoplasma genitalium P140 and P110 cytadhesins are reciprocally stabilized and required for cell adhesion and terminal-organelle development. *J Bacteriol,* 188**,** 8627-37.

BURGOS, R., PICH, O. Q., QUEROL, E. & PINOL, J. 2007. Functional analysis of the Mycoplasma genitalium MG312 protein reveals a specific requirement of the MG312 N-terminal domain for gliding motility. *J Bacteriol,* 189**,** 7014-23.

BURGOS, R., PICH, O. Q., QUEROL, E. & PINOL, J. 2008. Deletion of the Mycoplasma genitalium MG_217 gene modifies cell gliding behaviour by altering terminal organelle curvature. *Mol Microbiol,* 69**,** 1029-40.

CALISTO, B. M., BROTO, A., MARTINELLI, L., QUEROL, E., PINOL, J. & FITA, I. 2012. The EAGR box structure: a motif involved in mycoplasma motility. *Mol Microbiol,* 86**,** 382-93.

CAZANAVE, C., MANHART, L. E. & BEBEAR, C. 2012. Mycoplasma genitalium, an emerging sexually transmitted pathogen. *Med Mal Infect,* 42**,** 381-92.

CLOWARD, J. M. & KRAUSE, D. C. 2009. Mycoplasma pneumoniae J-domain protein required for terminal organelle function. *Mol Microbiol,* 71**,** 1296-307.

CLOWARD, J. M. & KRAUSE, D. C. 2010. Functional domain analysis of the Mycoplasma pneumoniae co-chaperone TopJ. *Mol Microbiol,* 77**,** 158-69.

CLOWARD, J. M. & KRAUSE, D. C. 2011. Loss of co-chaperone TopJ impacts adhesin P1 presentation and terminal organelle maturation in Mycoplasma pneumoniae. *Molecular Microbiology,* 81**,** 528-539.

CORDOVA, C. M., LARTIGUE, C., SIRAND-PUGNET, P., RENAUDIN, J., CUNHA, R. A. & BLANCHARD, A. 2002. Identification of the origin of replication of the Mycoplasma pulmonis chromosome and its use in oriC replicative plasmids. *J Bacteriol,* 184**,** 5426-35.

CORMACK, B. P., VALDIVIA, R. H. & FALKOW, S. 1996. FACS-optimized mutants of the green fluorescent protein (GFP). *Gene,* 173**,** 33-8.

CHANG, H. Y., JORDAN, J. L. & KRAUSE, D. C. 2011. Domain analysis of protein P30 in Mycoplasma pneumoniae cytadherence and gliding motility. *J Bacteriol,* 193**,** 1726-33.

CHAUDHRY, R., VARSHNEY, A. K. & MALHOTRA, P. 2007. Adhesion proteins of Mycoplasma pneumoniae. *Frontiers in Bioscience,* 12**,** 690-699.

DALLO, S. F., KANNAN, T. R., BLAYLOCK, M. W. & BASEMAN, J. B. 2002. Elongation factor Tu and E1 beta subunit of pyruvate dehydrogenase complex act as fibronectin binding proteins in Mycoplasma pneumoniae. *Mol Microbiol,* 46**,** 1041-51.

DHANDAYUTHAPANI, S., RASMUSSEN, W. G. & BASEMAN, J. B. 1999. Disruption of gene mg218 of Mycoplasma genitalium through homologous recombination leads to an adherence-deficient phenotype. *Proc Natl Acad Sci U S A,* 96**,** 5227-32.

DO NASCIMENTO, N. C., DOS SANTOS, A. P., CHU, Y., GUIMARAES, A. M., BAIRD, A. N., WEIL, A. B. & MESSICK, J. B. 2014. Microscopy and genomic analysis of Mycoplasma parvum strain Indiana. *Vet Res,* 45**,** 86.

DO NASCIMENTO, N. C., DOS SANTOS, A. P., CHU, Y., GUIMARAES, A. M., PAGLIARO, A. & MESSICK, J. B. 2013. Genome Sequence of Mycoplasma parvum (Formerly Eperythrozoon parvum), a Diminutive Hemoplasma of the Pig. *Genome Announc,* 1.

DOENCH, J. G., FUSI, N., SULLENDER, M., HEGDE, M., VAIMBERG, E. W., DONOVAN, K. F., SMITH, I., TOTHOVA, Z., WILEN, C., ORCHARD, R., VIRGIN, H. W., LISTGARTEN, J. & ROOT, D. E. 2016. Optimized sgRNA design to maximize activity and minimize off-target effects of CRISPR-Cas9. *Nat Biotechnol,* 34**,** 184-191.

DOMINGUEZ, A. A., LIM, W. A. & QI, L. S. 2016. Beyond editing: repurposing CRISPR-Cas9 for precision genome regulation and interrogation. *Nat Rev Mol Cell Biol,* 17**,** 5-15.

DUMKE, R., HAUSNER, M. & JACOBS, E. 2011. Role of Mycoplasma pneumoniae glyceraldehyde-3-phosphate dehydrogenase (GAPDH) in mediating interactions with the human extracellular matrix. *Microbiology,* 157**,** 2328-38.

DURET, S., ANDRE, A. & RENAUDIN, J. 2005. Specific gene targeting in Spiroplasma citri: improved vectors and production of unmarked mutations using site-specific recombination. *Microbiology,* 151**,** 2793-803.

DYBVIG, K. & CASSELL, G. H. 1987. Transposition of gram-positive transposon Tn916 in Acholeplasma laidlawii and Mycoplasma pulmonis. *Science,* 235**,** 1392-4.

EATON, M. D., MEIKLEJOHN, G. & VAN HERICK, W. 1944. Studies on the Etiology of Primary Atypical Pneumonia : A Filterable Agent Transmissible to Cotton Rats, Hamsters, and Chick Embryos. *J Exp Med,* 79**,** 649-68.

GARCIA-MORALES, L., GONZALEZ-GONZALEZ, L., QUEROL, E. & PINOL, J. 2016. A minimized motile machinery for Mycoplasma genitalium. *Mol Microbiol,* 100**,** 125-38.

GARCIA-OTIN, A. L. & GUILLOU, F. 2006. Mammalian genome targeting using site-specific recombinases. *Front Biosci,* 11**,** 1108-36.

GIBSON, D. G., BENDERS, G. A., ANDREWS-PFANNKOCH, C., DENISOVA, E. A., BADEN-TILLSON, H., ZAVERI, J., STOCKWELL, T. B., BROWNLEY, A., THOMAS, D. W., ALGIRE, M. A., MERRYMAN, C., YOUNG, L., NOSKOV, V. N., GLASS, J. I., VENTER, J. C., HUTCHISON, C. A., 3RD & SMITH, H. O. 2008a. Complete chemical synthesis, assembly, and cloning of a Mycoplasma genitalium genome. *Science,* 319**,** 1215-20.

GIBSON, D. G., BENDERS, G. A., AXELROD, K. C., ZAVERI, J., ALGIRE, M. A., MOODIE, M., MONTAGUE, M. G., VENTER, J. C., SMITH, H. O. & HUTCHISON, C. A., 3RD 2008b. One-step assembly in yeast of 25 overlapping DNA fragments to form a complete synthetic Mycoplasma genitalium genome. *Proc Natl Acad Sci U S A,* 105**,** 20404-9.

GIBSON, D. G., GLASS, J. I., LARTIGUE, C., NOSKOV, V. N., CHUANG, R. Y., ALGIRE, M. A., BENDERS, G. A., MONTAGUE, M. G., MA, L., MOODIE, M. M., MERRYMAN, C., VASHEE, S., KRISHNAKUMAR, R., ASSAD-GARCIA, N., ANDREWS-PFANNKOCH, C., DENISOVA, E. A., YOUNG, L., QI, Z. Q., SEGALL-SHAPIRO, T. H., CALVEY, C. H., PARMAR, P. P., HUTCHISON, C. A., 3RD, SMITH, H. O. & VENTER, J. C. 2010. Creation of a bacterial cell controlled by a chemically synthesized genome. *Science,* 329**,** 52-6.

GIL, J. C., CEDILLO, R. L., MAYAGOITIA, B. G. & PAZ, M. D. 1993. Isolation of Mycoplasma pneumoniae from asthmatic patients. *Ann Allergy,* 70**,** 23-5.

GLASS, J. I. 2012. Synthetic genomics and the construction of a synthetic bacterial cell. *Perspect Biol Med,* 55**,** 473-89.

GLASS, J. I., ASSAD-GARCIA, N., ALPEROVICH, N., YOOSEPH, S., LEWIS, M. R., MARUF, M., HUTCHISON, C. A., 3RD, SMITH, H. O. & VENTER, J. C. 2006a. Essential genes of a minimal bacterium. *Proc Natl Acad Sci U S A,* 103**,** 425-30.

GLASS, J. I., ASSAD-GARCIA, N., ALPEROVICH, N., YOOSEPH, S., LEWIS, M. R., MARUF, M., HUTCHISON, C. A., SMITH, H. O. & VENTER, J. C. 2006b. Essential genes of a minimal bacterium. *Proceedings of the National Academy of Sciences of the United States of America,* 103**,** 425-430.

GONZALEZ-GONZALEZ, L. 2015. Functional and structural analyses of the terminal oganelle of Mycoplasma genitalium. Universitat Autònoma de Barcelona.

GRIMSHAW, J. P., JELESAROV, I., SCHONFELD, H. J. & CHRISTEN, P. 2001. Reversible thermal transition in GrpE, the nucleotide exchange factor of the DnaK heat-shock system. *J Biol Chem,* 276**,** 6098-104.

GROEMPING, Y., KLOSTERMEIER, D., HERRMANN, C., VEIT, T., SEIDEL, R. & REINSTEIN, J. 2001. Regulation of ATPase and chaperone cycle of DnaK from Thermus thermophilus by the nucleotide exchange factor GrpE. *J Mol Biol,* 305**,** 1173-83.

GROSS, L. A., BAIRD, G. S., HOFFMAN, R. C., BALDRIDGE, K. K. & TSIEN, R. Y. 2000. The structure of the chromophore within DsRed, a red fluorescent protein from coral. *Proc Natl Acad Sci U S A,* 97**,** 11990-5.

GRUNDEL, A., FRIEDRICH, K., PFEIFFER, M., JACOBS, E. & DUMKE, R. 2015a. Subunits of the Pyruvate Dehydrogenase Cluster of Mycoplasma pneumoniae Are Surface-Displayed Proteins that Bind and Activate Human Plasminogen. *PLoS One,* 10**,** e0126600.

GRUNDEL, A., PFEIFFER, M., JACOBS, E. & DUMKE, R. 2015b. Network of Surface-Displayed Glycolytic Enzymes in Mycoplasma pneumoniae and Their Interactions with Human Plasminogen. *Infect Immun,* 84**,** 666-76.

GUELDENER, U., HEINISCH, J., KOEHLER, G. J., VOSS, D. & HEGEMANN, J. H. 2002. A second set of loxP marker cassettes for Cre-mediated multiple gene knockouts in budding yeast. *Nucleic Acids Res,* 30**,** e23.

GUELL, M., VAN NOORT, V., YUS, E., CHEN, W. H., LEIGH-BELL, J., MICHALODIMITRAKIS, K., YAMADA, T., ARUMUGAM, M., DOERKS, T., KUHNER, S., RODE, M., SUYAMA, M., SCHMIDT, S., GAVIN, A. C., BORK, P. & SERRANO, L. 2009. Transcriptome complexity in a genome-reduced bacterium. *Science,* 326**,** 1268-71.

GUR, E. & SAUER, R. T. 2008. Evolution of the ssrA degradation tag in Mycoplasma: specificity switch to a different protease. *Proc Natl Acad Sci U S A,* 105**,** 16113-8.

HADJANTONAKIS, A. K. & NAGY, A. 2001. The color of mice: in the light of GFP-variant reporters. *Histochem Cell Biol,* 115**,** 49-58.

HAHN, T. W., MOTHERSHED, E. A., WALDO, R. H., 3RD & KRAUSE, D. C. 1999. Construction and analysis of a modified Tn4001 conferring chloramphenicol resistance in Mycoplasma pneumoniae. *Plasmid,* 41**,** 120-4.

HAHN, T. W., WILLBY, M. J. & KRAUSE, D. C. 1998. HMW1 is required for cytadhesin P1 trafficking to the attachment organelle in Mycoplasma pneumoniae. *J Bacteriol,* 180**,** 1270-6.

HALBEDEL, S. & STULKE, J. 2007. Tools for the genetic analysis of Mycoplasma. *Int J Med Microbiol,* 297**,** 37-44.

HAMES, C., HALBEDEL, S., SCHILLING, O. & STULKE, J. 2005. Multiple-mutation reaction: a method for simultaneous introduction of multiple mutations into the glpK gene of Mycoplasma pneumoniae. *Appl Environ Microbiol,* 71**,** 4097-100.

HARRISON, C. 2003. GrpE, a nucleotide exchange factor for DnaK. *Cell Stress Chaperones,* 8**,** 218-24.

HARRISON, C. J., HAYER-HARTL, M., DI LIBERTO, M., HARTL, F. & KURIYAN, J. 1997. Crystal structure of the nucleotide exchange factor GrpE bound to the ATPase domain of the molecular chaperone DnaK. *Science,* 276**,** 431-5.

HASSELBRING, B. A., PAGE, C. A., SHEPPARD, E. S. & KRAUSE, D. C. 2006a. Transposon mutagenesis identifies genes associated with Mycoplasma pneumoniae gliding motility. *Journal of Bacteriology,* 188**,** 6335-6345.

HASSELBRING, B. M., JORDAN, J. L. & KRAUSE, D. C. 2005. Mutant analysis reveals a specific requirement for protein P30 in Mycoplasma pneumoniae gliding motility. *J Bacteriol,* 187**,** 6281-9.

HASSELBRING, B. M., JORDAN, J. L., KRAUSE, R. W. & KRAUSE, D. C. 2006b. Terminal organelle development in the cell wall-less bacterium Mycoplasma pneumoniae. *Proc Natl Acad Sci U S A,* 103**,** 16478-83.

HASSELBRING, B. M. & KRAUSE, D. C. 2007a. Cytoskeletal protein P41 is required to anchor the terminal organelle of the wall-less prokaryote Mycoplasma pneumoniae. *Mol Microbiol,* 63**,** 44-53.

HASSELBRING, B. M. & KRAUSE, D. C. 2007b. Proteins P24 and P41 function in the regulation of terminal-organelle development and gliding motility in Mycoplasma pneumoniae. *J Bacteriol,* 189**,** 7442-9.

HASSELBRING, B. M., SHEPPARD, E. S. & KRAUSE, D. C. 2012. P65 truncation impacts P30 dynamics during Mycoplasma pneumoniae gliding. *J Bacteriol,* 194**,** 3000-7.

HATCHEL, J. M. & BALISH, M. F. 2008. Attachment organelle ultrastructure correlates with phylogeny, not gliding motility properties, in Mycoplasma pneumoniae relatives. *Microbiology,* 154**,** 286-95.

HEGERMANN, J., HERRMANN, R. & MAYER, F. 2002. Cytoskeletal elements in the bacterium Mycoplasma pneumoniae. *Naturwissenschaften,* 89**,** 453-458.

HENDERSON, G. P. & JENSEN, G. J. 2006. Three-dimensional structure of Mycoplasma pneumoniae's attachment organelle and a model for its role in gliding motility. *Mol Microbiol,* 60**,** 376-85.

HUH, W. J., MYSOREKAR, I. U. & MILLS, J. C. 2010. Inducible activation of Cre recombinase in adult mice causes gastric epithelial atrophy, metaplasia, and regenerative changes in the absence of "floxed" alleles. *Am J Physiol Gastrointest Liver Physiol,* 299**,** G368-80.

HUTCHISON, C. A., 3RD, CHUANG, R. Y., NOSKOV, V. N., ASSAD-GARCIA, N., DEERINCK, T. J., ELLISMAN, M. H., GILL, J., KANNAN, K., KARAS, B. J., MA, L., PELLETIER, J. F., QI, Z. Q., RICHTER, R. A., STRYCHALSKI, E. A., SUN, L., SUZUKI, Y., TSVETANOVA, B., WISE, K. S., SMITH, H. O., GLASS, J. I., MERRYMAN, C., GIBSON, D. G. & VENTER, J. C. 2016. Design and synthesis of a minimal bacterial genome. *Science,* 351**,** aad6253.

IDAHL, A., LUNDIN, E., JURSTRAND, M., KUMLIN, U., ELGH, F., OHLSON, N. & OTTANDER, U. 2011. Chlamydia trachomatis and Mycoplasma genitalium plasma antibodies in relation to epithelial ovarian tumors. *Infect Dis Obstet Gynecol,* 2011**,** 824627.

JAFFE, J. D., STANGE-THOMANN, N., SMITH, C., DECAPRIO, D., FISHER, S., BUTLER, J., CALVO, S., ELKINS, T., FITZGERALD, M. G., HAFEZ, N., KODIRA, C. D., MAJOR, J., WANG, S., WILKINSON, J., NICOL, R., NUSBAUM, C., BIRREN, B., BERG, H. C. & CHURCH, G. M. 2004. The complete genome and proteome of Mycoplasma mobile. *Genome Res,* 14**,** 1447-61.

JARRELL, K. F. & MCBRIDE, M. J. 2008. The surprisingly diverse ways that prokaryotes move. *Nat Rev Microbiol,* 6**,** 466-76.

JINEK, M., CHYLINSKI, K., FONFARA, I., HAUER, M., DOUDNA, J. A. & CHARPENTIER, E. 2012. A programmable dual-RNA-guided DNA endonuclease in adaptive bacterial immunity. *Science,* 337**,** 816-21.

JORDAN, J. L., BERRY, K. M., BALISH, M. F. & KRAUSE, D. C. 2001. Stability and subcellular localization of cytadherence-associated protein P65 in Mycoplasma pneumoniae. *J Bacteriol,* 183**,** 7387-91.

JORDAN, J. L., CHANG, H. Y., BALISH, M. F., HOLT, L. S., BOSE, S. R., HASSELBRING, B. M., WALDO, R. H., 3RD, KRUNKOSKY, T. M. & KRAUSE, D. C. 2007. Protein P200 is dispensable for Mycoplasma pneumoniae hemadsorption but not gliding motility or colonization of differentiated bronchial epithelium. *Infect Immun,* 75**,** 518-22.

KANNAN, T. R. & BASEMAN, J. B. 2006. ADP-ribosylating and vacuolating cytotoxin of Mycoplasma pneumoniae represents unique virulence determinant among bacterial pathogens. *Proc Natl Acad Sci U S A,* 103**,** 6724-9.

KARASAWA, S., ARAKI, T., YAMAMOTO-HINO, M. & MIYAWAKI, A. 2003. A green-emitting fluorescent protein from Galaxeidae coral and its monomeric version for use in fluorescent labeling. *J Biol Chem,* 278**,** 34167-71.

KARR, J. R., SANGHVI, J. C., MACKLIN, D. N., GUTSCHOW, M. V., JACOBS, J. M., BOLIVAL, B., JR., ASSAD-GARCIA, N., GLASS, J. I. & COVERT, M. W. 2012. A whole-cell computational model predicts phenotype from genotype. *Cell,* 150**,** 389-401.

KASAI, T., NAKANE, D., ISHIDA, H., ANDO, H., KISO, M. & MIYATA, M. 2013. Role of binding in Mycoplasma mobile and Mycoplasma pneumoniae gliding analyzed through inhibition by synthesized sialylated compounds. *J Bacteriol,* 195**,** 429-35.

KAWAKITA, Y., KINOSHITA, M., FURUKAWA, Y., TULUM, I., TAHARA, Y. O., KATAYAMA, E., NAMBA, K. & MIYATA, M. 2016. Structural Study of MPN387, an Essential Protein for Gliding Motility of a Human-Pathogenic Bacterium, Mycoplasma pneumoniae. *J Bacteriol,* 198**,** 2352-9.

KAWAMOTO, A., MATSUO, L., KATO, T., YAMAMOTO, H., NAMBA, K. & MIYATA, M. 2016. Periodicity in Attachment Organelle Revealed by Electron Cryotomography Suggests Conformational Changes in Gliding Mechanism of Mycoplasma pneumoniae. *MBio,* 7**,** e00243-16.

KENRI, T., SETO, S., HORINO, A., SASAKI, Y., SASAKI, T. & MIYATA, M. 2004. Use of fluorescent-protein tagging to determine the subcellular localization of mycoplasma pneumoniae proteins encoded by the cytadherence regulatory locus. *J Bacteriol,* 186**,** 6944-55.

KLEINSTIVER, B. P., PATTANAYAK, V., PREW, M. S., TSAI, S. Q., NGUYEN, N. T., ZHENG, Z. & JOUNG, J. K. 2016. High-fidelity CRISPR-Cas9 nucleases with no detectable genome-wide off-target effects. *Nature,* 529**,** 490-5.

KNUDSEN, G. M., HOLCH, A. & GRAM, L. 2012. Subinhibitory concentrations of antibiotics affect stress and virulence gene expression in Listeria monocytogenes and cause enhanced stress sensitivity but do not affect Caco-2 cell invasion. *J Appl Microbiol,* 113**,** 1273-86.

KRAFT, M., CASSELL, G. H., HENSON, J. E., WATSON, H., WILLIAMSON, J., MARMION, B. P., GAYDOS, C. A. & MARTIN, R. J. 1998. Detection of Mycoplasma pneumoniae in the airways of adults with chronic asthma. *Am J Respir Crit Care Med,* 158**,** 998-1001.

KRAUSE, D. C. & BALISH, M. F. 2001. Structure, function, and assembly of the terminal organelle of Mycoplasma pneumoniae. *Fems Microbiology Letters,* 198**,** 1-7.

KRAUSE, D. C., PROFT, T., HEDREYDA, C. T., HILBERT, H., PLAGENS, H. & HERRMANN, R. 1997. Transposon mutagenesis reinforces the correlation between Mycoplasma pneumoniae cytoskeletal protein HMW2 and cytadherence. *J Bacteriol,* 179**,** 2668-77.

KRISHNAKUMAR, R., ASSAD-GARCIA, N., BENDERS, G. A., PHAN, Q., MONTAGUE, M. G. & GLASS, J. I. 2010. Targeted chromosomal knockouts in Mycoplasma pneumoniae. *Appl Environ Microbiol,* 76**,** 5297-9.

KURNER, J., FRANGAKIS, A. S. & BAUMEISTER, W. 2005. Cryo-electron tomography reveals the cytoskeletal structure of Spiroplasma melliferum. *Science,* 307**,** 436-8.

LANGER, S. J., GHAFOORI, A. P., BYRD, M. & LEINWAND, L. 2002. A genetic screen identifies novel non-compatible loxP sites. *Nucleic Acids Res,* 30**,** 3067-77.

LANZA, A. M., DYESS, T. J. & ALPER, H. S. 2012. Using the Cre/lox system for targeted integration into the human genome: loxFAS-loxP pairing and delayed introduction of Cre DNA improve gene swapping efficiency. *Biotechnol J,* 7**,** 898-908.

LAYH-SCHMITT, G., PODTELEJNIKOV, A. & MANN, M. 2000. Proteins complexed to the P1 adhesin of Mycoplasma pneumoniae. *Microbiology,* 146 (Pt 3)**,** 741-7.

LAZAREV, V. N., LEVITSKII, S. A., BASOVSKII, Y. I., CHUKIN, M. M., AKOPIAN, T. A., VERESHCHAGIN, V. V., KOSTRJUKOVA, E. S., KOVALEVA, G. Y., KAZANOV, M. D., MALKO, D. B., VITRESCHAK, A. G., SERNOVA, N. V., GELFAND, M. S., DEMINA, I. A., SEREBRYAKOVA, M. V., GALYAMINA, M. A., VTYURIN, N. N., ROGOV, S. I., ALEXEEV, D. G., LADYGINA, V. G. & GOVORUN, V. M. 2011. Complete genome and proteome of Acholeplasma laidlawii. *J Bacteriol,* 193**,** 4943-53.

LEE, G. & SAITO, I. 1998. Role of nucleotide sequences of loxP spacer region in Cre-mediated recombination. *Gene,* 216**,** 55-65.

LEE, S. W., BROWNING, G. F. & MARKHAM, P. F. 2008. Development of a replicable oriC plasmid for Mycoplasma gallisepticum and Mycoplasma imitans, and gene disruption through homologous recombination in M. gallisepticum. *Microbiology,* 154**,** 2571-80.

LIU, P., ZHENG, H., MENG, Q., TERAHARA, N., GU, W., WANG, S., ZHAO, G., NAKANE, D., WANG, W. & MIYATA, M. 2017. Chemotaxis without Conventional Two-Component System, Based on Cell Polarity and Aerobic Conditions in Helicity-Switching Swimming of Spiroplasma eriocheiris. *Front Microbiol,* 8**,** 58.

LIVET, J., WEISSMAN, T. A., KANG, H., DRAFT, R. W., LU, J., BENNIS, R. A., SANES, J. R. & LICHTMAN, J. W. 2007. Transgenic strategies for combinatorial expression of fluorescent proteins in the nervous system. *Nature,* 450**,** 56-62.

LOOMES, L. M., UEMURA, K., CHILDS, R. A., PAULSON, J. C., ROGERS, G. N., SCUDDER, P. R., MICHALSKI, J. C., HOUNSELL, E. F., TAYLOR-ROBINSON, D. & FEIZI, T. 1984. Erythrocyte receptors for Mycoplasma pneumoniae are sialylated oligosaccharides of Ii antigen type. *Nature,* 307**,** 560-3.

LOONSTRA, A., VOOIJS, M., BEVERLOO, H. B., ALLAK, B. A., VAN DRUNEN, E., KANAAR, R., BERNS, A. & JONKERS, J. 2001. Growth inhibition and DNA damage induced by Cre recombinase in mammalian cells. *Proc Natl Acad Sci U S A,* 98**,** 9209-14.

LLUCH-SENAR, M., MANCUSO, F. M., CLIMENTE-GONZALEZ, H., PENA-PAZ, M. I., SABIDO, E. & SERRANO, L. 2016. Rescuing discarded spectra: Full comprehensive analysis of a minimal proteome. *Proteomics,* 16**,** 554-63.

LLUCH-SENAR, M., QUEROL, E. & PINOL, J. 2010. Cell division in a minimal bacterium in the absence of ftsZ. *Mol Microbiol,* 78**,** 278-89.

MAGLENNON, G. A., COOK, B. S., MATTHEWS, D., DEENEY, A. S., BOSSE, J. T., LANGFORD, P. R., MASKELL, D. J., TUCKER, A. W., WREN, B. W., RYCROFT, A. N. & CONSORTIUM, B. R. T. 2013. Development of a self-replicating plasmid system for Mycoplasma hyopneumoniae. *Vet Res,* 44**,** 63.

MAHAIRAS, G. G. & MINION, F. C. 1989a. Random insertion of the gentamicin resistance transposon Tn4001 in Mycoplasma pulmonis. *Plasmid,* 21**,** 43-7.

MAHAIRAS, G. G. & MINION, F. C. 1989b. Transformation of Mycoplasma pulmonis: demonstration of homologous recombination, introduction of cloned genes, and preliminary description of an integrating shuttle system. *J Bacteriol,* 171**,** 1775-80.

MANHART, L. E., HOLMES, K. K., HUGHES, J. P., HOUSTON, L. S. & TOTTEN, P. A. 2007. Mycoplasma genitalium among young adults in the United States: an emerging sexually transmitted infection. *Am J Public Health,* 97**,** 1118-25.

MARISCAL, A. M., GONZALEZ-GONZALEZ, L., QUEROL, E. & PINOL, J. 2016. All-in-one construct for genome engineering using Cre-lox technology. *DNA Res,* 23**,** 263-70.

MARTINELLI, L., GARCIA-MORALES, L., QUEROL, E., PINOL, J., FITA, I. & CALISTO, B. M. 2016. Structure-Guided Mutations in the Terminal Organelle Protein MG491 Cause Major Motility and Morphologic Alterations on Mycoplasma genitalium. *PLoS Pathog,* 12**,** e1005533.

MARTINELLI, L., LALLI, D., GARCIA-MORALES, L., RATERA, M., QUEROL, E., PINOL, J., FITA, I. & CALISTO, B. M. 2015. A Major Determinant for Gliding Motility in Mycoplasma genitalium THE INTERACTION BETWEEN THE TERMINAL ORGANELLE PROTEINS MG200 AND MG491. *Journal of Biological Chemistry,* 290**,** 1699-1711.

MATZ, M. V., FRADKOV, A. F., LABAS, Y. A., SAVITSKY, A. P., ZARAISKY, A. G., MARKELOV, M. L. & LUKYANOV, S. A. 1999. Fluorescent proteins from nonbioluminescent Anthozoa species. *Nat Biotechnol,* 17**,** 969-73.

MCBRIDE, M. J. 2001. Bacterial gliding motility: multiple mechanisms for cell movement over surfaces. *Annu Rev Microbiol,* 55**,** 49-75.

MCGOWIN, C. L. & ANDERSON-SMITS, C. 2011. Mycoplasma genitalium: an emerging cause of sexually transmitted disease in women. *PLoS Pathog,* 7**,** e1001324.

MCGOWIN, C. L., POPOV, V. L. & PYLES, R. B. 2009. Intracellular Mycoplasma genitalium infection of human vaginal and cervical epithelial cells elicits distinct patterns of inflammatory cytokine secretion and provides a possible survival niche against macrophage-mediated killing. *BMC Microbiol,* 9**,** 139.

MENA, M. A., TREYNOR, T. P., MAYO, S. L. & DAUGHERTY, P. S. 2006. Blue fluorescent proteins with enhanced brightness and photostability from a structurally targeted library. *Nat Biotechnol,* 24**,** 1569-71.

MENG, K. E. & PFISTER, R. M. 1980. Intracellular structures of Mycoplasma pneumoniae revealed after membrane removal. *J Bacteriol,* 144**,** 390-9.

MERNAUGH, G. R., DALLO, S. F., HOLT, S. C. & BASEMAN, J. B. 1993. Properties of adhering and nonadhering populations of Mycoplasma genitalium. *Clin Infect Dis,* 17 Suppl 1**,** S69-78.

MIYATA, M. 2008. Centipede and inchworm models to explain Mycoplasma gliding. *Trends Microbiol,* 16**,** 6-12.

MIYATA, M. 2010. Unique Centipede Mechanism of Mycoplasma Gliding. *Annu Rev Microbiol*.

MIYATA, M. & HAMAGUCHI, T. 2016. Integrated Information and Prospects for Gliding Mechanism of the Pathogenic Bacterium Mycoplasma pneumoniae. *Front Microbiol,* 7**,** 960.

MUSATOVOVA, O., DHANDAYUTHAPANI, S. & BASEMAN, J. B. 2006. Transcriptional heat shock response in the smallest known self-replicating cell, Mycoplasma genitalium. *J Bacteriol,* 188**,** 2845-55.

NAGAI, R. & MIYATA, M. 2006. Gliding motility of Mycoplasma mobile can occur by repeated binding to N-acetylneuraminyllactose (sialyllactose) fixed on solid surfaces. *J Bacteriol,* 188**,** 6469-75.

NAGAI, T., IBATA, K., PARK, E. S., KUBOTA, M., MIKOSHIBA, K. & MIYAWAKI, A. 2002. A variant of yellow fluorescent protein with fast and efficient maturation for cell-biological applications. *Nat Biotechnol,* 20**,** 87-90.

NAGY, A. 2000. Cre recombinase: the universal reagent for genome tailoring. *Genesis,* 26**,** 99-109.

NAKANE, D., ADAN-KUBO, J., KENRI, T. & MIYATA, M. 2011. Isolation and Characterization of P1 Adhesin, a Leg Protein of the Gliding Bacterium Mycoplasma pneumoniae. *Journal of Bacteriology,* 193**,** 715-722.

NAKANE, D., KENRI, T., MATSUO, L. & MIYATA, M. 2015. Systematic Structural Analyses of Attachment Organelle in Mycoplasma pneumoniae. *PLoS Pathog,* 11**,** e1005299.

NAMIKI, K., GOODISON, S., PORVASNIK, S., ALLAN, R. W., ICZKOWSKI, K. A., URBANEK, C., REYES, L., SAKAMOTO, N. & ROSSER, C. J. 2009. Persistent exposure to Mycoplasma induces malignant transformation of human prostate cells. *PLoS One,* 4**,** e6872.

NAPIERALA MAVEDZENGE, S. & WEISS, H. A. 2009. Association of Mycoplasma genitalium and HIV infection: a systematic review and meta-analysis. *AIDS,* 23**,** 611-20.

NASH, H. A. 1977. Integration and excision of bacteriophage lambda. *Curr Top Microbiol Immunol,* 78**,** 171-99.

NCBI 2017. Ref_seq NC_000908.2.

PARRAGA-NINO, N., COLOME-CALLS, N., CANALS, F., QUEROL, E. & FERRER-NAVARRO, M. 2012. A comprehensive proteome of Mycoplasma genitalium. *J Proteome Res,* 11**,** 3305-16.

PICH, O. Q. 2008. Aïllament i caracterització de mutants de *Mycoplasma genitalium* deficients en motilitat. *Tesis doctoral*.

PICH, O. Q., BURGOS, R., FERRER-NAVARRO, M., QUEROL, E. & PINOL, J. 2006a. Mycoplasma genitalium mg200 and mg386 genes are involved in gliding motility but not in cytadherence. *Mol Microbiol,* 60**,** 1509-19.

PICH, O. Q., BURGOS, R., FERRER-NAVARRO, M., QUEROL, E. & PINOL, J. 2008. Role of Mycoplasma genitalium MG218 and MG317 cytoskeletal proteins in terminal organelle organization, gliding motility and cytadherence. *Microbiology,* 154**,** 3188-98.

PICH, O. Q., BURGOS, R., PLANELL, R., QUEROL, E. & PINOL, J. 2006b. Comparative analysis of antibiotic resistance gene markers in Mycoplasma genitalium: application to studies of the minimal gene complement. *Microbiology,* 152**,** 519-27.

PICH, O. Q., BURGOS, R., QUEROL, E. & PINOL, J. 2009. P110 and P140 cytadherence-related proteins are negative effectors of terminal organelle duplication in Mycoplasma genitalium. *PLoS One,* 4**,** e7452.

POLLACK, J. D., WILLIAMS, M. V. & MCELHANEY, R. N. 1997. The comparative metabolism of the mollicutes (Mycoplasmas): the utility for taxonomic classification and the relationship of putative gene annotation and phylogeny to enzymatic function in the smallest free-living cells. *Crit Rev Microbiol,* 23**,** 269-354.

POPHAM, P. L., HAHN, T. W., KREBES, K. A. & KRAUSE, D. C. 1997. Loss of HMW1 and HMW3 in noncytadhering mutants of Mycoplasma pneumoniae occurs post-translationally. *Proc Natl Acad Sci U S A,* 94**,** 13979-84.

QI, L. S., LARSON, M. H., GILBERT, L. A., DOUDNA, J. A., WEISSMAN, J. S., ARKIN, A. P. & LIM, W. A. 2013. Repurposing CRISPR as an RNA-guided platform for sequence-specific control of gene expression. *Cell,* 152**,** 1173-83.

RASMUSSEN, B., NOLLER, H. F., DAUBRESSE, G., OLIVA, B., MISULOVIN, Z., ROTHSTEIN, D. M., ELLESTAD, G. A., GLUZMAN, Y., TALLY, F. P. & CHOPRA, I. 1991. Molecular basis of tetracycline action: identification of analogs whose primary target is not the bacterial ribosome. *Antimicrob Agents Chemother,* 35**,** 2306-11.

RAZIN, S. 2006. *The Genus Mycoplasma and Related Genera (Class Mollicutes)*.

RAZIN, S., YOGEV, D. & NAOT, Y. 1998. Molecular biology and pathogenicity of mycoplasmas. *Microbiol Mol Biol Rev,* 62**,** 1094-156.

RELICH, R. F. & BALISH, M. F. 2011. Insights into the function of Mycoplasma pneumoniae protein P30 from orthologous gene replacement. *Microbiology,* 157**,** 2862-70.

ROMERO-ARROYO, C. E., JORDAN, J., PEACOCK, S. J., WILLBY, M. J., FARMER, M. A. & KRAUSE, D. C. 1999. Mycoplasma pneumoniae protein P30 is required for cytadherence and associated with proper cell development. *J Bacteriol,* 181**,** 1079-87.

SAMBROOK, J., RUSSELL, D. W. & SAMBROOK, J. 2006. *The condensed protocols from Molecular cloning : a laboratory manual,* Cold Spring Harbor, N.Y., Cold Spring Harbor Laboratory Press.

SCHEFFER, M. P., GONZALEZ-GONZALEZ, L., SEYBERT, A., RATERA, M., KUNZ, M., VALPUESTA, J. M., FITA, I., QUEROL, E., PINOL, J., MARTIN-BENITO, J. & FRANGAKIS, A. S. 2017. Structural characterization of the NAP;

the major adhesion complex of the human pathogen Mycoplasma genitalium. *Mol Microbiol,* 105**,** 869-879.

SCHMIDT, E. E., TAYLOR, D. S., PRIGGE, J. R., BARNETT, S. & CAPECCHI, M. R. 2000. Illegitimate Cre-dependent chromosome rearrangements in transgenic mouse spermatids. *Proc Natl Acad Sci U S A,* 97**,** 13702-7.

SCHRODER, H., LANGER, T., HARTL, F. U. & BUKAU, B. 1993. DnaK, DnaJ and GrpE form a cellular chaperone machinery capable of repairing heat-induced protein damage. *EMBO J,* 12**,** 4137-44.

SETO, S., KENRI, T., TOMIYAMA, T. & MIYATA, M. 2005. Involvement of P1 adhesin in gliding motility of Mycoplasma pneumoniae as revealed by the inhibitory effects of antibody under optimized gliding conditions. *Journal of Bacteriology,* 187**,** 1875-1877.

SETO, S., LAYH-SCHMITT, G., KENRI, T. & MIYATA, M. 2001. Visualization of the attachment organelle and cytadherence proteins of Mycoplasma pneumoniae by immunofluorescence microscopy. *J Bacteriol,* 183**,** 1621-30.

SETO, S. & MIYATA, M. 2003. Attachment organelle formation represented by localization of cytadherence proteins and formation of the electron-dense core in wild-type and mutant strains of Mycoplasma pneumoniae. *J Bacteriol,* 185**,** 1082-91.

SEYBERT, A., HERRMANN, R. & FRANGAKIS, A. S. 2006. Structural analysis of Mycoplasma pneumoniae by cryo-electron tomography. *J Struct Biol,* 156**,** 342-54.

SHARMA, S., CITTI, C., SAGNE, E., MARENDA, M. S., MARKHAM, P. F. & BROWNING, G. F. 2015. Development and host compatibility of plasmids for two important ruminant pathogens, Mycoplasma bovis and Mycoplasma agalactiae. *PLoS One,* 10**,** e0119000.

SHI, W., ZHOU, Y., WILD, J., ADLER, J. & GROSS, C. A. 1992. DnaK, DnaJ, and GrpE are required for flagellum synthesis in Escherichia coli. *J Bacteriol,* 174**,** 6256-63.

SHIMOMURA, O., JOHNSON, F. H. & SAIGA, Y. 1962. Extraction, purification and properties of aequorin, a bioluminescent protein from the luminous hydromedusan, Aequorea. *J Cell Comp Physiol,* 59**,** 223-39.

SMILEY, B. K. & MINION, F. C. 1993. Enhanced readthrough of opal (UGA) stop codons and production of Mycoplasma pneumoniae P1 epitopes in Escherichia coli. *Gene,* 134**,** 33-40.

STERNBERG, N. & HAMILTON, D. 1981. Bacteriophage P1 site-specific recombination. I. Recombination between loxP sites. *J Mol Biol,* 150**,** 467-86.

STERNBERG, N., HAMILTON, D. & HOESS, R. 1981. Bacteriophage P1 site-specific recombination. II. Recombination between loxP and the bacterial chromosome. *J Mol Biol,* 150**,** 487-507.

STEVENS, M. K. & KRAUSE, D. C. 1992. Mycoplasma pneumoniae cytadherence phase-variable protein HMW3 is a component of the attachment organelle. *J Bacteriol,* 174**,** 4265-74.

SZCZEPANEK, S. M., MAJUMDER, S., SHEPPARD, E. S., LIAO, X., ROOD, D., TULMAN, E. R., WYAND, S., KRAUSE, D. C., SILBART, L. K. & GEARY, S. J. 2012. Vaccination of BALB/c mice with an avirulent Mycoplasma pneumoniae P30 mutant results in disease exacerbation upon challenge with a virulent strain. *Infect Immun,* 80**,** 1007-14.

TAYLOR-ROBINSON, D. & JENSEN, J. S. 2011. Mycoplasma genitalium: from Chrysalis to multicolored butterfly. *Clin Microbiol Rev,* 24**,** 498-514.

TECHASAENSIRI, C., TAGLIABUE, C., CAGLE, M., IRANPOUR, P., KATZ, K., KANNAN, T. R., COALSON, J. J., BASEMAN, J. B. & HARDY, R. D. 2010. Variation in colonization, ADP-ribosylating and vacuolating cytotoxin, and pulmonary disease severity among mycoplasma pneumoniae strains. *Am J Respir Crit Care Med,* 182**,** 797-804.

THOMAS, C., JACOBS, E. & DUMKE, R. 2013. Characterization of pyruvate dehydrogenase subunit B and enolase as plasminogen-binding proteins in Mycoplasma pneumoniae. *Microbiology,* 159**,** 352-65.

TULLY, J. G., TAYLOR-ROBINSON, D., COLE, R. M. & ROSE, D. L. 1981. A newly discovered mycoplasma in the human urogenital tract. *Lancet,* 1**,** 1288-91.

TURAN, S., GALLA, M., ERNST, E., QIAO, J., VOELKEL, C., SCHIEDLMEIER, B., ZEHE, C. & BODE, J. 2011. Recombinase-mediated cassette exchange (RMCE): traditional concepts and current challenges. *J Mol Biol,* 407**,** 193-221.

UENO, P. M., TIMENETSKY, J., CENTONZE, V. E., WEWER, J. J., CAGLE, M., STEIN, M. A., KRISHNAN, M. & BASEMAN, J. B. 2008. Interaction of Mycoplasma genitalium with host cells: evidence for nuclear localization. *Microbiology,* 154**,** 3033-41.

VAN DUYNE, G. D. 2001. A structural view of cre-loxp site-specific recombination. *Annu Rev Biophys Biomol Struct,* 30**,** 87-104.

WAITES, K. B. & TALKINGTON, D. F. 2004. Mycoplasma pneumoniae and its role as a human pathogen. *Clin Microbiol Rev,* 17**,** 697-728, table of contents.

WAITES, K. B., XIAO, L., LIU, Y., BALISH, M. F. & ATKINSON, T. P. 2017. Mycoplasma pneumoniae from the Respiratory Tract and Beyond. *Clin Microbiol Rev,* 30**,** 747-809.

WEISBURG, W. G., TULLY, J. G., ROSE, D. L., PETZEL, J. P., OYAIZU, H., YANG, D., MANDELCO, L., SECHREST, J., LAWRENCE, T. G., VAN ETTEN, J. & ET AL. 1989. A phylogenetic analysis of the mycoplasmas: basis for their classification. *J Bacteriol,* 171**,** 6455-67.

WILLBY, M. J., BALISH, M. F., ROSS, S. M., LEE, K. K., JORDAN, J. L. & KRAUSE, D. C. 2004. HMW1 is required for stability and localization of HMW2 to the attachment organelle of Mycoplasma pneumoniae. *Journal of Bacteriology,* 186**,** 8221-8228.

WILLBY, M. J. & KRAUSE, D. C. 2002. Characterization of a Mycoplasma pneumoniae hmw3 mutant: implications for attachment organelle assembly. *J Bacteriol,* 184**,** 3061-8.

WILLIAMS, M., LOUW, A. I. & BIRKHOLTZ, L. M. 2007. Deletion mutagenesis of large areas in Plasmodium falciparum genes: a comparative study. *Malar J,* 6**,** 64.

WOESE, C. R., MANILOFF, J. & ZABLEN, L. B. 1980. Phylogenetic analysis of the mycoplasmas. *Proc Natl Acad Sci U S A,* 77**,** 494-8.

WOLGEMUTH, C. W., IGOSHIN, O. & OSTER, G. 2003. The motility of mollicutes. *Biophys J,* 85**,** 828-42.

WU, C. C., NAVEEN, V., CHIEN, C. H., CHANG, Y. W. & HSIAO, C. D. 2012. Crystal structure of DnaK protein complexed with nucleotide exchange factor GrpE in DnaK chaperone system: insight into intermolecular communication. *J Biol Chem,* 287**,** 21461-70.

XAVIER, J. C., PATIL, K. R. & ROCHA, I. 2014. Systems biology perspectives on minimal and simpler cells. *Microbiol Mol Biol Rev,* 78**,** 487-509.

YU, Y. & BRADLEY, A. 2001. Engineering chromosomal rearrangements in mice. *Nat Rev Genet,* 2**,** 780-90.

ZAPATA-HOMMER, O. & GRIESBECK, O. 2003. Efficiently folding and circularly permuted variants of the Sapphire mutant of GFP. *BMC Biotechnol,* 3**,** 5.

ZAREI, O., REZANIA, S. & MOUSAVI, A. 2013. Mycoplasma genitalium and cancer: a brief review. *Asian Pac J Cancer Prev,* 14**,** 3425-8.

ZIMMERMAN, C. U. & HERRMANN, R. 2005. Synthesis of a small, cysteine-rich, 29 amino acids long peptide in Mycoplasma pneumoniae. *FEMS Microbiol Lett,* 253**,** 315-21.